THE JOURNAL
OF
CHEMICAL PHYSICS

VOLUME 8 MARCH, 1940 NUMBER 3

The Infra-Red Absorption Spectrum of Methyl Amine

RALPH G. OWENS AND E. F. BARKER
University of Michigan, Ann Arbor, Michigan

(Received December 27, 1939)

The parallel type methyl amine band at 10μ has been resolved. Its center is at 1045.27 cm^{-1}, and the very regular structure of its P and R branches indicates a close approximation to axial symmetry. The mean of the two largest moments of inertia is 37.43×10^{-40} $g\cdot cm^2$. Assuming angles and distances for NH_2 as in ammonia, and for CH_3 as in methane, the C—N distance is computed to be 1.48×10^{-8} cm. Certain enhanced lines suggest a superposed perpendicular band. The 13μ band is partially resolved, and assigned to a motion corresponding to ν_3 in NH_3. The bands arising from vibrations characteristic of the amino and methyl groups have been examined but could not be resolved.

OBSERVATIONS upon the infra-red spectrum of methylamine vapor which have recently been published by Cleaves and Plyler[1] include the envelopes of a number of unresolved absorption bands, the frequencies of which have been assigned to various normal modes of vibration of the CH_3NH_2 molecule. The same spectrum has been under investigation in this laboratory with a slightly higher dispersion, the results being identical in some respects, but sufficiently different in others to justify further discussion.

The molecule approximates a rigid rotator which is almost, but not quite, axially symmetrical, and its spectrum is similar in many respects to those of CH_3OH and CH_3F. It may also be thought of as an ammonia derivative in which the methyl group has replaced one of the hydrogen atoms. There is a single plane of symmetry through the CN axis and bisecting the HNH angle. The motions associated with the fifteen vibrational degrees of freedom may be subdivided for convenience into three classes. Six of them represent the mutual oscillations of the methyl and amino groups; three others are characteristic of the amino group alone, while the remaining six belong primarily to the methyl radical.

MUTUAL VIBRATIONS OF THE METHYL AND AMINO GROUPS

The molecule may first be considered as consisting of two approximately rigid groups of atoms attached to one another through the C—N bond. Of the six characteristic motions of this structure (rotation and translation excluded) the simplest is the valence oscillation, which is accompanied by a change in electric moment nearly parallel to the CN axis. The corresponding absorption band lies close to 10μ, and, as represented by Cleaves and Plyler, has a narrow intense zero branch. Under somewhat higher resolution the rotational structure of this band appears, showing the remarkably regular pattern indicated in Fig. 1. The spectral range included in the slit was about 0.5 cm^{-1}. The zero branch remains quite narrow and unresolved, and the

[1] Cleaves and Plyler, J. Chem. Phys. **7**, 563 (1939).

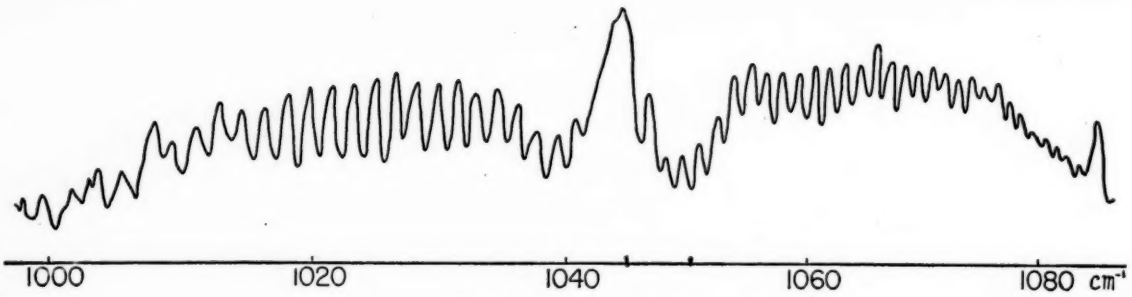

FIG. 1. The band at 10μ.

individual lines composing the wings show no observable splitting. This indicates that axial symmetry is closely approximated. Table I presents the positions of the observed lines, in wave numbers, reduced to vacuum.

An unusual feature of this band is the enhancement in intensity of certain lines, particularly of $+1$, although $+7$, $+15$ and others stand out above the envelope, and a strong narrow line appears at 1085 cm^{-1}, at the high frequency end of the band. This suggests that a weak perpendicular type band with relatively wide spacing is superposed upon the principal absorption. Further observations with different amounts of gas may reveal more detail.

A second mode of motion associated with the CN axis is the torsional oscillation. Cleaves and Plyler assign to it the frequency 620 cm^{-1}, and report a band envelope resembling that of a parallel vibration, with an intense though rather wide central maximum. Our observations seem hardly compatible with this. While an irregular pattern of rather weak absorption extends from 500 to 700 cm^{-1}, we have observed no region of particularly high intensity, and no characteristic band structure. It is of course possible that this absorption represents the fundamental band due to torsional oscillation, but we are inclined to believe that the frequency is too high* to be so interpreted, and that instead one or more difference bands are involved.

A pair of perpendicular vibrations are expected in which the C—N bond is deformed either in the plane of symmetry or normal to this plane. These are perhaps represented by rather weak bands at about 1130 cm^{-1} and 1150 cm^{-1}. Here the structure is quite complicated, with no very intense lines, and is not sufficiently resolved to permit an analysis.

The other two vibrations characteristic of a molecule considered as a pair of approximately rigid groups are torsional oscillations in which the hydrogens belonging to NH_2 move, either in the same sense or in opposite senses, along lines perpendicular to the N—H bond and parallel to the plane of symmetry. Thinking of the structure as a substituted ammonia, the first of these corresponds to the symmetrical NH_3 vibration ν_3, which gives rise to a pair of bands near 10μ, the doubling being a consequence of the two minimum potential function. This interesting characteristic must persist in methyl amine, though somewhat modified by the fact that whenever the N atom passes through the $H-H-CH_3$ plane from one equilibrium position to the other, the methyl group must rotate through an angle of 60° about its own symmetry axis. The resulting absorption band extends from about 710 cm^{-1} to about 850 cm^{-1}, its central portion having the structure indicated in Fig. 2.

TABLE I. *Observed wave numbers, reduced to vacuum, for lines in the 10μ band. J for the lower rotation state.*

P BRANCH	J	R BRANCH	P BRANCH	J	R BRANCH
——	0	1046.44	1026.23	11	1061.52
——	1	1047.86	1024.56	12	1062.77
1040.50	2	1049.30	1022.90	13	1064.08
1038.96	3	1050.71	1021.19	14	1065.39
1037.42	4	1052.11	1019.54	15	1066.70
1035.89	5	1053.45	1017.84	16	1067.90
1034.31	6	1054.85	1016.10	17	1069.10
1032.67	7	1056.21	1014.35	18	1070.24
1031.03	8	1057.56	1012.56	19	1071.38
1029.47	9	1058.86	1010.82	20	1072.59
1027.84	10	1060.22	1009.06	21	1073.73

*This supposition is supported by observations of Randall and Lawson, as yet unpublished, but kindly communicated to us. They find a region of rather strong absorption in the neighborhood of 270 cm^{-1}.

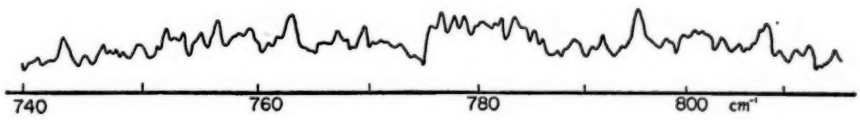

FIG. 2. A part of the 13μ band.

There is a rather strong central region around 780 cm^{-1}, obviously consisting of many lines, and flanked on either side by a fairly sharp maximum suggesting a Q branch. The positions of these maxima are 763 cm^{-1} and 795 cm^{-1}. The change in electric moment will include both parallel and perpendicular components.

The corresponding unsymmetrical oscillation introduces an angular momentum which must be compensated by a tilting of the methyl group. Thus the change in electric moment is principally in a direction normal to the symmetry plane of the molecule. This nondegenerate perpendicular vibration corresponds to the 6μ band, ν_4, of NH_3. It has not been identified in the spectrum, but may possibly lie in the 10μ region, or even as far out as 16μ.

VIBRATIONS CHARACTERISTIC OF NH_2

The symmetrical valence oscillation of the amino group should have both perpendicular and parallel components. The latter, though relatively less intense, is unmistakable because of its sharp Q branch, and the frequency may thus be determined. Our observations are so nearly identical with those presented by Cleaves and Plyler,* that it is not necessary to reproduce the curves. The zero branch is plainly indicated at 3360 cm^{-1}. The absorption pattern is not symmetrical with respect to this ordinate, however, but is much more intense on the high frequency side. Its appearance suggests a superposed perpendicular band at about 3410 cm^{-1} due to the unsymmetrical valence oscillation.

The symmetrical deformation oscillation of the NH_2 group, which includes both perpendicular and parallel components, is represented by a band at 1625 cm^{-1}. Our observations show no more detail than those of Cleaves and Plyler, as represented in Fig. 4 of their report.

VIBRATIONS OF THE METHYL RADICAL

The symmetrical and unsymmetrical valence oscillations in CH_3 yield superposed bands in the neighborhood of 3.5μ. A well-defined zero branch appears at 2820 cm^{-1}, with a somewhat similar maximum at 2964 cm^{-1}. These are also observed in Raman scattering as strong sharp lines.[2] Whether or not they are related through resonance with $2\delta_{CH}$ is not clear, but the question of resonance in this case is complicated by the lack of true axial symmetry or complete degeneracy. The center of the strong perpendicular type band appears to be around 2930 cm^{-1}.

The symmetrical and unsymmetrical deformation vibrations produce bands in the neighborhood of 7μ, which we find very poorly resolved. There seems to be a weak zero branch at 1385 cm^{-1}, and a broad complex absorption with its center near 1470 cm^{-1}.

MOLECULAR MOMENTS OF INERTIA

When the molecule is considered as a symmetrical rotator the term values may be written

$$W/hc = G(v) + F(J,K,v),$$

where

$$F(J,K,v) = X_1^v J(J+1) + X_{01}^v K^2 + X_2^v J^2(J+1)^2 + X_{02}^v K^4.$$

The mean of the two larger and nearly equal moments of inertia for the ground state is equal to $h/8\pi^2 c X_1^0$, which may be evaluated by the usual combination relations.

$$\Delta_2 F^0 = R(J+1) - P(J-1) = 2(2J+1)\{(X_1^0 + \tfrac{3}{2}X_2^0) + 2X_2^0(J+\tfrac{1}{2})^2\}.$$

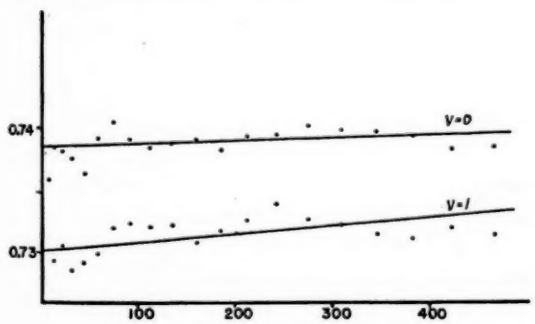

FIG. 3. $\Delta_2 F/2(2J+1)$ *vs.* $(J+\frac{1}{2})^2$.

* Reference 1, Fig. 6.

[2] Kirby-Smith and Bonner, J. Chem. Phys. 7, 880 (1939).

Fig. 3 shows $\Delta_2 F/2(2J+1)$ plotted against $(J+\frac{1}{2})^2$, the upper line corresponding to $v=0$, and the lower one to $v=1$. While the points scatter considerably, due in part to the superposition of one or more weak bands, they approximate straight lines with the constants

$$X_1^0=0.7385 \text{ cm}^{-1} \quad \text{and} \quad X_2^0=12\times10^{-7},$$
$$X_1^1=0.7300 \text{ cm}^{-1} \quad \text{and} \quad X_2^1=36\times10^{-7}.$$

The moment of inertia in the ground state is, therefore, 37.43×10^{-40} g cm^2, and the corresponding C−N distance is 1.48×10^{-8} cm, assuming angles and distances for NH_2 as in ammonia, and for CH_3 as in methane.

The band center is at 1045.27 cm^{-1}. Its position is obtained by extrapolating to $J=0$ the midpoints between successive pairs of lines chosen from the P and R branches. These midpoints are well represented by the equation

$$\tilde{\nu}=\nu_v+(X_1^1-X_1^0)J^2=1045.27-0.0085J^2.$$

The smallest moment of inertia would be obtained at once from the spacing between Q branches in any nondegenerate perpendicular band. If the enhanced lines in the 10μ region constitute such a band, with a mean spacing of about 6.2 cm^{-1}, the value of C is about 7.2×10^{-40} g·cm^2. This can hardly be considered as well established, however.

The examination of methyl amine was suggested to us by Professor J. G. Aston, of Pennsylvania State College, and it is a pleasure to acknowledge our indebtedness to him for a supply of ammonia-free material.

MARCH, 1940 JOURNAL OF CHEMICAL PHYSICS VOLUME 8

Spectral Transmission of Glucose Glass in the Near Infra-Red

WILLI M. COHN
El Cerrito—Berkeley, California

(Received November 13, 1939)

The transmission of samples of glucose glass varying in thermal history was previously investigated. This work covered the visible part of the spectrum. Transmission data in the near infra-red are presented now as far as could be obtained photographically (12,000A). No limit of absorption was found at long wave-lengths as far as tested. The possible use of organic glass for investigations in the near infra-red is discussed.

I. THE METHOD

THIS paper is a continuation of my paper.[1] Two series of glucose glasses have been tested prepared by somewhat different methods, see paper I. The series include samples GG 1, 2; and 3, 5, 6, 8, 9, respectively. (Glasses GG 4 and 7 were now omitted because of increased crystallization.) The samples range from clear to dark brown in color. The Hilger grating spectrograph of paper I was adapted for work in the near infra-red. The first order was used, the overlapping ultraviolet of the second order being eliminated by means of a No. 88 Wratten filter. A neutral wedge equal in length to the length of the slit was inserted in front of the slit as discussed in paper I. The width of the slit varied from 0.1 to 0.3 mm.

[1] Willi M. Cohn, "A Spectral Investigation of Glucose Glass," J. Chem. Phys. **6**, 65–67 (1938). (Cited as "paper I.")

Wedge spectra were obtained on Eastman plates, emulsions K, P, M, and Z using sensitivities I or 144. Plates of series M and Z were hypersensitized by means of ammonia. A reference spectrum of an incandescent lamp operated at a constant voltage, together with spectra of one or two glass samples were taken on a plate. The photometric reduction was carried out as discussed in paper I.

II. THE RESULTS

Transmission values D_λ as a function of the wave-length are presented in Table I. These data include results of both former and present investigations. We further computed the "relative transmission" of the samples by arbitrarily setting the transmission at λ6000 equal to 1.0. This permits an easier comparison of the two groups of samples. Fig. 1 shows the relative transmission as a function of the wave-length.

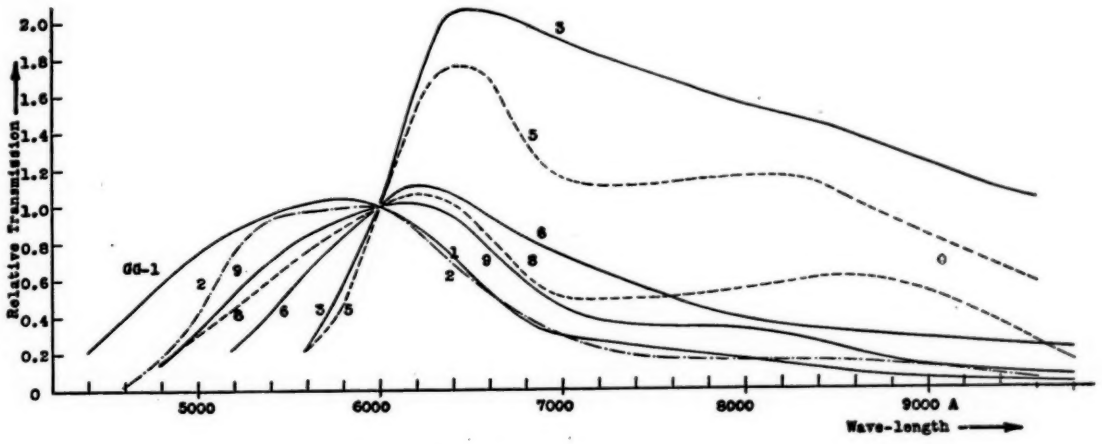

FIG. 1. Relative spectral transmission of glucose glasses varying in thermal history.

The results may be summarized as follows: Glucose glass shows, with increasing caramelization, a general absorption over the entire spectrum; a rather flat maximum of transmission; no narrow bands of absorption; and a shift of the maximum of transmission with an increase in coloring matter. Glasses GG 5 and 8 show secondary maxima of transmission at 8100 and 8600A, respectively. None of the samples reaches the limit of transmission at long wavelengths within the region investigated: Quantitative data could be determined from wedge spectra as far as 9800A, and the visual examination of spectra on plates Z could be carried out as far as 12,000A. (Since wedge spectra on plates Z are of less contrast than the remaining spectra we consider the results of the visual determinations of less weight than the remaining data.)

The comparatively high values of the transmission of glucose glass in the near infra-red seem of interest in connection with investigations in this region of the spectrum, particularly in regard to the ease of preparing containers of various shapes from this material.

TABLE I. *Glucose glass; transmission D_λ in the visible and near infra-red parts of the spectrum; thickness of layer 25.0 mm.*

WAVE-LENGTH IN A	GG-1 %	GG-2 %	GG-8 %	GG-9 %	GG-6 %	GG-3 %	GG-5 %
4400	8.4						
4600	15.2	2.1					
4800	22.9	11.8	9.2	11.6			
5000	29.1	29.3	17.0	26.2			
5200	33.6	53.3	25.4	44.4	10.2		
5400	36.9	66.9	33.6	59.2	19.4		
5600	39.0	69.0	41.8	70.6	29.8	3.0	(3.2)
5800	40.1	70.6	49.6	78.6	37.8	7.6	6.6
6000	38.6	71.3	56.2	84.6	45.8	13.6	14.4
6200	34.6	62.9	60.0	86.4	50.8	22.2	21.8
6400	28.2	48.7	57.2	80.2	49.2	28.0	25.4
6600	(20.4)	(37.1)	(46.6)	(65.4)	(43.2)	(28.0)	(24.4)
6800	14.5	28.2	34.6	49.6	37.2	27.0	19.4
7000	11.0	20.7	27.8	38.4	33.8	25.6	16.6
7200	10.4	15.5	27.6	32.4	29.8	24.4	16.0
7400	9.2	13.0	27.6	30.0	26.2	23.8	15.8
7600	8.3	11.9	28.0	29.4	22.8	22.4	16.0
7800	7.2	11.5	29.2	29.0	19.6	21.8	16.4
8000	6.3	11.3	30.2	27.8	17.2	20.6	16.6
8200	5.7	11.1	32.0	25.4	16.0	20.0	16.6
8400	4.2	10.9	33.8	21.8	14.8	19.6	16.2
8600	3.3	10.7	34.2	17.6	14.0	18.6	14.6
8800	2.7	10.3	33.0	13.6	13.2	17.6	13.2
9000	2.2	9.3	29.4	11.0	12.4	16.4	11.8
9200	2.0	7.8	25.6	9.6	11.8	15.8	10.8
9400	1.7	5.3	20.2	8.0	11.0	14.6	9.6
9600	1.5	2.3	13.6	6.8	10.4	14.2	8.2
9800	(1.3)		8.4	(6.0)	9.4		(7.2)

III. SUMMARY

The presence of small amounts of colloidal carbon formed during caramelization causes characteristic changes in color and spectral transmission of glucose glass. All samples show comparatively high values of transmission in the infra-red as far as tested (12,000A). For a comparison of the color and spectral transmission of glucose glass and inorganic glass prepared with the addition of carbon, see our paper.[2] My thanks to Dr. George S. Parks of Stanford University in connection with these investigations were expressed in my former paper dealing with glucose glass.

[2] Willi M. Cohn, "Color and spectral transmission of some inorganic and organic glasses containing carbon." To be published soon.

Intensities of Electronic Transitions in Molecular Spectra

IX. Calculations on the Long Wave-Length Halogen Spectra*

ROBERT S. MULLIKEN
University of Chicago, Chicago, Illinois
(Received December 8, 1939)

The dipole strength D_{NQ} for the perpendicular-type $N \rightarrow Q$ transitions in the long wave-length spectra of the halogen molecules is computed theoretically according to each of two approximations (LCAO and AO) for the wave functions. The work illustrates the behavior of antisymmetrical wave functions in transition moment calculations, and justifies the ignoring (as an approximation) of closed shells. The overlapping and dipole moment integrals $\int[\phi(np\sigma)][\phi(np\sigma')]dv$ and $\int[\phi(np\sigma)]y[\phi(np\pi_y')]dv$ are evaluated using Slater's approximate atomic orbitals for the ϕ's. The calculated D_{NQ} values for both approximations show the same rapid variation with atomic number as do the observed values, except for iodine, where the anomalous smallness of the observed value may reasonably be attributed to strong case c effects. The LCAO calculated values are consistently much larger than the AO values; the latter agree surprisingly well with the experimental values (cf. Table I). The calculations show D_{NQ} to be very sensitive to variations of the internuclear distance r, and to variation of the effective charge Z^* in the Slater atomic orbitals used. It is pointed out that the former variation may require reconsideration of work in which repulsive potential energy curves are deduced from intensity data on absorption continua. A qualitative discussion is given of the effects on D_{NQ} of various possible improvements of the wave functions used. In connection with this, calculations have been made which show that the energy of the $\sigma_u 1s$ antibonding state of H_2^+ in LCAO approximation is minimized when Z^* for $1s$ is (roughly) 0.84, for normal internuclear distance. This contrasts with $Z^*=1.228$ determined by Finkelstein and Horowitz for the $\sigma_g 1s$ bonding state, and suggests that to improve molecular wave functions Z^* should be increased for bonding but decreased for antibonding molecular orbitals.

I. INTRODUCTION

IN earlier papers,[1,2] the possibility of making significant quantum-mechanical calculations of absolute intensities in molecular spectra has been explored, and its importance for the interpretation of experimental data has been emphasized. The calculations previously reported have been for transitions of the special very intense "$N \rightarrow V$" type. In diatomic molecules, $N \rightarrow V$ transitions are polarized parallel to the axis of the molecule.

Calculations of the intensities of the $N \rightarrow V$ spectra of the halogens and comparisons with observation have already been given in one of the previous papers,[1] except that the calculation of the overlapping integral S has not been detailed. This is included in Section II of the present paper.

The present paper is devoted to calculations on the weak perpendicular-type transitions $N \rightarrow {}^{1,3}Q_1$ of the long wave-length absorption spectra of the halogen molecules. The results of these calculations are compared with observed absolute dipole strengths.[3] These were evaluated in a separate paper.[4]

The calculations are based on certain assumed electron configurations for states N and Q; these have been discussed in previous papers[5] and now seem to be well assured. The electron configuration of any molecular state can be expressed either in terms of AO's (atomic orbitals) or of MO's (molecular orbitals). These correspond to two different approximations to the electronic structure. Calculations are made below corresponding to both.

Before proceeding further, it should be mentioned that there really must be *two* Q complexes, i.e., two ${}^{1,3}Q$ sets of states in the halogen molecules.[5] One comprises ${}^{1,3}\Pi_u$, the other ${}^{1,3}\Pi_g$, states; it is predicted that the latter should be somewhat the higher in energy. According to the

* Reported at the 1938 Chicago meeting of the American Physical Society; Phys. Rev. 55, 239(A) (1939).

[1] R. S. Mulliken, J. Chem. Phys. 7, 14, 20 (1939).

[2] R. S. Mulliken, J. Chem. Phys. 7, 121, and later (1939).

[3] The comparison of observed with calculated *dipole strengths* D (cf. reference 1 for definitions) has advantages over the comparison of observed and calculated f values, which was used in previous papers of this series (references 1, 2). Namely, a complete theoretical calculation can readily be made for each D, whereas for a purely theoretical f, the *frequency* of the transition would have to be calculated in addition. In previous papers (cf. reference 2, footnote 2), this was avoided by using "semi-theoretical f's" combining calculated D's with observed ν's.

[4] R. S. Mulliken, Phys. Rev. (in press).

[5] R. S. Mulliken, Phys. Rev. 46, 549 (1934).

selection rules for homopolar molecules, transitions from the normal state $N\ {}^1\Sigma^+_g$ can occur only to the ${}^{1,3}\Pi_u$ set, which is then to be identified with the observed Q complex. Hence we have ${}^{1,3}Q_u$ (observed), and ${}^{1,3}Q_g$ (predicted). Although only the former is of immediate interest, it is desirable for a systematic understanding to consider both. This is true especially because in the mixed halogens (see X of this series), transitions to *both* Q complexes are allowed, and are apparently observed.[5]

The electron configurations and state-species of states N, Q_u, and Q_g are as follows (inner-shell electrons are omitted):

$$\textit{AO approximation:}\quad \begin{cases} N: (np\sigma\cdot np\sigma')(np\pi)^4(np\pi')^4,\ {}^1\Sigma^+_g \\ {}^{3,1}Q_u,\ {}^{3,1}Q_g \begin{Bmatrix} np\sigma^2\ np\pi^3\ np\sigma'\ np\pi'^4 \\ np\sigma\ np\pi^4\ np\sigma'^2\ np\pi'^3 \end{Bmatrix}, {}^{3,1}\Pi_u,\ {}^{3,1}\Pi_g \end{cases} \tag{1a}$$

$$\textit{MO approximation:}\quad \begin{cases} N: (\sigma_g np)^2(\pi_u np)^4(\pi_g np)^4,\ {}^1\Sigma^+_g \\ {}^{3,1}Q_u: \sigma_g np^2\ \pi_u np^4\ \pi_g np^3\ \sigma_u np,\ {}^{3,1}\Pi_u \\ {}^{3,1}Q_g: \sigma_g np^2\ \pi_u np^3\ \pi_g np^4\ \sigma_u np,\ {}^{3,1}\Pi_g. \end{cases} \tag{1b}$$

In (1*a*) and (1*b*), $n=2$, 3, 4, 5, for F_2, Cl_2, Br_2, I_2. The primed and unprimed symbols refer to the two atoms of the molecule.

For the Q_u and Q_g states jointly, two equivalent electron configurations are given for the AO approximation in (1a). The actual Q_u and Q_g wave functions correspond to "resonance" between these two configurations, that is they are two 50,50 linear combinations of wave functions corresponding to the two configurations. These wave functions are discussed at the beginning of Section III.

If we use AO chemical bond terminology,[6] two three-electron bonds (one σ, one π), equivalent in strength to one (weak) ordinary bond, may be said to exist in the Q_u states (both the ${}^3Q_u$ and the ${}^1Q_u$). The Q_g states may be said to have two three-electron antibonds, equivalent to one weak ordinary antibond. [The term "antibond," not hitherto used, seems suitable.]

In MO chemical bond terminology, the Q_u states (both ${}^3Q$ and ${}^1Q$) as described by (1b) have two σ (strong) and four π (weak) bonding electrons, and one σ (strong) and three π (weak) antibonding electrons, giving a net bonding effect equivalent to one strong σ and one weak π bonding electron, or two half-bonds, one σ (strong) and one π (weak). Similarly in the Q_g states, the net effect is equivalent to two half-antibonds, one σ, one π.

[6] L. Pauling, *The Nature of the Chemical Bond* (Cornell University Press, Ithaca, 1939), Chapter VIII.

II. Calculation of $N\rightarrow{}^{1,3}Q$ Dipole Strengths, MO and LCAO Theory

Referring to Eq. (18) of a related paper,[4] it is seen that the sum of the dipole strengths of $N\rightarrow{}^3Q_1$ and $N\rightarrow{}^1Q$ in the halogen spectra should be equal to the quantity D_{NQ}.[3] This represents the dipole strength which $N\rightarrow{}^1Q_x$ or $N\rightarrow{}^1Q_y$ would have for Λ,S coupling. D_{NQ} is equal to the square of Q_{NQ}, which we wish here to calculate quantum-mechanically. By Eq. (17) of the paper just mentioned,[4]

$$Q_{NQ}=\int[\psi(N)][\textstyle\sum_i x_i][\psi_0({}^1\Pi_x)]dv$$
$$=\int[\psi(N)][\textstyle\sum_i y_i][\psi_0({}^1\Pi_y)]dv, \tag{2}$$

where the summation Σ_i is over all the electrons in the molecule. To evaluate this integral, we proceed as in Sections 4 and 5 of a previous paper.[1] We shall begin with the MO approximation. The discussion will be given in considerable detail, in order to make clear certain points that will arise repeatedly in the calculation of Q integrals.

The antisymmetrical wave function $\psi(N)$ corresponding to the MO electron configuration in (1b) is as follows:[7, 8]

[7] The antisymmetrical wave functions of molecules in terms of MO's are constructed in the same way as are antisymmetrical wave functions of atoms in terms of AO's. See J. C. Slater, Phys. Rev. **34**, 1293 (1929); **38**, 1112–1115 (1931).

[8] The normalization factor $(n!)^{-\frac{1}{2}}$ is strictly correct only if all the MO's used are mutually orthogonal (cf. J. C. Slater, reference 7).

$$\psi(N)=(n!)^{-\frac{1}{2}}\sum_P(-1)^P P\pi^*_{y\alpha}(1)\pi^*_{y\beta}(2)\cdots, \quad (3)$$

where . . . stands for $\pi^*_{x\alpha}(3)\pi^*_{x\beta}(4)\pi_{y\alpha}(5)\pi_{y\beta}(6)\times\pi_{x\alpha}(7)\pi_{x\beta}(8)\sigma_\alpha(9)\sigma_\beta(10)$ and so on down through all the closed shells and the n electrons. The single-electron wave function symbol $\pi^*_{y\alpha}(1)$ is an abbreviation for $\pi_g np_y(1)\alpha(1)$; and so on; π^*_y, π^*_x, π_y, π_x, σ stand here for $\pi_g np_y$, $\pi_g np_x$, $\pi_u np_y$, $\pi_u np_x$, and $\sigma_g np$, respectively, and α and β for the two possible states of the electron spin. P refers to any permutation of electrons among the single-electron wave functions. The quantity $(-1)^P$ is $+1$ for even, -1 for odd permutations. For the degenerate π MO's we are here using real forms π_x and π_y: $\pi_x=f(\rho,z)\cos\phi$, $\pi_y=f(\rho,z)\sin\phi$, with axes x, y perpendicular to the molecule axis, $\rho=(x^2+y^2)^{\frac{1}{2}}$, and $\phi=\tan^{-1}y/x$.

The antisymmetrical MO configuration wave function for $\psi_0(^1Q_y)$ is[8, 9]

$$\psi_0(^1Q_y)=2^{-\frac{1}{2}}(\psi_k+\psi_l),$$

with

$$\psi_k=(n!)^{-\frac{1}{2}}\sum_P\pm P\pi^*_{y\alpha}(1)\sigma^*_\beta(2)\cdots, \quad (4)$$

$$\psi_l=(n!)^{-\frac{1}{2}}\sum_P\pm P\sigma^*_\alpha(1)\pi^*_{y\beta}(2)\cdots,$$

where the dotted parts are the same as in Eq. (3). The symbol σ^* is an abbreviation for $\sigma_u np$. $\psi_0(^1Q_x)$ is just like $\psi_0(^1Q_y)$ except that, in ψ_k and ψ_l, x and y are exchanged in the three π^* factors in the basic permutation. In passing, it may be noted that the $\psi_0(^3Q_1)$ wave functions differ from the $\psi_0(^1Q)$ only in having a negative sign before ψ_l in the first of Eqs. (4).

Putting the results of Eq. (3) and (4) into Eq. (2), and reducing the double Σ_P summations to single ones in the manner given by Slater (reference 7, p. 1115), one finds

$$Q_{NQ}^{(y)}=2^{-\frac{1}{2}}\int[\pi^*_{y\alpha}(1)\pi^*_{y\beta}(2)\cdots]$$

$$\times[y_1+y_2+\cdots+y_n][\sum_P\pm P(\pi^*_{y\alpha}(1)\sigma^*_\beta(2)\cdots$$

$$+\sigma^*_\alpha(1)\pi^*_{y\beta}(2)\cdots)]d\tau. \quad (5)$$

[9] For the very best MO approximation ψ, analogous to the Hartree ψ of an atom (cf. Slater, reference 7), some of the MO's would no longer be quite orthogonal. (*Many* are *always* orthogonal for reasons of symmetry.) However, the corrections then required in the normalization factor and in the value of Q_{NQ} from Eq. (5) would be relatively unimportant, and may properly be neglected here.

If the MO's in Eqs. (5) are all mutually orthogonal, as may be assumed with negligible error,[9] it is found that all but two of the very numerous integrals contained in Eq. (5) vanish. These two are

$$\int[\pi^*_{y\alpha}(1)\pi^*_{y\beta}(2)\cdots]y_2$$

$$\times[\pi^*_{y\alpha}(1)\sigma^*_\beta(2)\cdots]d\tau=\int\pi^*_y y\sigma^* dv,$$

and

$$\int[\pi^*_{y\alpha}(1)\pi^*_{y\beta}(2)\cdots]y_1$$

$$\times[\sigma^*_\alpha(1)\pi^*_{y\beta}(2)\cdots]d\tau=\int\pi^*_y y\sigma^* dv.$$

Hence

$$Q_{NQ}=2^{\frac{1}{2}}\int(\pi_g np_y)y(\sigma_u np)dv$$

$$=2^{\frac{1}{2}}\int(\pi_g np_x)x(\sigma_u np)dv. \quad (6)$$

This result is exactly the same as if from the beginning we had ignored all shells of electrons which *remain closed during the transition.*[10] Eq. (6) is exactly the same as if we were dealing with a two-electron problem corresponding to a transition

$$(\pi_g np_y)^2\rightarrow(\pi_g np_y)(\sigma_u np)$$

or

$$(\pi_g np_x)^2\rightarrow(\pi_g np_x)(\sigma_u np).$$

For if we treat this two-electron problem just as we treated the transition $(\sigma_g 1s)^2\rightarrow(\sigma_g 1s)(\sigma_u 1s)$ of H_2 in a previous paper,[1] writing equations analogous to Eqs. (8) and (9) of that paper, we arrive at the present Eq. (6), which is analogous to Eq. (10) of that paper.

To make as accurate as possible a calculation of Q_{NQ} by Eq. (6), we should use the most accurate possible (Hartree-type) forms for the MO's $\pi_g np$ and $\sigma_u np$ in Eq. (6).[9] If we knew these, Q_{NQ} might turn out to be fairly accurate, but unfortunately we do not know them. For a rough calculation, however, we may use the well-known rough LCAO forms to approximate our MO's.

The normalized LCAO MO's needed, in real

[10] For the present purpose, $\pi_g np_x$ and $\pi_g np_y$ belong in effect to two different shells, of which one *or the other* remains closed during the transition.

form, are:[5,1]

$$\pi_g np_z=(np\pi_z-np\pi_z')/2^{\frac{1}{2}}(1-S_{\pi\pi'})^{\frac{1}{2}},$$
$$\pi_g np_y=(np\pi_y-np\pi_y')/2^{\frac{1}{2}}(1-S_{\pi\pi'})^{\frac{1}{2}}, \quad (7)$$
$$\sigma_u np=(np\sigma-np\sigma')/2^{\frac{1}{2}}(1-S_{\sigma\sigma'})^{\frac{1}{2}},$$

where the overlapping integrals $S_{\pi\pi'}$ and $S_{\sigma\sigma'}$ are

$$S_{\pi\pi'}=\int(np\pi_z)(np\pi'_z)dv,$$
$$S_{\sigma\sigma'}=\int(np\sigma)(np\sigma')dv. \quad (8)$$

The AO's $np\sigma$ and $np\sigma'$ are here to be taken *both to have the same sign in the region where they overlap* in the middle of the molecule.

Introducing the LCAO forms for $\pi_g np$ and $\sigma_u np$ (cf. Eqs. (7)), Eq. (6) reduces to

$$-Q_{NQ}=2^{\frac{1}{2}}(1-S_{\pi\pi'})^{-\frac{1}{2}}(1-S_{\sigma\sigma'})^{-\frac{1}{2}}(Q_{\pi\sigma'}-Q_{\pi\sigma}), \quad (9)$$

where

$$Q_{\pi\sigma'}=\int(np\pi_z)x(np\sigma')dv$$
$$=\int(np\pi_y)y(np\sigma')dv, \quad (10)$$
$$Q_{\pi\sigma}=\int(np\pi_z)x(np\sigma)dv$$
$$=\int(np\pi_y)y(np\sigma)dv=0. \quad (11)$$

Since $Q_{\pi\sigma}=0$, it remains to evaluate $Q_{\pi\sigma'}$. For this purpose, we must introduce analytical forms for the AO's np_x and $np\sigma$. Suitable are the radially nodeless forms given by Zener and Slater.[11] The lack of radial nodes can be seen to be of negligible importance for our calculations. Nevertheless, the use of these simple forms for the AO's introduces an additional element of approximation into our calculations.

If A and B refer to the two atoms, the Slater functions are of the forms

$$np_x=N_{n^*}x_A r_A^{n^*-2}\exp[-hr_A], \quad (12)$$
$$np\sigma'=N_{n^*}z_B r_B^{n^*-2}\exp[-hr_B], \quad (13)$$

where

$$h=Z^*/a_0n^*, \quad (14)$$

with a_0 equal to the Bohr radius of the normal hydrogen atom, and $n^*=2$, 3, 3.7, 4, $Z^*=5.12$, 6.1, 7.6, and 7.6 for the respective atoms F, Cl, Br, and I.[12] The normalizing factors N_{n^*} are readily determined to have the values $(h^5/\pi)^{\frac{1}{2}}$, $(2h^7/15\pi)^{\frac{1}{2}}$, and $(h^9/105\pi)^{\frac{1}{2}}$, for F, Cl, and I, respectively; the calculation for Br has not been made here. In Eqs. (12), (13), x_A and r_A refer to the x or r coordinate measured from the center of the A atom, with similar meanings for z_B and r_B.

Taking the origin of coordinates at the center of the molecule, with the z axis directed from B to A, and letting r be the distance between the nuclei, we have $z_B=z+r/2$, $x_A=x$, and so on. Introducing these relations into Eqs. (12), (13), and the latter into Eq. (11), we have

$$Q_{\pi\sigma'}=\int N_{n^*}{}^2x^2(z+\tfrac{1}{2}r)(r_Ar_B)^{n^*-2}$$
$$\times\exp[-h(r_A+r_B)dv]. \quad (15)$$

The integrations can be effected without obstacle after transformation to confocal elliptic coordinates ξ, η, ϕ, where $\xi=(r_A+r_B)/r$, $\eta=(r_A-r_B)/r$. The results for F_2, Cl_2, and I_2 (Br_2 has not been done) are as follows:

$$F_2: \quad Q_{\pi\sigma'}=\tfrac{1}{2}re^{-\gamma}(1+\gamma+0.4\gamma^2+\gamma^3/15), \quad (16)$$

where

$$\gamma=rh; \quad (17)$$

$$Cl_2: \quad Q_{\pi\sigma'}=\tfrac{1}{2}re^{-\gamma}(1+\gamma+34\gamma^2/75+3\gamma^3/25$$
$$+31\gamma^4/1575+\gamma^5/525); \quad (18)$$

$$I_2: \quad Q_{\pi\sigma'}=\tfrac{1}{2}re^{-\gamma}(1+\gamma+33\gamma^2/70$$
$$+29\gamma^3/210+41\gamma^4/1470+\gamma^5/245$$
$$+29\gamma^6/49\times1350+\gamma^7/49\times675). \quad (19)$$

For the respective molecules F_2, Cl_2, I_2, one finds

$$\gamma=2.56r/a_0, \quad 2.03r/a_0, \quad \text{and} \quad 1.9r/a_0.$$

In order to complete the evaluation of Q_{NQ} using Eq. (12), we need the quantities $S_{\sigma\sigma'}$ and $S_{\pi\pi'}$. One could of course neglect these without gross error, but they can be evaluated fairly easily, and will be needed later. Substituting Eqs. (12), (13) into Eqs. (8), transforming to

[11] J. C. Slater, Phys. Rev. **36**, 57 (1930).

[12] The values of the parameters are those given by Slater, except for fluorine, where Zener's $Z^*=5.12$ (Phys. Rev. **36**, 51 (1930)) has been used instead of Slater's $Z^*=5.2$.

elliptic coordinates, and integrating, the results are as follows:[13]

$$\begin{aligned} \mathrm{F}_2\colon\ S_{\sigma\sigma'}&=e^{-\gamma}(\gamma^4/15+2\gamma^3/15-\gamma^2/5-\gamma-1),\\ S_{\pi\pi'}&=e^{-\gamma}(1+\gamma+0.4\gamma^2+\gamma^3/15). \end{aligned} \tag{20}$$

It is of interest that the expression for $S_{\pi\pi'}$ in Eqs. (20) is exactly the same as that for $Q_{\pi\sigma'}$ in Eq. (16) except for the omission of a factor $\frac{1}{2}r$ which in the latter betokens its dipole-moment character. The same relation between $S_{\pi\pi'}$ and $Q_{\pi\sigma'}$ holds in general,[14] so we need not give the $S_{\pi\pi'}$ equations explicitly for Cl_2 and I_2.

$$\begin{aligned} \mathrm{Cl}_2\colon\ S_{\sigma\sigma'}=e^{-\gamma}&(\gamma^6/525+13\gamma^5/1575\\ &+34\gamma^4/1575-2\gamma^3/75\\ &-9\gamma^2/25-\gamma-1). \end{aligned} \tag{21}$$

$$\begin{aligned} \mathrm{I}_2\colon\ S_{\sigma\sigma'}=e^{-\gamma}&(\gamma^8/33075+23\gamma^7/66150\\ &+67\gamma^6/66150+\gamma^5/294\\ &-\gamma^4/735-17\gamma^3/210\\ &-29\gamma^2/70-\gamma-1). \end{aligned} \tag{22}$$

III. Calculation of $N\rightarrow{}^{1,3}Q$ Dipole Strengths: AO Theory

Before calculating numerical values of Q_{NQ} and D_{NQ}, let us evaluate Q_{NQ} in terms of the AO approximation. The antisymmetrical AO wave functions for states N and pure ^1Q are as follows:[15]

$$\psi(N)=A(n!)^{-\frac{1}{2}}(\psi_{\mathrm{I}}+\psi_{\mathrm{II}}), \tag{23}$$

$$\psi_0(^1Q_y)=B(n!)^{-\frac{1}{2}}(\psi_{\mathrm{III}}+\psi_{\mathrm{IV}}+\psi_{\mathrm{V}}+\psi_{\mathrm{VI}}), \tag{24}$$

where A and B are normalization factors, and

$$\begin{aligned} \psi_{\mathrm{I}}&=N_{\mathrm{I}}\sum_P(-1)^P P\sigma_\alpha(1)\sigma_\beta'(2)\pi_{y\alpha}(3)\pi_{y\beta}(4)\\ &\qquad\times\pi_{y\alpha}'(5)\pi_{y\beta}'(6)\cdots,\\ \psi_{\mathrm{II}}&=N_{\mathrm{II}}\sum_P\pm P\sigma_\alpha'(1)\sigma_\beta(2)\pi_{y\alpha}(3)\\ &\qquad\times\pi_{y\beta}(4)\pi_{y\alpha}'(5)\pi_{y\beta}'(6)\cdots. \end{aligned} \tag{25}$$

$$\begin{aligned} \psi_{\mathrm{III}}&=N_{\mathrm{III}}\sum_P\pm P\sigma_\alpha'(1)\sigma_\beta'(2)\sigma_\alpha(3)\pi_{y\beta}'(4)\\ &\qquad\times\pi_{y\alpha}(5)\pi_{y\beta}(6)\cdots,\\ \psi_{\mathrm{IV}}&=N_{\mathrm{IV}}\sum_P\pm P\sigma_\alpha(1)\sigma_\beta(2)\sigma_\alpha'(3)\pi_{y\beta}(4)\\ &\qquad\times\pi_{y\alpha}'(5)\pi_{y\beta}'(6)\cdots,\\ \psi_{\mathrm{V}}&=N_{\mathrm{V}}\sum_P\pm P\sigma_\alpha'(1)\sigma_\beta'(2)\pi_{y\alpha}'(3)\sigma_\beta(4)\\ &\qquad\times\pi_{y\alpha}(5)\pi_{y\beta}(6)\cdots,\\ \psi_{\mathrm{VI}}&=N_{\mathrm{VI}}\sum_P\pm P\sigma_\alpha(1)\sigma_\beta(2)\pi_{y\alpha}(3)\sigma_\beta'(4)\\ &\qquad\times\pi_{y\alpha}'(5)\pi_{y\beta}(6)\cdots. \end{aligned} \tag{26}$$

The . . . stands for $\pi_{x\alpha}(7)\pi_{x\beta}(8)\pi_{x\alpha}'(9)\pi_{x\beta}'(10)$ and so on with suitable additional single-electron functions occupied by inner-shell electrons $11\cdots n$. The symbols σ, π_y, π_x stand here for $np\sigma$, $np\pi_y$, and $np\pi_x$ of atom A, σ', π_y', π_x' for the same AO's of atom B. The AO's $np\sigma$ and $np\sigma'$ are to be taken with the *same sign* in the region where they overlap strongly. $\psi_0(^1Q_x)$ is like $\psi_0(^1Q_y)$ except that x's and y's replace each other throughout.

The wave function given by Eq. (24) is one of four possible independent linear combinations of the four ψ's of Eqs. (26). The four independent combinations, differing only in choice of signs (and slightly in the value of B) in Eq. (24), may be described and identified as follows. The sign combinations $++++$, $++--$, $+-+-$, $+--+$ correspond to the y component of the respective states ^1Q_u, $^3Q_{1u}$, ^1Q_g, $^3Q_{1g}$ (cf. Section I and Eqs. (1) in regard to the Q_g states).

Introducing $\psi(N)$ and $\psi_0(^1Q)$ from Eqs. (23)–(26) into Eq. (2), and reducing the double Σ_P's to single Σ_P's (thereby at the same time removing the $(n!)^{-\frac{1}{2}}$ factors) in the manner given by Slater,[16] we obtain

$$\begin{aligned} Q_{NQ}=AB(&J_{\mathrm{I,III}}+J_{\mathrm{I,IV}}+J_{\mathrm{I,V}}+J_{\mathrm{I,VI}}\\ &+J_{\mathrm{II,III}}+J_{\mathrm{II,IV}}+J_{\mathrm{II,V}}+J_{\mathrm{II,VI}}), \end{aligned} \tag{27}$$

where, for example,

$$\begin{aligned} J_{\mathrm{I,III}}=N_{\mathrm{I}}N_{\mathrm{III}}\int&[\sigma_\alpha(1)\sigma_\beta'(2)\pi_{y\alpha}(3)\pi_{y\beta}(4)\\ &\times\pi_{y\alpha}'(5)\pi_{y\beta}'(6)\cdots][y_1+y_2+\cdots+y_n]\\ &[\textstyle\sum_P\pm P\sigma_\alpha'(1)\sigma_\beta'(2)\sigma_\alpha(3)\pi_{y\beta}'(4)\pi_{y\alpha}(5)\\ &\times\pi_{y\beta}(6)\cdots]d\tau. \end{aligned} \tag{28}$$

[13] For $2p$ AO's, $S_{\sigma\sigma'}$ and $S_{\pi\pi'}$ are given (under the respective designations $S_{00}^{\frac{1}{2}}$ and $S_{11}^{\frac{1}{2}}$) by J. H. Bartlett, Jr., Phys. Rev. **37**, 512 and 522 (Table IX), 1931.

[14] This can be seen as follows: in Eq. (12), the part of the integral which comes from the z in the factor $(z+\frac{1}{2}r)$ of the integrand vanishes. The remainder of the integral, except for the factor $\frac{1}{2}r$, is exactly $S_{\pi\pi'}$.

[15] The method is that of J. C. Slater, Phys. Rev. **38**, 1109 (1931).

[16] Reference 7, p. 1115.

To obtain Q_{NQ}, we have to evaluate the eight J integrals, also A and B. Roughly, $A=2^{-\frac{1}{2}}$ and $B=\frac{1}{2}$, and $N_{\rm I}=\cdots N_{\rm VI}=1$. These relations would be exact if $\psi_{\rm I}$ and $\psi_{\rm II}$ in Eq. (23) were orthogonal, likewise $\psi_{\rm III}\cdots\psi_{\rm VI}$ in Eq. (24), and the various AO's in Eqs. (25) and (26). The lack of orthogonality arises mainly[17] from the fact that AO's of two different atoms occur in each ψ of Eqs. (23)–(26), and any two such AO's, if alike in λ and (if $\lambda>0$) in x or y character, depart more or less from orthogonality.

Now it can be shown that, if we neglect unimportant factors, each of the J's can be reduced to a four-electron integral,[18] for example

$$J_{\rm I,\,III}=\nu_{\rm I}\nu_{\rm III}\int[\sigma_\alpha(1)\sigma_\beta'(2)\pi_{y\alpha}'(3)\pi_{y\beta}'(4)]\times[y_1+y_2+y_3+y_4][\sum_P\pm P\sigma_\alpha'(1)\sigma_\beta'(2)\times\sigma_\alpha(3)\pi_{y\beta}'(4)]d\tau. \quad (29)$$

[17] If the best Hartree AO's are used, AO's even of the *same* atom[7] may not be orthogonal if alike in l, λ, and x or y type; but for our purposes we can safely neglect this additional possibility.

[18] The proof is as follows. Consider for example $J_{\rm I,\,III}$ of Eq. (28). In the first place, all terms coming from $y_7\cdots y_n$ are easily seen to vanish. Next, let us write $\pi_{y\alpha}'(3)\pi_{y\beta}'(4)\pi_{y\alpha}(5)\pi_{y\beta}(6)$ instead of $\pi_{y\alpha}(3)\pi_{y\beta}(4)\times\pi_{y\alpha}'(5)\pi_{y\beta}'(6)$ in the first part of $J_{\rm I,\,III}$. This does not alter the latter's value, as can be seen by going back to $\psi_{\rm I}$ in Eqs. (25) and first making the change there. We see that the terms from y_5+y_6 now vanish, leaving only those from y_1 to y_4. Now consider the contributions to J of all permutations P of wave functions among electrons $5\cdots n$. It is found that the total effect of these is to introduce a factor which is a product $\Pi_{k,\,l}(1-S_{kl}^2)$ of all possible quantities $(1-S_{kl}^2)$, where $S_{kl}=\int\phi_k\phi_l d\nu$, that can be formed from pairs of wave functions k,l selected from among those occupied by electrons $5\cdots n$ in the basic or identity permutation. Note also that electrons $5\cdots n$ are assigned to *the same set of closed shells* in the part of the integrand preceding as in that following the symbol P in Eq. (28).

Now if we similarly consider the quantities $N_{\rm I}$ and $N_{\rm III}$, each of them is found to contain a factor $[1/\Pi_{k,\,l}(1-S_{kl}^2)]^{\frac{1}{2}}$. In the calculation of J, these factors just cancel the above factor $\Pi(1-S_{kl}^2)$. This suggests that we would obtain correct results by simply omitting all but four electrons and a set of four one-electron wave functions from the ψ's of Eqs. (25)–(26). The wave functions to be dropped are those occupied by electrons $7\cdots n$ in Eqs. (25)–(26), together with *two* out of those occupied by electrons 1 to 6; the choice of these two varies, however, from one J to another.

The foregoing proof that J can be reduced to a four-electron integral chosen as above described is exact and rigorous except for one thing. Among the permutations in Eq. (28), we have not yet considered those which exchange the arguments of electrons 1 to 4 with those of $5\cdots n$. These have the effect of introducing a further factor $\Pi_{h,\,l}(1-S_{h,l}^2)$, where h corresponds to arguments of electrons in the group $1\cdots4$, l to arguments of electrons in the group $5\cdots n$. They also introduce some additive contributions to J which are not expressible simply by a multiplying factor. It appears that these effects are largely but not exactly canceled out by similar effects in the N product. The conclusion then is that the four-electron J expression is a good approximation to the n-electron expression, but is not quite exact. (It appears that in *special cases* the error might be serious.)

From each n-electron integral $J_{R,\,S}$ all those $n-4$ one-electron wave functions whose electrons *belong to the same closed shells*[19] *both in* ψ_R *and in* ψ_S are eliminated in forming the four-electron integral.[18] In obtaining Eq. (29), for example, the basic permutation in $\psi_{\rm I}$ is first altered by exchanging one-electron functions between electrons 3, 4 and 5, 6 (this does not alter the value of $\psi_{\rm I}$), whereupon it is seen that all the electrons $5\cdots n$ are now in identical closed shells in $\psi_{\rm I}$ and $\psi_{\rm III}$, while the electrons 1 to 4 are *not* in like closed shells in $\psi_{\rm I}$ and $\psi_{\rm III}$. To a sufficient approximation,[18] $\nu_{\rm I}=\nu_{\rm III}=1$ in Eq. (29); the ν's have the same relation to 4-electron ψ's as do the N's to the n-electron ψ's of Eqs. (25), (26).

The four-electron J's are now easily reduced to expressions in terms of one-electron integrals. Each J yields two nonvanishing contributions. When all these are put into Eq. (27), the result is

$$Q_{NQ}=4AB[2S_{\sigma\sigma'}Q_{\pi\sigma'}-(1+S^2_{\sigma\sigma'})Q_{\pi\sigma}], \quad (30)$$

where $Q_{\pi\sigma'}$ and $Q_{\pi\sigma}$ are as in Eqs. (10), (11). One finds

$$1/A^2=2(1+S^2_{\sigma\sigma'})(1+\cdots);\qquad 1/B^2=4(1-S^2_{\sigma\sigma'})+\cdots, \quad (31)$$

from which, to a close approximation,

$$Q_{NQ}=2^{\frac{1}{2}}(1-S^4_{\sigma\sigma'})^{-\frac{1}{2}}\times(2S_{\sigma\sigma'}Q_{\pi\sigma'}-(1+S^2_{\sigma\sigma'})Q_{\pi\sigma}]. \quad (32)$$

As was noted above (cf. Eq. (10)), $Q_{\pi\sigma}=0$ if ordinary np AO's are used.

IV. Calculation of $N\rightarrow{}^{1,3}Q$ Dipole Strengths; Comparison with Experiment

Using Eqs. (9), (32) together with Eqs. (10), (14), (16)–(22), we can now compute the quantities Q_{NQ} and D_{NQ} theoretically for the transitions $N\rightarrow{}^{1,3}Q$ in F_2, Cl_2, and I_2, for both the LCAO MO and the AO approximations. The values so computed for F_2, Cl_2, and I_2 for their respective equilibrium internuclear separations, also interpolated values for Br_2, are given in

[19] For this purpose, a closed shell consists of *two* electrons with opposite spins occupying the *same AO*, e.g., $np\pi_y$.

Table I, together with corresponding experimental values taken from the analysis in another paper.[4] In the case of F_2, Q_{NQ} and D_{NQ} have been computed for three different values of r.

Everything considered, the correspondence between observed and calculated quantities is extremely gratifying, if for the moment we omit iodine from consideration. In the other halogens, the AO calculated values are rather close to the observed. Notably, the AO calculated D values parallel very closely the twenty-fold increase in the observed D values from F_2 to Br_2. The LCAO calculated values agree less well than the AO both in being several times too large, and in showing too great a ratio of intensity between F_2 and Br_2; however, the progressive increase from F_2 to Br_2 is qualitatively correct.

In calculations on $N \rightarrow V$ transitions, the scanty experimental intensity values seemed to fall about midway between LCAO and AO calculated values.[2] The present data and evidence on $N \rightarrow Q$ transitions, and further similar evidence to be presented in X of this series, tend to indicate that the AO approximation is the better.[20] This indication cannot be taken as proof, however, because of the additional approximations involved in the use of Slater AO's for $N \rightarrow Q$ transitions, and not involved for $N \rightarrow V$ transitions, where the forms of the AO's drop out.[2]

The observed agreements for the $N \rightarrow Q$ halogen spectra give confirmation to the existing interpretation of the observed bands and continua in terms of electron configurations and electronic states (cf. Eqs. (1)).

It remains to explain why the observed D_{NQ} for iodine is so out of line with those for the other halogens, and with the calculated values. In this connection, it is probably significant that the D_{NQ} values for HI and CH_3I (to be discussed in X of this series) are likewise abnormally small compared with those of the other hydrogen and methyl halides.

Empirically, there is a striking correlation in iodine of abnormally high intensity of $N \rightarrow Q_0$, attributable only to strong case c effects, with the abnormally low intensity of $N \rightarrow {}^{3,1}Q_1$. There are also indications of a similar correlation in CH_3I (see X of this series). It seems fairly safe, then, to attribute the low Q_{NQ} of iodine to some kind of case c disturbance. It might for instance be that one or both of the N and Q wave functions become so much admixed with others that considerable added contributions appear in the expressions for Q_{NQ} in Eqs. (9) and (32), and happen to be opposite in sign to $Q_{\pi\sigma'}$, thus partly canceling the latter.

[20] In this connection, the writer would like to emphasize again that the LCAO approximation, used here, represents only a crude approach to the best MO approximation.

V. Conclusions. Discussion of Approximations

The calculations for F_2 in Table I illustrate that D_{NQ} may vary very rapidly with the internuclear distance r. It would be of interest to make similar calculations for the other halogens.* If the result for F_2 is at all typical, existing determinations of upper potential energy curves from intensity distributions in continuous $N \rightarrow Q$ spectra (halogens, hydrogen and alkyl halides) should undergo reconsideration. Rapid variation of D_{NQ} with r would considerably alter ν_{max} and the intensity distribution for a continuum corresponding to a given upper and lower potential energy curve.[21]

Referring to Eqs. (9) or (32) and (16), it will be seen that the variation of D with r comes in mainly through the parameter $\gamma = rZ^*/n^*a_0$. Hence D_{NQ} should be about equally as sensitive to change in the assumed value of Z^*/n^* as to variation of r. Thus for F_2, an increase of 20 percent in Z^* would cause the computed D_{NQ} in Table I to be decreased to about one-tenth its value according to the AO, or to about one-fourth its value according to the LCAO method. It is therefore of interest to consider whether our Z^* values were well chosen.

For the computations reported in Table I, the Z^* values suggested by Slater for free atoms were used. It is, however, known that when the variation method is used to minimize the energy of molecular wave functions, treating Z^* as a parameter, the optimum value of the latter may be considerably different than for free atoms.

* *Note added in proof.*—Calculations being made by Dr. A. Sayvetz, show similar rapid variation for all the halogens.

[21] H. M. James and A. S. Coolidge, Phys. Rev. **55**, 184 (1939) have also found a considerable variation of D with r in the case of the transition $\sigma_g 1s\, 2s\sigma_g, {}^3\Sigma_g^+ \rightarrow \sigma_g 1s\, \sigma_u 1s, {}^3\Sigma_u^+$ of the hydrogen molecule. Their calculations were made with accurate wave functions.

The method has been applied principally to the normal states of H_2^+ and of H_2, where (both in AO and in LCAO approximations), values near 1.2 are found for Z^*, as compared with 1.00 for the free atoms.[22]

In the normal states of H_2^+ and H_2, orbitals or interactions are purely bonding. In the halogen N and Q states, antibonding as well as bonding interactions are present. It therefore seemed desirable to investigate minimization of the energy by varying Z^* for an antibonding state.

The simplest example of the latter is the $\sigma_u 1s$ antibonding MO of H_2^+, given in LCAO approximation by

$$\sigma_u 1s \approx (\phi_{1s} - \phi_{1s}')/(1 - S_{1s,\,1s'}).$$

On minimizing the energy for $r = 2a_0$ (near r_e of normal H_2^+), the best Z^* was found to be roughly 0.84. This may be contrasted with the optimum Z^* value 1.228 found by Finkelstein and Horowitz for the $\sigma_g 1s$ bonding MO of H_2^+. The comparison indicates that the optimum Z^* is increased for bonding but decreased for antibonding states.[22a]

In the $N \rightarrow Q$ halogen spectra in MO approximation, an electron jumps from one antibonding MO ($\pi_g np$) to another ($\sigma_u np$). Using, in the LCAO forms, Z^* values less than for the free atoms would increase the computed D_{NQ} values, thus making their agreement with experiment worse than before;[22a] quite possibly not *much* worse, however, since it appears probable that the Z^* changes may be relatively much smaller than in the case of H_2^+.

Turning now to the AO approximation (cf. Eqs. (1), (23)–(32)), a qualitative examination shows that a nearly nonbonding π AO of state N and a bonded σ AO of state Q are involved in the integrals $S_{\sigma\sigma'}$ and $Q_{\pi\sigma'}$ which appear in the expression for Q_{NQ}. Presumably, then, the optimum Z^* is about equal for π to the Slater value, but larger for σ. The calculated D_{NQ} is then somewhat decreased. Thus the effects on D_{NQ} of optimizing Z^* are apparently opposite for the LCAO and AO approximations, giving improved agreement with experiment only in the latter case.[22a]

A fault of the Slater AO's, not removed by

[22] Cf., e.g., L. Pauling and E. Bright Wilson, Jr., *Introduction to Quantum Mechanics* (McGraw-Hill, New York, 1935), pp. 331, 349.

[22a] Analogy to H_2 and H_2^+, assumed here, may of course possibly not be a reliable guide for estimating in the case of halogen molecules whether the optimum Z^* is greater or less than for free atoms. Also, the absence of radial nodes in the Slater functions may conceivably affect our arguments (except for fluorine).

TABLE I. *Calculated and observed dipole strengths for $N \rightarrow Q$ in the halogens.*

MOLECULE	PARAMETERS[2]		INTEGRALS[3]			DIPOLE STRENGTH[4]					
						LCAO CALC.[5]		AO CALC.[6]		OBS.[7]	
$r_e(A)$[1]	$\frac{1}{2}r(A)$	γ	$S_{\sigma\sigma'}$	$S_{\pi\pi'}$	$Q_{\pi\sigma'}(A)$	$Q_{NQ}(A)$	$D_{NQ}(A^2)$	Q_{NQ}	D_{NQ}	Q_{NQ}	D_{NQ}
F_2	0.64	6.21	0.235	0.077	0.0494	0.083	0.0069	0.033	0.0011		
1.45±.05	0.70	6.8	0.187	0.053	0.037	0.060	0.0036	0.020	0.00040	0.018	0.00034
	0.75	7.28	0.151	0.038	0.0285	0.045	0.0020	0.012	0.00014		
Cl_2 1.983	0.99	7.64	0.302	0.100	0.0985	0.178	0.0317	0.084	0.0071	0.053	0.0028
Br_2 2.284	1.14	8.88				[0.204]	[0.0416]	[0.110]	[0.0121]	0.077 or 0.084	0.0060 or 0.0070
I_2 2.667	1.33	9.57	0.392	0.091	0.121	0.230	0.0529	0.136	0.0185	(0.025)	(0.0006)

[1] The equilibrium internuclear distances r_e are from band spectrum data except for F_2, where the value given was obtained by L. O. Brockway, J. Am. Chem. Soc. **60**, 1348 (1938), and is rather uncertain. [2] The parameters are: r is the internuclear distance, and $\gamma = rZ^*/n^*a_0$, with $Z^* = 5.12$, 6.1, 7.6, and 7.6, $n^* = 2$, 3, 3.7, 4 for F, Cl, Br, and I, respectively. [3] Cf. Eqs. (16)–(22). [4] The dipole strength D_{NQ} is the square of Q_{NQ}; the latter, given by Eq. (2) of the text, is conveniently measured in angstrom units (A). Q_{NQ} has not been calculated for Br_2; the "calculated" values given in brackets for Q_{NQ} have been interpolated between those calculated for Cl_2 and for I_2, and the bracketed D_{NQ} values are the squares of these. [5] Cf. Eqs. (9), (10) of the text. [6] Cf. Eqs. (32), (10) of text. [7] The observed D_{NQ} values are obtained by adding the D values for $N \rightarrow {}^3Q_1$ and $N \rightarrow {}^1Q$ given in the last column of Table I of reference 4 (cf. text above, preceding Eq. (2)). For Br_2, the two values given here correspond to the alternative interpretations I and II of reference 4. For I_2, the value is an average of those corresponding to interpretations I and II of reference 4, but is in any case based on very rough data, and may be in error by a factor as large as 3 or 5.

optimizing Z^*, is that they correspond to an inverse square field. The best AO's would correspond to a Z^* decreasing from inside out, to an asymptotic value 1 at large r. Qualitative consideration indicates that such best AO's of two atoms would overlap more, and thus increase D_{NQ}, as compared with those based on constant Z^*. Hence it appears that this kind of improvement in the wave functions would make the calculated D_{NQ}'s agree less well than before with experiment, for both AO and LCAO approximations.[22a]

On the basis of the foregoing discussion, it appears not very useful to try to improve the wave functions by improving the forms of the AO's used in the AO or LCAO approximation. Fortuitously, perhaps, the simple unimproved Slater AO's give relatively good results. It may seem anomalous that improved wave functions can give worse calculated D_{NQ} values,[22a] but this is entirely possible so long as the wave functions used are still at best only rough approximations. Apparently it happens that *those parts* of the wave functions which are of predominant importance for D_{NQ} are more nearly correct using the original Slater AO's than when each wave function *as a whole* is improved[22a] by varying Z^*. It should be borne in mind, however, that the observed D_{NQ} values, since they are rather small, and thus relatively sensitive to perturbing effects, should be used with some caution as a test of the goodness of various approximations.

For the sake of completeness, we may consider the improvement of the Slater AO's in molecular wave functions by "polarization." In the MO approximation, we may reasonably expect this to give better calculated D_{NQ} values, since in the case of MO's "polarization" means essentially getting away from the limitations of the very simple LCAO approximation, in the direction of using "true" or "best" MO's.[23] Taking as an example the $\sigma_u np$ and $\pi_g np$ MO's of a halogen molecule, we may write expansions in pairs of AO's as follows, writing the presumably most important terms first:

$$\sigma_u np = \alpha(np\sigma - np\sigma') + \beta(nd\sigma - nd\sigma') + \gamma(ns\sigma - ns\sigma') + \cdots, \quad (33)$$

$$\pi_g np_x = a(np\pi_x - np\pi_x') + b(nd\pi_x - nd\pi_x') + \cdots.$$

The first pair of terms in each of Eqs. (33) gives the LCAO approximation, further pairs may be thought of as corresponding to the use of *polarized* AO's, thus:

$$\begin{aligned} \sigma_u np &= \delta(np\sigma_{\text{pol}} - np\sigma'_{\text{pol}}), \\ \pi_g np &= \epsilon(np\pi_{\text{pol}} - np\pi'_{\text{pol}}), \end{aligned} \quad (34)$$

where

$$(np\sigma_{\text{pol}}) = k(np\sigma) + l(nd\sigma) + \cdots \quad (35)$$

is an example of a polarized AO.

In Eq. (33), α, β, γ and so on can be treated as parameters in a variation problem. To minimize the energy of an antibonding $\sigma_u np$ MO expressed in the form (33) or (34)–(35), overlapping of the two AO's $np\sigma_{\text{pol}}$ and $np\sigma'_{\text{pol}}$ in Eqs. (34) should be diminished. From the forms of $np\sigma$ and $nd\sigma$ one readily sees that for this purpose β/α in (33), or l/k in (35), should have *negative sign*. Numerical values, and further coefficients, might be obtained by calculations. If we substitute polarized AO's obtained in this manner for the ordinary AO's in Eqs. (9)–(11), the latter expressions for Q_{NQ} are converted from rough LCAO-approximation-MO equations to best-MO equations.

In Eq. (11), the integral $Q_{\pi\sigma}$, hitherto vanishing, now assumes importance. Considering just the effect of $nd\sigma$, which except in F_2 is probably the principal polarizing term in Eq. (35), we now have

$$Q_{\pi\sigma} = \int (np\pi_y)(y)l(nd\sigma)dv,$$

with l negative (see above). Since

$$\int (np\pi_y)y(nd\sigma)dv$$

is *large* and *negative*, it is seen that $Q_{\pi\sigma}$ assumes a considerable positive value. At the same time, $Q_{\pi\sigma'}$ of Eq. (10) is somewhat diminished because of the diminished overlapping of the polarized AO's now involved. Thus without much doubt

[23] Compare the work of H. M. James and A. S. Coolidge, J. Chem. Phys. **1**, 825 (1933); **3**, 129 (1935). Here, to be sure, an expansion in terms of elliptical coordinates is used (also containing extra terms in r_{12} and $\eta_1\eta_2$ carrying the wave functions even beyond the best MO approximation), but the principle is the same as for an expansion in pairs of AO's.

polarization causes $Q_{\pi\sigma}$ partly to cancel[24] $Q_{\pi\sigma'}$ and so to reduce the calculated MO approximation D_{NQ}, making it agree better with the observed value.[25] This improvement most probably much outweighs the contrary effects[22a] obtained by optimizing Z^*.

The effect on D_{NQ} of using polarized AO's is quite different in the AO than in the MO approximation. Referring to an earlier paragraph on the variation of Z^* in the AO approximation, similar remarks now apply for improvement of the AO's by polarization. The only AO's for which improvement is important are the $np\sigma$ AO's in state Q. These are occupied by electrons which are somewhat bonding, so to minimize the energy the polarization should be such as to give *increased overlapping*. This would be obtained by using Eq. (35) with l/k positive, instead of negative as for best polarization of the LCAO MO's.

The effects of such polarization on Q_{NQ} can be seen from Eq. (32). $S_{\sigma\sigma'}$ and $Q_{\pi\sigma'}$ are increased, while $Q_{\pi\sigma}$ takes on a negative value, so that D_{NQ} is increased. Agreement with experiment is made worse, opposing[22a] the effect obtained by optimizing Z^*.

[24] *Presumably* $Q_{\pi\sigma}$ does not become so large as to *more than* cancel $Q_{\pi\sigma'}$, but this cannot be shown by the present qualitative arguments.

[25] This applies to the heavier halogens. For F_2 the result is not qualitatively obvious, but presumably still holds, since the best-MO approximation pretty surely should give better D_{NQ} values than the LCAO approximation.

MARCH, 1940 JOURNAL OF CHEMICAL PHYSICS VOLUME 8

The Hydrogen Isotope Exchange Reaction

J. O. HALFORD
Department of Chemistry, University of Michigan, Ann Arbor, Michigan

(Received August 25, 1939)

The possibility of deriving the equilibrium constants for the higher deuterium substitutions from the isotope exchange coefficient is examined with the aid of calculations on the ammonia and methane reactions with water. If the experiment is carried to solutions at equilibrium with water containing as much as 25 percent D_2O and the error in a single measurement does not exceed 1.0 percent the second constant is determined to within 10 percent of the correct value. As a standard of comparison against which the experimental results may be examined to advantage, an equation is developed showing the relation between the equilibrium constant for the first substitution and the exchange factor at higher deuterium fractions, subject to the assumption that each successive substitution of D for H produces the same frequency shift. The evaluation of frequency shifts from exchange data is considered.

THE study of hydrogen isotope exchange equilibria has been restricted almost exclusively to systems of low deuterium fraction in which only a negligible proportion of the molecules can acquire more than one deuterium atom. For exchange reactions involving water this restriction limits the interpretation to the first of the n reactions

$$AH_n + p\text{DOH} = AH_{n-p}D_p + p\text{HOH}. \quad (1)$$

In principle the measurement and interpretation need not be so limited. It is possible to perform exchange experiments over a wide range of isotope fractions involving systems in which the higher deuterium substitution products are present at considerable concentrations. From such experiments, if they were sufficiently accurate, all the equilibrium constants of the reactions expressed by Eq. (1) could be derived. The success of an actual interpretation, however, is limited by the accuracy of the individual distribution measurement and by the fact that the relative scarcity of deuterium makes it impractical to obtain data over the entire range of isotope compositions.

In the following paragraphs it is shown by calculations with the ammonia and methane reactions that the constant for the second substitution can be obtained with a fair degree of accuracy even with a liberal allowance for experi-

mental error and that the satisfactory determination of the higher constants would involve a greater precision than is normally achieved. The equilibrium constants are derived from the distribution by trial. The extrapolation to zero deuterium fraction for K_1 and the selection of first approximations to K_2 and K_3 are facilitated by the use of some limiting algebraic relations. For their development it is convenient to define β_A by the equation

$$\beta_A=\sum_{p=1}^{p=n} pA_p/\sum_{p=0}^{p=n} A_p, \tag{2}$$

in which A_p represents the number of molecules of $AH_{n-p}D_p$ in the equilibrium mixture. Eq. (2) then describes the exchange experiment in terms of the average number of D atoms per molecule of AH_n and its deuterium substitution products.

Each substance $AH_{n-p}D_p$ will come to equilibrium with H_2O, DOH and AH_n in accordance with reaction 1 for which the mass law expression is

$$A_p=A_0K_pR^p. \tag{3}$$

The concentration ratio DOH/HOH has been represented by R. Eqs. (2) and (3) are combined to yield the relation

$$\beta_A=\sum_{p=1}^{p=n} pK_pR^p/1+\sum_{p=1}^{p=n} K_pR^p. \tag{4}$$

The corresponding expression for β_{H_2O} takes the form

$$\beta_{H_2O}=R(1+2KR)/(1+R+KR^2), \tag{5}$$

with K denoting the equilibrium constant of the reaction

$$2DOH=H_2O+D_2O. \tag{6}$$

In order to develop Eq. (4) any further it is necessary to assume relations between the n constants K_p. The numerical or symmetry effect can be separated from the other statistical factors by means of the equation

$$K_p=\frac{k_p}{2^p}\frac{n!}{(n-p)!p!}. \tag{7}$$

If k_p is set equal to $k_1{}^p$ it follows that

$$K_p=\left(\frac{K_1'}{n}\right)^p\frac{n!}{(n-p)!p!}. \tag{8}$$

Eq. (8) describes the limiting case for which the same factors of mass, moment of inertia and frequency could be used to calculate the equilibrium constant of each successive reaction in the series

$$AH_{n-p}D_p+DOH=AH_{n-p-1}D_{p+1}+H_2O.$$

This condition is fulfilled closely enough by the mass and inertia factors but may be far from true for the vibrational effect. Consequently the derivation leads to a relation in which K_1' varies with β_A in a manner determined primarily by the change in frequency shift with successive substitution of D for H.

Equation (8) is equivalent to a conclusion reached by Brodskii.[1] It is combined with Eq. (4) and simplified as follows:

$$\beta_A=\frac{\sum_{p=1}^{p=n}\left(\frac{K_1'R}{n}\right)^p\frac{n!}{(n-p)!(p-1)!}}{1+\sum_{p=1}^{p=n}\left(\frac{K_1'R}{n}\right)^p\frac{n!}{(n-p)!p!}}=\frac{nK_1'R}{n+K_1'R}. \tag{9}$$

It follows that

$$K_1'=n\beta_A/R(n-\beta_A) \tag{10}$$

for the limiting case under consideration.

The numerical factor introduced into Eq. (7) requires no justification, since it merely sets the probability of occurrence of $AH_{n-p}D_p$ proportional to the number of permutations of $(n-p)$ atoms of the one isotope with p atoms of the other. It is of interest, however, to consider the relation of this factor to the symmetry number which occurs in the simplified form of the partition function or sum over states.

In the general case, $AH_{n-p}D_p$ may represent several molecules, the number depending on the symmetry number σ_0 of AH_n. To the ith molecule is assigned the symmetry number σ_{pi}. The constant K_{pi} of the reaction

$$AH_n+pDOH=(AH_{n-p}D_p)_i+pH_2O \tag{11}$$

then becomes

$$K_{pi}=(k_{pi}/2^p)(\sigma_0/\sigma_{pi}). \tag{12}$$

The relations equivalent to Eqs. (7) and (8) are obtained by summing over the i molecules:

$$K_p=\sum_i K_{pi}=\frac{1}{2^p}\sum_i k_{pi}\frac{\sigma_0}{\sigma_{pi}}=\frac{k_p}{2^p}\sum_i\frac{\sigma_0}{\sigma_{pi}}. \tag{13}$$

[1] Brodskii, Trans. Faraday Soc. **33**, 1180 (1937).

TABLE I. *Statistical constants for ammonia-water and methane-water exchange reactions at 25°C.*

	$\left(\frac{M_p}{M_0}\right)^{\frac{3}{2}}$	$\left(\frac{A_pB_pC_p}{A_0B_0C_0}\right)^{\frac{1}{2}}$	$-\Delta\nu$ (cm^{-1})	K_p	$\left(\frac{K_1}{n}\right)^p \frac{n!}{(n-p)!p!}$
H_2O	1.000	1.000	0	—	—
DOH	1.085	1.659	1133$^{\Delta}$	—	—
D_2O	1.172	2.632	2377$^{\Delta}$	—	—
NH_3	1.000	1.000	0	—	—
NH_2D	1.090	1.457	1097*	1.214	1.214
NHD_2	1.183	2.043	2417*	0.804	0.491
ND_3	1.278	2.752	3850*	0.223	0.066
CH_4	1.000	1.000	0	—	—
CH_3D	1.096	1.342	1161‡	1.747	1.747
CH_2D_2	1.194	1.776	2441‡	1.495	1.145
CHD_3	1.296	2.269	3725‡	0.553	0.333
CD_4	1.400	2.827	5004‡	0.073	0.036

Δ Barker and Sleator, J. Chem. Phys. **3**, 660 (1935).
* Howard, J. Chem. Phys. **3**, 208 (1935).
‡ Benedict, Morikawa, Barnes and Taylor, J. Chem. Phys. **5**, 1 (1937).

TABLE II. *Ammonia exchange reaction at 25°C. Distribution from molecular constants.*

R	%D_2O	β	K_1'
0.6	24.09	0.702_7	1.529_4
.4	17.22	$.482_5$	1.437_3
.3	13.40	$.365_3$	1.386_5
.2	9.27	$.244_7$	1.332_3
.1	4.81	$.122_3$	1.274_8
.05	2.45	.0610	1.244_9
0	0	0	1.214

The factor k_p is a weighted average of the values of k_{pi}. If both Eqs. (7) and (13) are correct it is necessary to set $\sum_i \sigma_0/\sigma_{pi}$ equal to $n!/(n-p)!p!$.

In the limiting case for which $\sigma_0=1$ each σ_{pi} must be equal to unity because each substitution of D for H will result in a recognizably different molecule. The ratio σ_0/σ_{pi} is equal to unity and the sum over the i forms will be equal to the number of forms $n!/(n-p)!p!$, that is, to the number of distinguishable permutations of pD atoms with $(n-p)$H atoms. If, however, σ_0 equals *abc*, the product of a set of numbers representing equivalent arrangements produced by internal rotation or rotation of the entire molecule, the substitution of pD atoms will eliminate one or more of these factors, so that σ_{pi} might be equal to a and σ_0/σ_{pi} equal to bc. The rotational operations corresponding to b and c, when performed upon the substitution product, are no longer symmetry operations, but instead show the equivalence of bc of the total possible permutations. In this way they give to the form of symmetry number a a statistical weight equal to the number of permutations which can be shown to be equivalent by performing just those rotations which were eliminated as symmetry operations by the substitution. None of the $n!/(n-p)!p!$ permutations are lost and each one must belong to one of the i forms. The quantity $\sum_i \sigma_0/\sigma_{pi}$ must therefore be independent of the actual symmetry numbers and equal to the number of permutations. It can be shown, in addition, that this relation is a necessary consequence of the accepted principle that the difference between isotopes of slightly different mass, such as Cl^{35} and Cl^{37}, may be taken into account or neglected at will without introducing significant statistical errors.

For the purpose of illustrating the sensitivity of K_2 and K_3 to variations in the distribution values from which they have been calculated, it has seemed preferable to use the ammonia and methane reactions, rather than to set up a purely hypothetical case. All molecular data necessary to a complete description of these systems are available. Table I summarizes the values of K_p at 25°C together with the mass ratios, moment ratios and frequencies used in their calculation. K_p has been obtained from the relation $K_p=L_p/L_{DOH}{}^p$ where

$$L_p=\left(\frac{M_p}{M_0}\right)^{\frac{3}{2}}\left(\frac{A_pB_pC_p}{A_0B_0C_0}\right)^{\frac{1}{2}} e^{-hc\Delta\nu/2kT}\frac{n!}{(n-p)!p!}. \quad (14)$$

Factors of the form $(1-e^{-hc\nu/kT})$, associated with individual frequencies, have been omitted from Eq. (14) because their contribution to K_p is negligible. The moment ratios are based upon the assumption that interatomic distances and bond angles do not change with the isotope substitution. The tetrahedral angle has been used for methane, and for water and ammonia, respectively, the angles taken are 105° and 113°. It is possible that some of the frequency shifts may be in error, since they are based in part upon calculated quantities. For example, the data of Ginsburg and Barker[2] set the first methane shift at 1088, which would give a constant about

[2] Ginsburg and Barker, J. Chem. Phys. **3**, 668 (1935).

TABLE III. *Methane exchange reaction at 25°C. Distribution from molecular constants.*

R	%D_2O	β	K_1'
0.6	24.09	0.928_4	2.014_9
.4	17.22	$.653_5$	1.952_8
.3	13.40	$.502_0$	1.913_3
.2	9.27	$.346_5$	1.866_8
.1	4.81	$.173_3$	1.811_7
.05	2.45	.0871	1.780_8
0	0	0	1.747

15 percent lower than the value of 1.747 which appears in the table. This difference is not important for the present purpose.

The constants of Table I are used to yield values of β, in accordance with Eq. (5), for selected values of R. These quantities, together with K_1 from Eq. (10) and, for reference, the deuterium oxide concentration of the equilibrium water in the conventional units, are presented in Tables II and III, respectively, for the ammonia and methane reactions.

The practical experimental range has been taken to involve equilibration with water containing not more than 25 percent D_2O, although for highest accuracy in determining the constants K_p the distribution should cover the entire range of isotope fractions, and each constant should be derived mainly from the distribution in the region in which $AH_{n-p}D_p$ contains its maximum fraction of the deuterium. Tables II and III show the character to be expected for typical isotope exchange data involving small molecules in which the replaceable hydrogens are linked to a single atom. Such data could be conveniently extrapolated to zero deuterium fraction to yield the limiting value of K_1 by plotting both K_1' and β/R against R and taking the best intercept common to the two functions. For selecting a preliminary value of K_2 from experimental data, a comparison of K_1' with the quantities appearing in Tables I, II and III should prove to be useful. In this connection, it is observed that the deviation of K_1' from K_1 at a given value of R is about the same for the ammonia and methane reactions, in spite of the fact that K_2 is much closer to K_1^2/n in the latter case. This indicates that the deviation of K_1 from constancy is larger for larger values of n, other factors being constant.

In testing the sensitivity of K_2 to uncertainties in the data from which it is derived, it is assumed that each experimental value of β will be accurate to 1.0 percent, and that β values used in the interpretation will be taken from a smooth curve of β against R, so that the sum of the errors in two β values separated by 0.3 unit on the R scale will not exceed 1.0 percent. In Tables IV and V are shown K_2 and K_3 as derived from K_1 and values of β at $R=0.3$ and $R=0.6$ with these quantities differing from those of Tables II and III in the manner indicated in the first three columns. The fourth and sixth columns show K_2 and K_3, the fifth and seventh the corresponding frequency shifts when the entire deviation from Eq. (8) is assumed to be due to the frequencies. This assumption introduces an error of 18 cm^{-1} in $\Delta\nu_2$ for ammonia and would have a much smaller effect in the interpretation of data for larger molecules.

The largest tabulated deviation of K_2 from the correct value is 8.2 percent. The corresponding error in $\Delta\nu_2$ is 53 cm^{-1}, of which 18 cm^{-1} could be accounted for in a more detailed calculation. It is interesting to observe that this is considerably smaller than the difference of 73 cm^{-1} between the calculated and observed values of $\Delta\nu_1$ for methane to which reference was made in connection with Table I. It is evident that the determination of K_2 and $\Delta\nu_2$ from exchange equilibrium data of reasonable accuracy is feasible, but that satisfactory evaluation of the corresponding quantities for the third substitution would require measurements of higher precision extending over a wider range of isotope fractions. Exchange data can thus provide an additional condition which must be met by an assignment of frequencies to a series of molecules $AH_{n-p}D_p$.

There are no recorded exchange experiments

TABLE IV. *Ammonia exchange reaction at 25°C; Variation of K_2 and K_3 with K_1 and β.*

1.0% VARIATION						
K_1	$\beta(0.3)$	$\beta(0.6)$	K_2	$\Delta\nu_2(2417)$	K_3	$\Delta\nu_3(3850)$
0	0	0	0.804	2399	0.223	3796
0	–	0	.738	2364	.285	3899
0	–	–	.763	2377	.233	3815
–	0	–	.855	2424	.150	3632
–	0	+	.805	2400	.255	3853

with any substance for which $n>1$ which extend over a sufficient range of isotope fractions to permit an accurate interpretation along the lines illustrated above. Some results[3] obtained in this laboratory with acetone, however, may be examined with profit in spite of their inadequacy. They are shown in Table VI.

From the last four listed measurements it appears that the limiting K_1 at 25°C should be about 2.45, giving 0.82 for the exchange factor. This is in very close agreement with the reciprocal of Brodskii's exchange factor of 1.22 and agrees well with the calculated result of K. Wirtz.[4] A factor for internal rotation or torsional vibration of the methyl group, equal in the first approximation to $(4/3)^{\frac{1}{2}}$, is introduced into Eq. (14), and $\Delta\nu_1$ is calculated to be -1217 cm^{-1}. This method of taking internal rotation into account, which has been used by Hobden, Johnston, Weldon and Wilson,[5] by Halford and Pecherer,[6] and by Wirtz, is equivalent to an assumption that the contribution of this type of motion to the exchange equilibrium constant is not sensitive to the height of the potential barrier. The frequency shift determines the temperature dependence of the equilibrium constant and permits the calculation of K_1 at 80°C to be 2.37, a value considerably higher than the experimental one at this temperature. The calculated value is taken to be the more reliable and is combined with the first two measurements of Table VI to yield $K_2=4.1$ and $\Delta\nu_2=-2650$ cm^{-1}. These are minimum magnitudes consistent with available information.

With this interpretation the acetone reaction falls at least qualitatively into line with other exchange reactions. The frequency shift produced by single substitution in the methyl group is numerically greater than $\Delta\nu_1$ for methane by an amount comparable to the parallel difference observed between the alcohols and water. In addition, the relation between the indicated values of $\Delta\nu_1$ and $\Delta\nu_2$ for acetone is similar to that observed for water, ammonia and methane.

TABLE V. *Methane exchange reaction at 25°C; Variation of K_2 and K_3 with K_1 and β.*

1.0% Variation						
K_1	β(0.3)	β(0.6)	K_2	$\Delta\nu_2$(2441)	K_3	$\Delta\nu_3$(3725)
0	0	0	1.495	2433	0.553	3694
0	+	0	1.605	2461	.458	3615
0	+	+	1.555	2450	.558	3698
+	0	+	1.412	2409	.680	3780
+	0	−	1.514	2438	.479	3634

TABLE VI. *Acetone exchange reaction.*

Temp. (°C)	%D_2O	R	β	K_1'
80	5.17	0.1080	0.2789	2.71
80	4.14	.0857	.2153	2.61
80	1.89	.0384	.0860	2.27
80*	0.919	.01852	.0400	2.17
60	1.136	.02293	.0524	2.31
40, 35	1.167	.02356	.0561	2.40

* Reversed reaction, subject to larger experimental error.

[3] Halford, Anderson, Bates and Swisher, J. Am. Chem. Soc. **57**, 1663 (1935).
[4] Wirtz, Zeits. f. physik. Chemie, **B31**, 309 (1936).
[5] Hobden, Johnston, Weldon and Wilson, J. Chem. Soc. 61 (1939).
[6] Halford and Pecherer, J. Chem. Phys. **6**, 571 (1938)

On the Heterogeneous Ortho- Paraconversion on Paramagnetic Crystals

L. FARKAS AND L. SANDLER
Department of Physical Chemistry, Hebrew University, Jerusalem, and the Daniel Sieff Institute, Rehovoth, Palestine
(Received December 13, 1939)

The rate of conversion of parahydrogen and of ortho-deuterium is measured on paramagnetic crystals, *viz.*, $CuSO_4$, $NiCl_2$ and neodymium oxalate. In the last case, crystals of approximately uniform size were used so that the total converting area was known. The conversion rate has a maximum at 0°C and it is shown that below this temperature the desorption rate of the H_2 and the D_2 is rate-determining. Hence, the ratio of the rates for H_2 and D_2 is not far from unity. The rate of desorption increases with increasing temperature and at higher temperatures, the rate of conversion on the surface becomes the slow process. The ratio of the rates for H_2 and D_2 becomes nearly 11 in this region. The heat of adsorption of the hydrogen on neodymium oxalate is about 2.4 kcal./mole.

THE collision of hydrogen or deuterium molecules with paramagnetic ions or molecules causes with a certain small probability[1-5] an ortho- paraconversion in the former. This conversion is induced by the inhomogeneous magnetic field of the paramagnetic particle.[6]

The ortho- paraconversion on the surface of certain catalysts is also of paramagnetic nature. This is indicated by the experiments of Bonhoeffer, Farkas and Rummel[7] which have made it very probable that in the case of charcoal, unsaturated, paramagnetic carbon atoms are responsible for the conversion. The conversion takes place in this case "inside the adsorption layer," with a monomolecular mechanism. Taylor and Diamond[8] have demonstrated that the ortho-paraconversion is much more rapid on the surface of paramagnetic crystals than it is on diamagnetic materials. The present experiments deal with the ortho- paraconversion on paramagnetic crystals in a temperature region in which the amount of hydrogen adsorbed on the crystal is negligible and the conversion takes place during the collision process of the hydrogen molecule with the surface.

There are two different types of collision processes during which an ortho- paraconversion may take place. (1) Simple collisions for which the hydrogen (or deuterium) molecule remains only for a short time in interaction with the crystal. The order of magnitude of this time is $\sigma/3c \sim 10^{-13}$ sec. (σ denotes the diameter of the hydrogen molecule, c its mean velocity). (2) Adsorptive collisions, when the mean time of sojourn of the hydrogen on the surface is still short compared with the time needed for establishing the ortho- para-equilibrium but long compared with 10^{-13} sec.

In the simple collision processes we should expect an ortho- paratransition with approximately the same probability as it occurs in the gaseous state. This is about $5 \cdot 10^{-13}$ per collision. If, however, the time of interaction of the hydrogen with the crystals is longer than 10^{-13} sec. the transition probability during each of such a process may become larger. This will be discussed further below. The approximate amount of crystal surface required to obtain a measurable ortho- paraconversion by simple collision processes is easily estimated. If N is the number of hydrogen molecules per cc, they strike $Nc/4$ times a surface of 1 cm². The half-lifetime of the conversion will be given by the expression

$$\tau = \frac{4 \ln 2}{\gamma N c} \frac{Nv}{s}, \qquad (1)$$

if γ is the transition probability, v the total volume of the vessel, and s the total surface. Inserting the numerical values we obtain $\tau = 3.3 \cdot 10^7 v/s$ sec. Hence in a vessel of 20 cc and with a surface of

[1] L. Farkas and H. Sachsse, Zeits. f. physik. Chemie **B23**, 1 (1933).
[2] L. Farkas and H. Sachsse, Zeits. f. physik. Chemie **B23**, 19 (1933).
[3] A. Farkas, L. Farkas and P. Harteck, Proc. Roy. Soc. **A144**, 481 (1934).
[4] A. Farkas and L. Farkas, Proc. Roy. Soc. **A152**, 152 (1935).
[5] L. Farkas and U. Garbatski, J. Chem. Phys. **6**, 260 (1938).
[6] E. Wigner, Zeits. f. physik. Chemie **B23**, 28 (1933).
[7] Bonhoeffer, A. Farkas and Rummel, Zeits. f. physik. Chemie **B21**, 225 (1933).
[8] Taylor and Diamond, J. Am. Chem. Soc. **57**, 1251 (1935).

10^5 cm^2 the half-lifetime of the conversion will be 110 min. The surface of 10^5 cm^2 could be realized, e.g., by 1.7 cc substance consisting of little cubes of 10^{-12} cm^3 ($=1\mu^3$) volume.

Experiments with Parahydrogen on $CuSO_4$ and $NiCl_2$ (Anhydrous)

In a vessel of 27 cc 65 percent parahydrogen was brought into contact with 3 g of $CuSO_4$ powder at 25°C. The copper sulphate was dehydrated before the experiment by heating it in vacuum. It disintegrated into a fine powder during this process. Parahydrogen was then introduced into the vessel and the rate of conversion followed by the microconductivity method.[9] The conversion proceeded according to the equation

$$u_t = u_0 e^{-kt}, \qquad (2)$$

where u_t and u_0 denote the concentration of parahydrogen above the equilibrium concentration at the times t and $t=0$. The half-time of conversion was 45 minutes, so that $k=\ln 2/45$ min.$^{-1}$. Using the same crystal powder, Eq. (2) was well reproducible on successive days. No special precautions were needed to prevent poisoning of the surface of the catalyst and it could be left in the vacuum without making efforts to exclude tap grease, etc.

The conversion of p-H_2 on the paramagnetic $CuSO_4$ is exactly of first order—the lifetime being independent of the pressure in the range (0.2 mm–60 mm) investigated. On the other hand, the rate of conversion is increased proportionally with the amount of $CuSO_4$ used. The rate was the same no matter whether the $CuSO_4$ was in one heap at the bottom of a thick tube, or whether it was spread over a larger surface. This shows that the hydrogen penetrates rapidly into the space between the particles of the powder and the rate of this diffusion is fast compared with the rate of conversion.

Using $NiCl_2$ as catalyst at 25°C similar results were obtained. However, the diamagnetic $ZnSO_4$ powder, dehydrated in the same way, failed to induce any measurable conversion within 6 days even when used in ten times greater amounts than the $CuSO_4$ was used.

[9] A. Farkas, Zeits. f. physik. Chemie **B22**, 344 (1933); A. Farkas and L. Farkas, Proc. Roy. Soc. **A144**, 467 (1934).

Conversion of Orthodeuterium on $CuSO_4$ and $NiCl_2$

The ortho- paraconversion of deuterium, investigated in a similar way, proved to be about ten times slower than that of hydrogen. The same ratio for the rate constants has been observed in presence of paramagnetic gases.[4, 5] The slower rate of conversion of deuterium is due to the smaller magnetic moment of the deuteron, the rate of conversion being, *ceteris paribus*, proportional to the square of the nuclear magnetic moment of the material to be converted.[6, 10]

These experiments prove that in the present case the kinetics of the conversion is analogous to that in the gaseous state, the absolute rate being proportional to the number of molecules striking the paramagnetic surface, each collision inducing with a small probability an ortho-paratransition.

In the heterogeneous catalyses hitherto investigated the conversion took place at low temperatures in the van der Waals adsorption layer and the rate of conversion was determined by the desorption velocity. Consequently, as soon as the adsorption layer became saturated with hydrogen, the absolute rate of conversion became independent of pressure. The reason for this is that the time of sojourn of the H_2 or D_2 on the surface is so large that the ortho- para-equilibrium is practically established for the molecules leaving the surface. This is the situation already at moderately low pressures and since the rates of desorption for light and heavy hydrogen are not very different, a low ratio of conversion rates was observed.[11]

Estimate of the Collision Efficiency

In order to gain some information on the transition probability of the ortho- paraconversion during the collision process with the paramagnetic solid, two series of experiments were carried out. (1) Estimation of the collision efficiency at ordinary temperature. (2) Investigation of the temperature dependence of the conversion rate.

In order to determine the collision efficiency of

[10] Kalckar and Teller, Proc. Roy. Soc. **A150**, 520 (1935).

[11] The difference of the desorption rates is caused by the difference in zero point energies of H_2 and D_2, that of the latter being somewhat smaller and the desorption rate correspondingly lower.

the conversion it is essential to estimate the total surface of the paramagnetic solid.

Neodymium oxalate-hydrate crystals were chosen for this purpose as they form very small crystals of fairly well defined shape, when precipitated from nitrate solution. As they are not hygroscopic, they can conveniently be handled and also examined under the microscope. They were obtained by precipitating neodymium nitrate with oxalic acid at 50°C in dilute (0.05 molar) solution. The half-time of the parahydrogen conversion with 1 g of substance in a reaction vessel of 27 cc volume was 7.3 minutes. Examination of the crystals under the microscope showed that they formed prisms of a length between 0.5 and 50μ. As there was a possibility that still smaller crystals were present, which could not be seen under microscope, the substance was sedimented several times in water, rejecting alternately the upper and lower fractions. The remaining substance—approximately $\frac{1}{6}$ of the original amount—gave a half-time of conversion of 5.4 min./g in the vessel of 27 cc volume. The crystal size was found to be much more uniform, the larger ones missing entirely. The average length of the prisms was 1μ. Since the rate of conversion was not much changed by the process of sedimentation, it appears that submicroscopic crystals were not present in appreciable amounts in the original sample.

According to Eq. (1), 1 g of neodymium oxalate (0.57 cc), consisting of particles of $1\mu^3$ size, should give in a vessel of 27 cc volume a half-time of conversion of 260′. The actually observed conversion was about 45 times faster. This discrepancy can be established, independently of Eq. (1), by comparing the conversion caused by Nd^{+++} ions in water solution, with the conversion on neodymium oxalate crystals. Assuming that the concentration of the Nd ion on the surface of the crystal powder corresponds to its concentration in the bulk of the solid, 1 g of our powder has $2.5 \cdot 10^{19}$ ions on its surface. In a vessel of 27 cc this corresponds to a concentration of $1.8 \cdot 10^{-3}$ mole/liter which in aqueous solution would induce a paraconversion with the half-time[2] of 160′. Thus the rate is about 30 times slower than found on the surface of the powder. In fact the half-lifetime of the conversion on the solid should be even slower than 160′ if we take into account that the paramagnetic ions on the crystal can be approached from one side only. From these comparisons it is evident that the rate of conversion on the paramagnetic solid is about 30–50 times quicker than we would expect if it proceeded by simple collisions, as described in the first section. The simplest explanation of this result is that the time of sojourn of a hydrogen molecule on the surface is longer than the time of interaction in simple collision processes which we estimated to be 10^{-13} sec.

In order to understand the implications of this finding, we must consider the probability of conversion as a function of the time of sojourn ϑ on the surface. According to a formula previously derived,[6] the probability of conversion is proportional to the square of ϑ, if ϑ is very small compared with the rotational period of the molecule, $\vartheta < 2J/h$, where J is the moment of inertia of the molecule. If ϑ approaches this quantity, the probability of conversion increases less rapidly and should, according to these formulae, cease to increase after ϑ has reached the value of about $2J/h$. Actually the approximations used in reference 6 break down if $\vartheta > 2J/h$ and a closer investigation shows that the conversion probability continues to increase, for $\vartheta > 2J/h$, proportionally with the first power of ϑ. Since even in the liquid or in the gas phase the time of collision is not far from $2J/h$, we can assume that the roughly 50 times greater conversion probability of the collision with the crystal surface is caused by the 50 times longer duration of this collision, i.e., a 50 times longer time of sojourn of the H_2 or D_2 atom on the crystal surface than would correspond to a "simple collision." This indicates that the concentration of H_2 molecules on the crystal surface is about 50 times higher than in the gas phase, corresponding to a heat of adsorption Q of

$$e^{Q/RT} = 50, \tag{3}$$

i.e., $Q = 2.4$ kcal.

Temperature Dependence of the Conversion

In Fig. 1 the values of the half-lifetime of the conversion at 10 mm pressure are plotted as a function of the temperature. They represent the average values obtained in various runs with 1 g

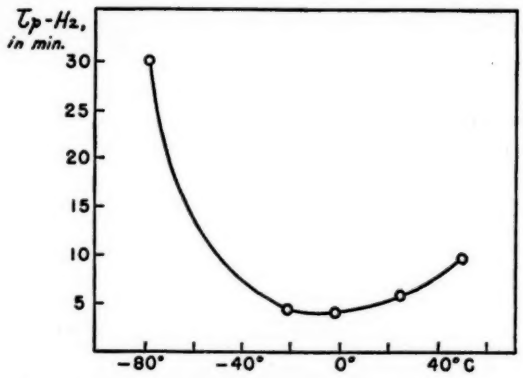

FIG. 1. Conversion rate of parahydrogen as function of temperature.

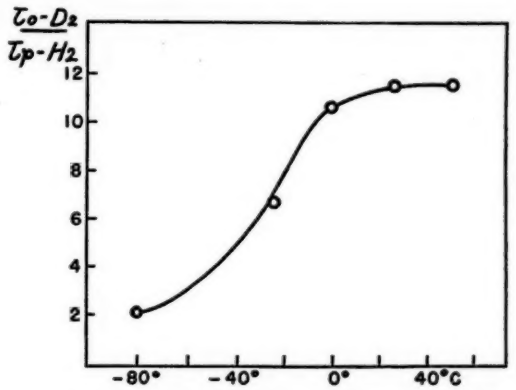

FIG. 2. Temperature dependence of the ratio of conversion rates of parahydrogen to orthodeuterium.

neodymium oxalate hydrate of 1μ grain size in our vessel of 27 cc volume. The curve in Fig. 2 represents[12] the ratio of the half-lifetime obtained with orthodeuterium to that obtained with parahydrogen. The curve in Fig. 1 has a minimum at 0°C (fastest conversion). At this point the ratio of conversion rates of light and heavy hydrogen, which is at higher temperatures constant (about 11) begins to decrease with decreasing temperature. It is obvious that on the two sides of the minimum point two different processes are rate determining for the conversion. At the low temperature side the rate of conversion is determined by the rate of desorption, the number of hydrogen or deuterium molecules which are given off by the surface in the para and ortho states corresponding to thermal equilibrium. In this temperature region, the conversion rates for light and heavy hydrogen differ only because of the somewhat lower desorption rate of deuterium. On the other hand, at high temperatures the mean time of adsorption is becoming shorter and the simple collisions begin to predominate. This causes the decrease of the rate of conversion. The ratio for the conversion rates of light and heavy hydrogen evidently approaches the value 11 in this region, corresponding to the ratio of conversion probabilities in simple collisions.

In the high temperature region, not the rate of desorption, but the rate of conversion on the surface is rate determining. The probability that a molecule is converted while on the surface is proportional to its time of sojourn ϑ. The total amount of conversion per cm² surface is, therefore, proportional to $\vartheta Nc/4$, where $Nc/4$ is the number of molecules striking 1 cm² of the surface per second. On the other hand, the total amount of hydrogen, adsorbed on 1 cm² of the surface is also $\vartheta Nc/4$ so that the rate of conversion in the high temperature region is proportional to the adsorbed amount. This latter quantity again is proportional to $\exp(-Q/RT)$ where Q is the heat of adsorption.

Figure 1 shows that the rate of conversion in the high temperature region decreases by a factor of about 2 if the temperature is raised by 50°. This gives the equation

$$\exp[Q(R/T-R/(T+50))]=2$$

or

$$Q=R\cdot\ln 2(0.00057)\sim 2.4 \text{ kcal.} \qquad (4)$$

in surprisingly good agreement with (3).

It is not certain up to what temperature the above described decrease of the conversion rate will continue, since at high temperatures other types of conversion, due to the activated adsorption, may become predominant.

The present experiments are promising for measuring very small amounts of adsorption, the measurement of which has caused great difficulties thus far. At 10 mm pressure, the adsorbed layer is 0.001 molecular. The work here outlined allows also a measurement of both the amount of surface which is blocked for H_2 by other adsorbed gases, and also the amount of surface left open. Most previous methods permit only the determination of the area *covered* by foreign gases, not of the area left open.

[12] More recent experiments indicate that the ratio of the two conversion rates is somewhat higher at high temperatures than given in Fig. 2. It is 10.5 at 0°C; 12.5 at 25°C and 13.5 at 50°C.

Vibration Spectra and Molecular Structure

IX. Further Studies of the Vapors of the Fatty Acid Series

ROBERT C. HERMAN
Palmer Physical Laboratory, Princeton University, Princeton, New Jersey

(Received November 30, 1939)

The monomer spectra of the vapors of C_3H_7COOH, C_3H_7COOD and C_4H_9COOH have been obtained in the near infra-red with a rocksalt spectrometer. The association of each of the following molecules: HCOOH, HCOOD and C_3H_7COOD has been studied in the vapor phase by measuring the variation with temperature and pressure of the intensity of some association band. The bond strengths obtained for these fatty acids are 6.2, 6.4 and 6.9 kcal. per mole per bond, respectively. The fact that the bond strengths for light and heavy formic acids agree within the experimental error although the determinations were carried out with different bands is further evidence that the spectroscopic method is satisfactory. The lower value obtained for the bond strength in formic acid by this method compared to the vapor density value is discussed. In addition, it is suggested from the experimental data available at the present time, that it does not seem possible to claim the existence of a simple linear relationship between the bond strength and $\Delta\nu/\nu$. Some results concerning ν(CH) absorption in the first five members of the fatty acid series are given.

SOME time ago Badger and Bauer[1] suggested that the frequency shift which a band ν(X−H) experiences when hydrogen bonding takes place might be a semi-quantitative measure of the energy of bonding. They plotted $\Delta\nu/\nu$ corresponding to the frequency shift of a band due to hydrogen bonding against the bond strength in the hope that some approximate proportionality existed between these two quantities and found that a straight line roughly fitted the data known at that time. Any such simple relationship would be of great importance because it would lead to a knowledge of the bond strength from the relatively simple determination of the frequency shift which occurs when hydrogen bonding takes place. However, the existence of such a relationship must be checked by the addition of reliable points to their plot. It is desirable to know the bond strength more accurately than is possible by estimations from latent heats. It would also be preferable to obtain the frequency shift by studying the vapor where possible so that the question of shifts due to the interactions present in the liquid phase and at times in solution would be avoided. From the results reported in this paper, as well as from earlier work[2–4] it is possible to attempt the check mentioned above. In the present work, values of $\Delta\nu/\nu$ have been obtained for the shift of ν(OH) to ν(OHO) for the vapors of butyric and valeric acids. Comparing these values with those obtained for the first three members of the fatty acid series one finds that they are only roughly the same, their average value being about 0.136. This is in fair agreement with $\Delta\nu/\nu$ calculated from the results of other investigations on acetic acid.[5, 6] There is a frequency shift of the fundamental ν(OH) band in the first four members of the series of about 70, 63, 68 and 66 cm^{-1} per kcal. of bond energy, respectively. Fig. 1 is a plot of $\Delta\nu/\nu$ *vs.* bond strength which includes the original points given by Badger and Bauer. In addition are included points which represent the first four members of the fatty acid series as well as other points for which we have employed bond strengths estimated by Pauling from latent heats of sublimation.[7] The difficulty of making such estimates is shown by the different values obtained from latent heats of sublimation and latent heats of vaporization.[8] Since we have no

[1] R. M. Badger and S. H. Bauer, J. Chem. Phys. **5**, 839 (1937).
[2] L. G. Bonner and R. Hofstadter, J. Chem. Phys. **6**, 531 (1938).
[3] R. C. Herman and R. Hofstadter, J. Chem. Phys. **6**, 534 (1938).
[4] R. C. Herman and R. Hofstadter, J. Chem. Phys. **7**, 460 (1939).
[5] A. M. Buswell, W. H. Rodebush and M. F. Roy, J. Am. Chem. Soc. **60**, 2239 (1938).
[6] M. M. Davies and G. B. B. M. Sutherland, J. Chem. Phys. **6**, 755, 767 (1938).
[7] L. C. Pauling, *Nature of the Chemical Bond* (Cornell Univ. Press, 1939).
[8] Badger and Bauer (reference 1) obtained the bond strength in the first members of the alcohol series by plotting the latent heat of vaporization against the number of carbon atoms in the molecule and extrapolating back to

way of knowing how reliable these estimates are, we must tentatively employ the bond strengths that are given. An inspection of the plot shows that the points representing the few substances for which both $\Delta\nu/\nu$ and bond strength are known do not lead to any clear relationship. The absence of any definite regularity is indeed not at all in disaccord with general considerations since there seems to be no *a priori* reason to expect a correlation between the bond strength and $\Delta\nu/\nu$. If it is possible that the bond strengths for water and the alcohols are in error, a precise knowledge of the bond strengths might lead to some empirical relationship. It would be very desirable to devise some direct method of obtaining accurately the bond strengths of substances like water and the alcohols which are not sufficiently associated in the vapor phase to employ known methods with any degree of success.

The present work shows that the spectroscopic method is a satisfactory method of determining bond strengths. The procedure of determining the amount of association at various temperatures and pressures and therefore the bond strength by measuring the intensity of some association band in the vapor phase could of course not be regarded as satisfactory if different bands led one to different values for the heat of association or if the absorption constant of the band under investigation varied markedly with the temperature. Recently, Davies and Sutherland[6] studied the association of several carboxylic acids in CCl_4 solution by measuring the variation with temperature of the integral absorption of the monomeric ν(OH) band. They obtained heats of association which varied from 6 to 10 kcal. per mole compared to the value of about 15 kcal. per mole known from vapor density measurements. They attribute this variation to a variation of the absorption constant with the temperature when working with solutions. We have found no evidence for any variation with temperature of the absorption constant of the association bands that we have studied in the vapor, and from a study of HCOOH and HCOOD find that to within the experimental error different bands lead to the same value of the heat of association.

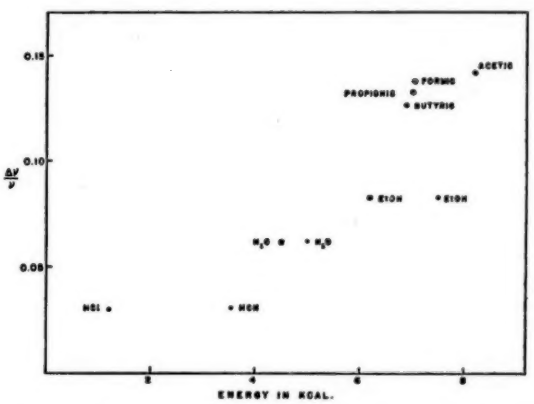

FIG. 1. Plot of $\Delta\nu/\nu$ for a fundamental band *vs.* bond strength in kcal. per mole. The closed circles are some of the original points given by Badger and Bauer. The squares represent points which have been plotted by using Pauling's value for the bond strength, obtained from heats of sublimation. The bond strength's employed for formic and acetic acids are those given by the vapor density method while those for propionic and butyric acids have been obtained spectroscopically.

During the past few years several spectroscopic investigations of association in the carboxylic acids have been made. Badger and Bauer[9] investigated the variation with temperature of the second harmonic of the OH band in acetic acid and obtained rough agreement with the data of MacDougall[10] found by the vapor density method. Studies made in this laboratory on the vapor of

zero carbon atoms. The 7.5 kcal. of energy remaining was attributed to hydrogen bonding and since it was assumed that each molecule has two neighbors a bond strength of 7.5 kcal. per mole per bond was obtained. However, according to the x-ray diffraction experiments of G. G. Harvey, J. Chem. Phys. **6**, 111 (1938); **7**, 878 (1939) both methyl and ethyl alcohol are not completely coordinated at room temperature so that the estimate of the bond strength would be expected to be too low. From latent heats of sublimation, on the other hand, Pauling (reference 7) estimates that the bond strength in methyl and ethyl alcohol is 6.2 kcal. per mole per bond. Thus, from present evidence one can only conclude that the bond strength for alcohol probably lies between 6.2 and something over 7.5 kcal. per mole per bond. Likewise, the estimate of the bond strength of water (about 5 kcal. per mole per bond) made by assuming that the latent heat of vaporization is almost entirely due to hydrogen bonding and that the number of hydrogen bonds per molecule is two, would be expected to be too low since Cross, Burnham and Leighton, J. Am. Chem. Soc. **59**, 1134 (1937) have found that water is not completely coordinated near and above the melting point. In fact it has been estimated that at 40°C the average number of hydrogen bonds per water molecule is already only somewhat greater than half the maximum number possible. If Pauling's (reference 7) estimate of a hydrogen bond strength of 4.5 kcal. per mole per bond for water is correct, this would imply that an appreciable part of the latent heat of vaporization of water is due to van der Waals and other forces.

[9] R. M. Badger and S. H. Bauer, J. Chem. Phys. **5**, 605 (1937).

[10] F. H. MacDougall, J. Am. Chem. Soc. **58**, 2585 (1936).

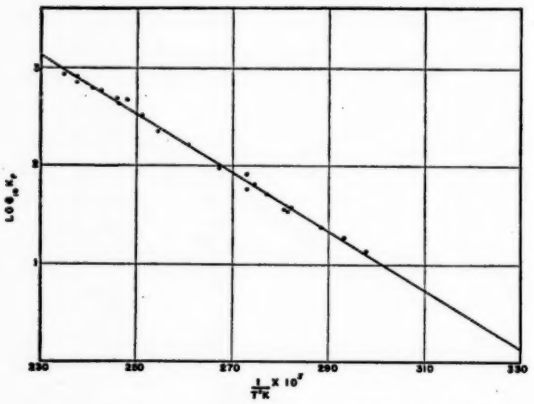

FIG. 2. Equilibrium constant for C_3H_7COOD.

acetic acid-*d* (CH_3COOD) by means of the ν(ODO) association band led to a heat of association of 15,900 calories per mole as compared to the value 16,400 calories per mole obtained by MacDougall.[3] Apart from the work of Davies and Sutherland mentioned above the heat of association of propionic acid-*d* (C_2H_5COOD) vapor has been obtained recently and found to be 14,100 calories per mole.[4] It is the purpose of this paper to discuss further results that have been obtained for light formic acid, formic acid-*d* (HCOOD) and butyric acid-*d* (C_3H_7COOD). It seemed desirable to investigate the formic acids first because it would be possible to compare the results with Coolidge's vapor density determination[11] and second in order to see whether the method employed would give consistent results when two different bands are studied in the same compound.[12] The monomer spectra of the vapors of butyric and valeric acids and butyric acid-*d* as well as some results on ν(CH) absorption in the first five members of the fatty acid series are reported here also.

EXPERIMENTAL

All the light acids employed were Kahlbaum products and were purified by vacuum distillation. Butyric acid-*d* (C_3H_7COOD) was prepared in vacuum by mixing a slight excess of butyryl chloride (Eastman) with 99.6 percent heavy water and was purified by pumping and several distillations. Only middle fractions were retained for this as well as the other compounds employed. The vapor pressure of this compound as well as its infra-red spectrum indicated that less than several percent of water was present. The hydrogen-deuterium gas mixture obtained from the reaction of the heavy butyric acid with magnesium was analyzed in a mass spectrograph and the resulting D/H ratio was 40.[13] Formic acid-*d* was prepared by exchanging light formic acid (Kahlbaum) with 99.6 percent heavy water several times. Between successive exchanges the water was removed by means of anhydrous copper sulphate. This method had been employed previously by Hofstadter in this laboratory.[14] In the attempt to prepare HCOOD with a greater D/H ratio than had been obtained previously, the anhydrous copper sulphate employed was initially exchanged with heavy water. Although the four exchanges carried out should have yielded a product with a D/H ratio of about 140, the final sample had a ratio of 16. Because a final dehydration had to be performed the sample eventually employed in the infra-red experiments had a D/H ratio of 12. The first of these D/H ratios was determined in the same way as that mentioned above for butyric acid-*d*. The other ratio was obtained from a comparison of the depths of the OH and OD bands found in a high temperature and pressure spectrum. This method has been employed by Hofstadter[14] who found good agreement between the D/H ratio found in this way and by means of the mass spectrograph. That both the light and heavy formic acids were free from water was known from a comparison of their vapor pressures with data obtained by Coolidge.[15]

The experimental arrangement employed to determine the association properties of the formic acids was the same as that used for acetic acid-*d*[3] and the determination of the heat of association of butyric acid-*d* was made with the same apparatus employed for propionic acid-*d* in this laboratory.[4] Different arrangements had to be employed because of the very different vapor pressure curves of these compounds. Intensities

[11] A. S. Coolidge, J. Am. Chem. Soc. **50**, 2166 (1928).

[12] These are the same compounds for our purposes because the experimental error is too large to show any difference due to zero point energy.

[13] We wish to thank Mr. W. Guyer for analyzing our hydrogen-deuterium gas mixtures.

[14] R. Hofstadter, J. Chem. Phys. **6**, 540 (1938).

[15] A. S. Coolidge, J. Am. Chem. Soc. **52**, 1874 (1930).

were measured at various pressures and temperatures at the bottom of the O−D−O association band for HCOOD and C_3H_7COOD whereas for HCOOH the association band at 7.38μ was used because the O−H−O association band falls in the region of C−H valence vibrations. Several times during a determination, the transmission was obtained with the sample frozen out of the absorption cell in order to check background absorption which remained constant. It was found necessary, as usual, to wait a considerable length of time between points in order for equilibrium to set in. Otherwise, points on the log K_p *vs.* $1/T$ curve were found to scatter badly. In all the association measurements, pressures were measured directly with a mercury manometer and temperatures by means of a calibrated thermocouple. However, the pressures noted in the infra-red spectra shown in Figs. 5 and 6 were calculated from the temperature of the liquid in a side tube, except in the case of butyric acid-*d* (Fig. 5) where it was measured directly. The general technique employed will not be discussed here since it has been reported in previous communications.[3, 4]

Results and Discussion

As in the determination of the heat of association of propionic acid-*d*,[4] the absorption constant for the O−D−O association band in butyric acid-*d* was assumed to be the same as that in acetic acid-*d*. In a previous communication it was remarked that the addition of a CH_2 group in going from one fatty acid to the next would probably not affect appreciably the absorption

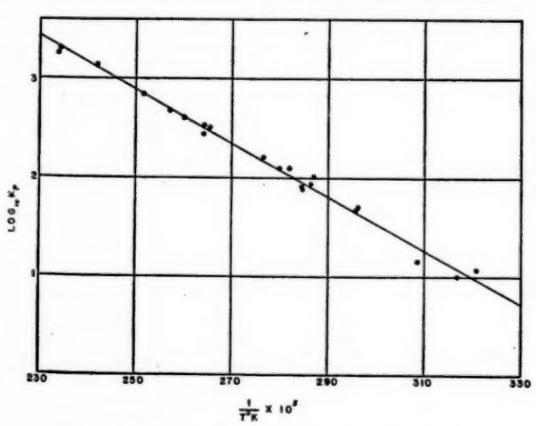

FIG. 3. Equilibrium constant for HCOOH.

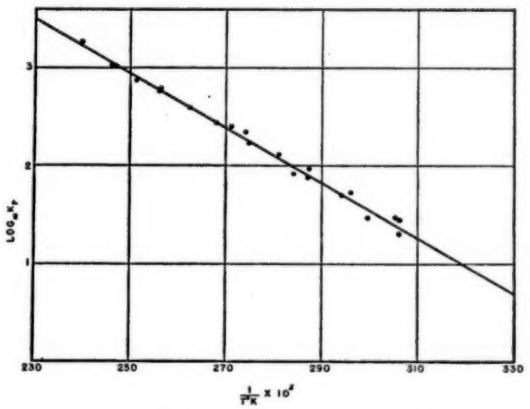

FIG. 4. Equilibrium constant for HCOOD.

constant of the O−D−O band.[4] Fig. 2 shows the results obtained for butyric acid-*d* on the basis of this assumption. From the slope of the best straight line the heat of association obtained is 13,800±700 calories per mole. This value is practically the same as that obtained for propionic acid-*d*. Calculations were made for this acid choosing an absorption constant differing by 20 percent from that above. The fact that there were no noticeable deviations from linearity of the curve on the log K_p *vs.* $1/T$ plot shows that both the heat of association and the absorption constant are not in error by more than about 5 and 20 percent, respectively.[16] Moreover, over the higher temperature range p_D/p (where p_D is the partial pressure of double molecules and p the total pressure) was kept practically constant so that the slope of the curve in that region is practically independent of the choice of absorption constant.[16]

Light formic acid was investigated in order to see whether this method would give results in agreement with the vapor density measurements obtained by Coolidge. The 7.38μ band which was employed is a dimer band and is not mixed with any monomer band as can be seen from an inspection of the monomer and dimer spectra of this compound obtained by Bonner and Hofstadter.[2] Since Coolidge's data were available, an absorption constant was determined for this band in the same way that the absorption constant for the O−D−O band in acetic acid-*d* was determined from MacDougall's data. The

[16] R. C. Herman and R. Hofstadter, J. Chem. Phys. **7**, 630 (1939).

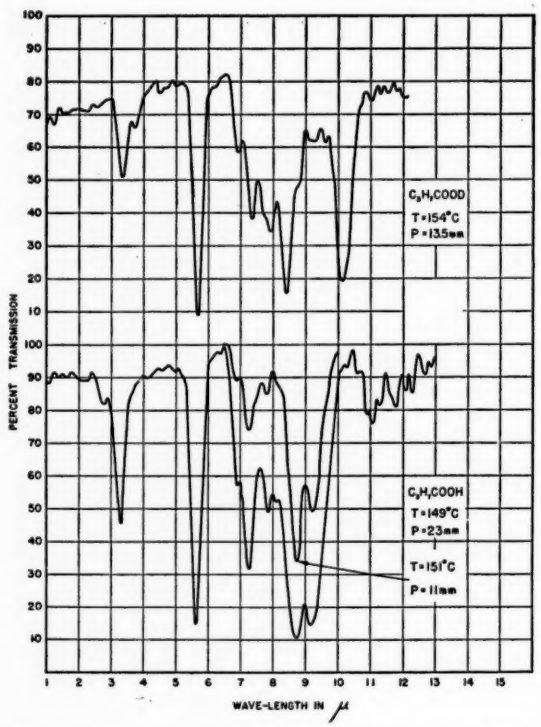

FIG. 5. Absorption spectra of C_3H_7COOH and C_3H_7COOD. Absorption cell length 22 cm.

value of the absorption constant for the 7.38μ band in HCOOH obtained in this way is 5×10^4 cm² per mole.[17] It should be remarked that by a method of trial and error one could find the value of the absorption constant for which the data on the log K_p *vs.* $1/T$ plot would give a best straight line. This is effectively what was done in the case of butyric acid-*d*. The association data for HCOOH are shown in Fig. 3 and the heat of association obtained from the slope is $12{,}400\pm700$ calories per mole as compared with Coolidge's value of 14,135 calories per mole. These two values differ by an amount larger than the experimental error and it was this discrepancy which in part prompted the further experiments on HCOOD for which a different band (the O−D−O association band) could be employed. An absorption constant for the O−D−O band was obtained in the same way as for the 7.38μ band in HCOOH and is 7.4×10^4 cm² per mole.[17] Since there was some light formic acid present, the vapor was assumed to contain an equilibrium mixture of two types of single molecules and three types of double molecules. If one takes this into consideration it is simple to show that

$$K_p=\frac{[1-(1+1/f)x]^2p}{(1+1/f)x},$$

where

$$x=p_D/p=-\frac{RT\log_{10}I/I_0}{\beta p}.$$

β is the absorption constant, p the total pressure and f the D/H ratio in the acid position. We should mention that in obtaining β for HCOOD we assumed that double molecules with one D

[17] All the absorption constants quoted in this paper have been obtained from the formula

$$I/I_0=10^{-\beta\rho_D l},$$

where ρ_D is the density in moles per cm³ and l the length of the absorption path in cm.

TABLE I.

ACID	INVESTIGATOR	METHOD	HEAT OF ASSOCIATION IN CAL./MOLE
HCOOH[a]	Coolidge[11]	V.D.*	14,135
	Ramsperger and Porter[b]	V.D.	14,100 (av. value)
	this paper	S**	12,400
HCOOD	this paper	S	12 800
CH_3COOH[c]	MacDougall[10]	V.D.	16,400
	Nernst and von Wartenburg[d]	V.D.	15,000
	Fenton and Garner[18]	V.D.	13,790
	Badger and Bauer[9]	S(Harmonic)	rough agreement with MacDougall
	Davies and Sutherland[6]	S(CCl_4 sol.)	9300***
CH_3COOD	Herman and Hofstadter[3]	S	15,900
C_2H_5COOD	Herman and Hofstadter[4]	S	14,100
C_3H_7COOD	this paper	S	13,800
$C_6H_{13}COOH$	Fenton and Garner[18]	V.D.	7050***

* Vapor density method.
** Spectroscopic method employing the fundamental band of a vapor unless stated otherwise.
*** Unreliable.
[a] For other work on formic acid see H. C. Ramsperger and C. W. Porter, J. Am. Chem. Soc. **50**, 3036 (1928).
[b] H. C. Ramsperger and C. W. Porter, J. Am. Chem. Soc. **48**, 1267 (1926).
[c] For earlier work on the vapor density of acetic acid see: W. Ramsay and S. Young, J. Chem. Soc. **49**, 790 (1886); S. Young, Proc. Roy. Dublin Soc. **12**, 374 (1909–1910); Drucker and Ullman, Zeits. f. physik. Chemie **74**, 604 (1910); Holland, Zeits. f. Electrochem. **18**, 234 (1913).
[d] Nernst and von Wartenburg, Zeits. f. Electrochem. **22**, 37 (1916).

atom and one H atom in the dimer ring contribute half the amount that double molecules with two D atoms contribute to the intensity of the O−D−O band. From the results for HCOOD shown in Fig. 4 we obtain a heat of association of 12,800±700 calories per mole.

Although the formic acids in the absorption cells were examined over a period of days at temperatures as high as 150°C, no decomposition was observed, so that the pressures recorded were those of the acid alone. The fact that the heavy formic acid was not completely deuterated could be taken into account as mentioned above. From a plot of $\log I/I_0$ *vs.* ρ_D (the density of dimer molecules calculated by means of Coolidge's data) it was evident that Beer's law was obeyed for all but some of the points employed on the low temperature part of the curves shown in Figs. 3 and 4. Furthermore, the absorption constants were not found to depend upon the temperature in the range studied. The O−D−O band in HCOOD was mixed with a weak monomer band due to HCOOH. Under the conditions employed this monomer band was negligibly small. The presence of a monomer band, however, would cause the intensity of the dimer band to decrease more slowly than for the dimer band alone and would lead to a higher rather than a lower heat of association. Thus, the effect of the 8.30μ band on the long wave-length side of the 7.38μ band studied in light formic acid and the small monomer band superposed on the O−D−O band in heavy formic acid does not explain the lower heats of association obtained by this method. We do not think that the other factors considered; namely, slit width (we employed constant slit width in each case) or adsorption account for this discrepancy either. Because of the care with which Coolidge's determination was made it seems that the discrepancy resulting from these two different methods may be real. Perhaps it is caused by the fact that the vapor density method includes all types of association whereas this method does not. Or it may be due to the presence of higher polymers. Because of the scattering of points in Figs. 3 and 4 it is difficult to say exactly what this difference is but from our results on acetic acid it does not seem that our error would be as large as 1500 calories per mole.

TABLE II. *Positions of monomer absorption bands.*

Valeric Acid		Butyric Acid		Butyric Acid-*d*	
$\lambda(\mu)$	(cm^{-1})	$\lambda(\mu)$	(cm^{-1})	$\lambda(\mu)$	(cm^{-1})
2.70	3703	2.80	3571	3.33	3003
3.33	3003	3.31	3021	3.70	2703
5.63	1770	5.65	1770	5.68	1760
6.80	1471	6.91	1447	6.90	1449
7.30	1370	7.30	1370	7.32	1366
8.00	1250	7.90	1266	7.90	1266
8.80	1136	8.12	1232	8.40*	1190
9.17	1091	8.77	1140	9.25	1081
10.5	952	9.23	1083	10.1	990
12.2	820	11.	909		
		12.	833		

* Asymmetry on long wave-length side.

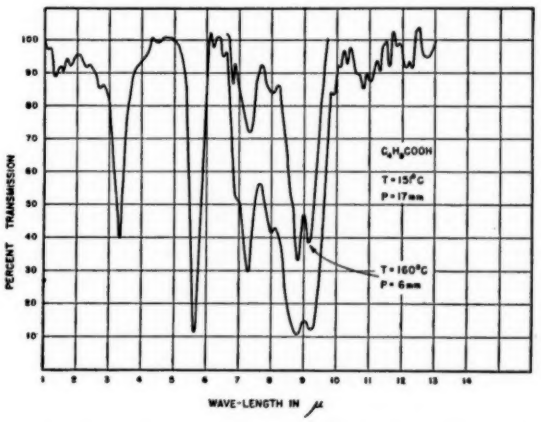

FIG. 6. Absorption spectrum of C_4H_9COOH. Absorption cell length 22 cm.

As far as we are aware the heats of association of only very few of the fatty acids have been obtained by the vapor density method, namely, formic, acetic and heptoic acids. In Table I we have gathered some of the results obtained by this method as well as others obtained spectroscopically. Fenton and Garner[18] state that although the values they obtained for the heat of association of heptoic acid do not possess much value by themselves, the results indicate that the heat of association of this acid is decidedly lower than that of acetic acid and suggest the investigation of acids with intermediate chain length. From our results there is no indication that the bond strength is decreasing with chain length as far up the series as butyric acid. It should be interesting to investigate carefully a member higher in the series to see whether the bond

[18] Fenton and Garner, J. Chem. Soc. 694 (1930).

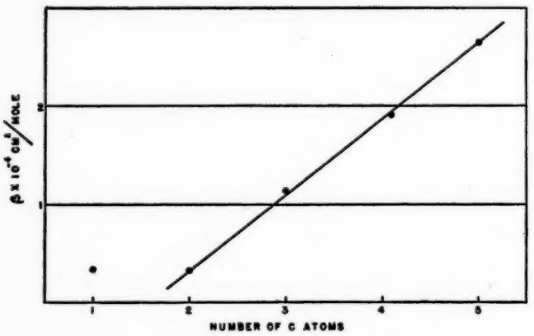

FIG. 7. Plot of the absorption constant for the band ν(CH) *vs.* the number of carbon atoms in each fatty acid molecule (reference 22).

strength remains roughly constant as this investigation shows or decreases as Fenton and Garner's work on heptoic acid indicates.

The monomer spectra of the vapors of valeric acid and butyric acid and butyric acid-*d* are shown in Figs. 5 and 6 and band centers are listed in Table II. Since the degree of dissociation is rather large for these compounds under conditions for which the vapor pressure is high enough to obtain sufficient absorption, it was not possible to obtain good dimer spectra. As in the other fatty acids studied the high frequency region is interpretable. An inspection of the spectra in this and earlier papers[2-4,14] shows that the position of the $\nu(C=0)$ frequency in the carboxyl group is practically independent of the length of the attached hydrocarbon chain. This result has been obtained previously by means of the Raman effect.[19] The question of assigning bands beyond $\nu(C=0)$ must be left until further work is done with higher resolution. However, it is likely that the band appearing near 6.9μ in these higher acids is due to some hydrocarbon chain frequency and perhaps the band in the vicinity of 10.5μ in the spectra of the higher members of the series which have D atoms in the acid position, contains the OD bending frequency which appears at about 11μ in heavy phenol (C_6H_5OD).[20]

If one studies the monomer spectra of the fatty acids with progressively longer hydrocarbon chains it is evident that the band associated with CH valence vibrations becomes deeper. We have obtained absorption constants for this band in the first five members of the series by measuring the depth of the band below the background with a wide slit. The following relation holds approximately for all but the first member:

$$\beta_N=\beta_{\text{acetic}}+0.77(N-2)$$

where N is the number of carbon atoms in the molecule and β_{acetic} is about 3.2×10^4 cm² per mole. We also find that the ν(CH) absorption constants for formic and acetic acids are about the same. These results are shown in Fig. 7. It seems then that each CH_2 group added to the hydrocarbon chain increases CH absorption by about the same amount and also that the contribution to CH absorption of the CH group in formic acid is about the same as that of the CH_3 group in acetic acid. Similar results have been found in the case of the alcohols by Henri. These results are probably only approximately correct since Bonino in the case of the alcohols has shown that as one goes to higher members of the series, the deviations from linearity become greater and greater.[21]

ACKNOWLEDGMENT

I wish to thank Professors E. P. Wigner and H. Eyring for profitable discussions. I also wish to thank Professor E. R. Caley of the Chemistry Department for the gift of some pure copper sulphate. I am indebted to Professor J. A. Wheeler for many helpful criticisms while preparing this paper. Finally, I wish to express my appreciation to Dr. R. Hofstadter for his constant help and encouragement.

[19] K. W. F. Kohlrausch, F. Koppl and A. Pongratz, Zeits. f. physik. Chemie **B21**, 242 (1933); **B22**, 359 (1933).

[20] V. Williams, R. Hofstadter and R. C. Herman, J. Chem. Phys. **7**, 802 (1939).

[21] A complete account of this point may be found in Schaefer and Matossi, *Das Ultrarote Spektrum* (1930), p. 280.

Reactions of Free Radicals with Organic Compounds Containing Atoms with Unshared Electron Pairs*

FRANCIS OWEN RICE, W. D. WALTERS† AND P. M. RUOFF‡
The Johns Hopkins University, Baltimore, Maryland

(Received December 13, 1939)

An experimental test for the reaction $CH_3+CH_3OCH_2CH_3\rightarrow CH_3OCH_3+CH_3CH_2$ was made by decomposing methyl ethyl ether both alone and in presence of azomethane, and examining the products for dimethyl ether; none was detected, and if this reaction occurs at all it is only to the extent of a very few percent. A similar test for the reaction $CH_3+CH_3CH_2CH_2NH_2\rightarrow CH_3NH_2+CH_3CH_2CH_2$ was made by decomposing pure *n*-propylamine in a flowing system, but this also gave a negative result. The products formed in the promoted decomposition of dimethyl ether were found to be essentially the same as those formed in the normal decomposition.

1. INTRODUCTION

IN a recent paper,[1] the whole question of the nature of the elementary reactions between radicals and molecules was considered, and the conclusion was reached that, in general, the most favored reaction would be removal of a hydrogen atom from the organic molecule by the free radical. On the other hand, the reaction that might be expected to have the smallest probability of occurring is the reaction between a free radical and a carbon atom having four valences joined to four univalent atoms or groups. Such a "shielded" carbon atom would be difficult to attack, and the reaction would be by far the least likely sort to occur.

However, atoms like chlorine, oxygen, or nitrogen are not shielded to the same extent as carbon, all having at least one pair of unbonded electrons. Since we know that free radicals attack doubly and triply bonded carbon atoms, it appeared desirable to investigate experimentally whether any similar sort of reaction occurs between radicals and atoms having one or more unshared electron pairs.

If free radicals react with an atom having an exposed pair of electrons, we would expect that introduction of methyl radicals into an ether, amine, or alkyl chloride would lead to the production of the corresponding methyl derivatives, according to the following equations:

$$CH_3+R-O-R'\rightarrow R-O-CH_3+R'$$
$$CH_3+RNH_2\rightarrow CH_3NH_2+R$$
$$CH_3+RCl\rightarrow CH_3Cl+R.$$

In view of the importance of this question, we attempted to obtain experimental evidence for reactions of this type by investigating three decompositions, namely the ordinary decomposition of methyl ethyl ether, the promoted decomposition of this compound, using azomethane as promoter, and the ordinary decomposition of normal propylamine.

2. EXPERIMENTAL

The method used in this investigation was to introduce a known amount of substance into a heated reaction vessel until the desired amount of decomposition, as measured by the pressure change on the manometer, had occurred. The sample was then quickly removed from the furnace, condensed at liquid nitrogen temperature, and separated into various fractions by distillation in a Podbielniak still. In order to carry out such a distillation, a larger sample is needed than can be contained in the small reaction vessel ordinarily used for rate measurements. Therefore a large furnace was constructed containing a 12-liter flask surrounded by two graphite hemispheres approximately 5 cm thick, contained in an oven made of $\frac{3}{8}$" transite board, and heated by inside windings of 16-gage Nichrome wire. The oven was insulated by Sil-O-Cel brick. We found that under these conditions, with a working temperature range of

* In part, from a dissertation submitted by W. D. Walters to the Johns Hopkins University in partial fulfillment of the requirements for the degree of Doctor of Philosophy.

† Wm. R. Warner Fellow in Chemistry, 1934–1938. Present address, University of Rochester.

‡ Hormal Foundation Fellow, 1934–1938.

[1] Rice and Teller, J. Chem. Phys. **6**, 489 (1938).

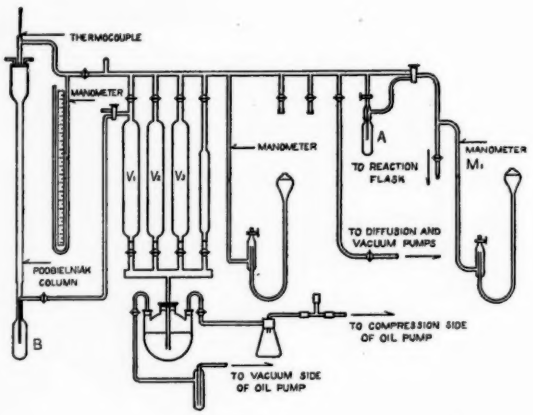

FIG. 1.

450–550°C, there was very little oxidation of the graphite hemispheres. The temperature was measured by means of a Chrome-Alumel thermocouple introduced into a well in the reaction vessel; the thermocouple checked to ±1°C, at the boiling point of sulfur. The reaction flask was connected directly to the distillation apparatus so that a sample could be readily removed and separated into fractions.

In Fig. 1 we show a sketch of the complete apparatus with the exception of the furnace and the reaction vessel. At the beginning of a run, the reaction flask was pumped out and brought up to temperature, and the substrate was introduced from the small flask A. When we were studying the promoted reaction with methyl ethyl ether, it was necessary to make up mixtures of known composition in flask A and evaporate the whole of the material into the reaction flask to prevent error due to selective evaporation. We could follow the course of the reaction by means of the manometer M_1, and at any selected point during the reaction, could quickly pump out the contents of the reaction vessel by connecting it to flask A, cooled in liquid nitrogen, and connecting flask A in turn to the flasks V_1, V_2, V_3, which could be used as a sort of Toepler pump. We did not try to remove more than about 95 percent of the contents of the reaction flask, and simply applied a correction for the amount not removed which we could determine from the reading of the manometer M_1. The contents of the small flask A, and of the bulbs V_1, V_2, V_3, were then transferred to the flask B and distilled through the Podbielniak column, the products being collected again in the bulbs V_1, V_2, V_3; these bulbs were in a glass box and were calibrated so that a measurement of the pressure and the temperature gave the molar contents. The results of the Podbielniak distillation were supplemented when necessary by gas analyses.

The decomposition of *n*-propylamine was studied by a flowing method in an apparatus described in a previous paper.[2] The apparatus used permitted us to make a complete over-all analysis, but we did not do this since we were interested primarily in finding out if any methylamine was present. Accordingly, we simply distilled the contents of the liquid-air trap, using a Podbielniak column, and looked for indications of a break in the distillation curve at the boiling point of methylamine.

3. Decomposition of Methyl Ethyl Ether

The methyl ethyl ether used in these experiments was a commercial sample which was distilled carefully in the Podbielniak column and stored at −80°C until needed. The results of experiments 1 and 2, which were carried out with pure methyl ethyl ether, are summarized in Table I.[3] Considerable amounts of aldehydes are formed as intermediates, and some formaldehyde polymerizes in the first trap A_1. We placed some aniline in the distillation flask B in order to keep the aldehydes in this flask and to prevent

TABLE I. *Decomposition of pure methyl ethyl ether.*

Exp. No.	Temp. °C	In. Press. mm	Time. Min.	% Press. Increase
1	448	596	40	20.0
2	473	401	63	50.5

Products found by Podbielniak distillation. The three fractions were not analyzed; fraction 1 should contain CH_4, CO, and H_2; fraction 2, C_2H_6 and C_2H_4; fraction 3, C_3H_8, C_4H_{10}, and CH_3OCH_3.

Exp. No.	Amount of $CH_3OC_2H_5$ taken cc at NTP	Fraction 1 B. P. < −157°C cc at NTP	Fraction 2 B. P. −90±5°C cc at NTP	Fraction 3 B. P. −73 to +7°C cc at NTP
1	3236	609.5	401.1	113.2
2	2160	1078	358.0	90.7

[2] Rice, Ruoff, and Rodowskas, J. Am. Chem. Soc. **60**, 955 (1938).

[3] These results may be compared with those of previous workers who analyzed the gaseous products. See Glass and Hinshelwood, J. Chem. Soc. 1804 (1929); Ure and Young, J. Phys. Chem. **37**, 1169 (1933).

TABLE II. *Induced decomposition of methyl ethyl ether using azomethane. Experiment 4.*

TEMP. °C	VOL. ETHER cc NTP	VOL. CH_3NNCH_3 cc NTP	% CH_3NNCH_3	IN. PRESS. MM	% PRESS. INCREASE	TIME MIN.
297	3351	19.1	0.57	473.5	16.4	92

Results of distillation and analysis of products cc at NTP

CO	H_2	CH_4	C_2H_4	C_2H_6	$CH_3OC_2H_5$
124.7	44.3	347	10.2	94.4	2878

[a] Ether decomposed = 3351 − 2878 = 473 cc at NTP.
[b] From the above data we estimate that there were about 400 cc (at NTP) of aldehydes and higher boiling compounds that were not decomposed.

TABLE III. *Induced decomposition of methyl ethyl ether using azomethane. Experiment 5.*

TEMP. °C	VOL. ETHER cc NTP	VOL. CH_3NNCH_3 cc NTP	% CH_3NNCH_3	IN. PRESS. MM	% PRESS. INCREASE	TIME MIN.
300	2884	102.3	3.43	426.0	55.8	280

Results of distillation and analysis of products cc at NTP

CO	H_2	CH_4	C_2H_4	C_2H_6	$CH_3OC_2H_5$
630	132	1347	5.9	264	1553

[a] Ether decomposed = 2884 − 1553 = 1331 cc at NTP.
[b] From the above data we estimate that there were about 600 cc (at NTP) of aldehydes and higher boiling compounds that were not decomposed.

them from polymerizing and clogging up the Podbielniak column.

There was no break whatsoever in the distillation curve at the boiling point of dimethyl ether, and the whole fraction collected between −73 and 7°C amounted to barely 10 percent of the total products. Since there is the possibility that in these experiments we are not dealing with radical reactions, or at least, that the radical chain[4] occurs only to a small extent, we decided to study the promoted decomposition of methyl ethyl ether under conditions where the pure substance is stable.

4. PROMOTED DECOMPOSITION OF METHYL ETHYL ETHER

We first made a run with pure methyl ethyl ether at 299°C and an initial pressure of 410 mm. After 277 minutes, the pressure was 413.4 mm, so that there was only 0.8 percent pressure increase. We then performed two experiments at approximately the same temperature by using a mixture of methyl ethyl ether and azomethane. As in runs 1 and 2, we distilled the products, but in these experiments we also made a complete over-all analysis of all the fractions; the results are summarized in Tables II and III. In none of the experiments was there any break in the distillation curve at the boiling point (−24°C) of dimethyl ether. While we did not look so carefully for a break in the case of propane and butane, the distillation curve showed no trace of inflection at these boiling points either. The absence of these compounds indicates that radicals attack neither the carbon nor oxygen atoms of the ether. Both acetaldehyde and formaldehyde were formed in the promoted decomposition; in a fraction in the correct boiling range, the presence of acetaldehyde was proved by its characteristic odor and a test with Schiff's reagent; formaldehyde appeared as its polymer, which was identified by its odor and by the red color produced by its solution in the presence of resorcinol and sodium hydroxide.

As in experiments 1 and 2, there was a small fraction of gas (90–100 cc) collected over the temperature range −73 to +7°C. This fraction appeared to be more or less independent of the size of the original sample, as well as of the amount decomposing. In view of the appearance of these samples which constitute a small, but appreciable amount of the products, we decided to make up known mixtures of ethane, methyl ethyl ether, and dimethyl ether, with the object

[4] See in this connection Staveley and Hinshelwood, Proc. Roy. Soc. **A159**, 198 (1937), who have shown that at 560°C the reaction is inhibited by nitric oxide and that the minimum chain length is 7.5.

TABLE IV. *Thermal decomposition of n-propylamine.*

Moles passed through furnace (39.3 g)	0.664
Moles decomposed	0.02
Percent decomposed	3
Temperature, °C	650
Pressure, mm	10
Time of run (minutes)	10
Moles of gas not condensed by liquid air	0.012
" " C_2 and C_3 hydrocarbons	0.011
" " NH_3	0.005
" " CH_3NH_2	——
" " $CH_3CH_2NH_2$	——

of determining the smallest amount of dimethyl ether that we could detect under conditions similar to those in the distillation of the products of decomposition. We found that we could just detect 47.5 cc of dimethyl ether, which gave a slight break in the distillation curve, whereas with 97 cc we could obtain a definite and true boiling point.

In experiment 5, 1332 cc of methyl ethyl ether were decomposed, and 5 percent should give a detectable break in the distillation curve. In experiment 4, where we decomposed only 472 cc of methyl ethyl ether, we can conclude that any production of dimethyl ether was less than 10 percent of the amount of methyl ethyl ether decomposed.

Assuming that each molecule of azomethane gives two methyl radicals, the number of ether molecules decomposed by the addition of each radical in experiment 4 is 17 and in experiment 5 is 7. Although no special weight can be given to our two results, it is interesting to note that they indicate that the chain length at a given temperature is inversely proportional to the square root of the concentration of the azomethane.

5. DECOMPOSITION OF *n*-PROPYLAMINE

The decomposition of propylamine has been investigated by Sickman and O. K. Rice.[5] They concluded from a study of the decomposition at low pressures that the reaction is probably a chain. The decomposition of ethylamine proceeds[6] through the intermediate formation of diethylhydrazine according to the equation $2C_2H_5NH_2 \rightarrow C_2H_5NHNHC_2H_5$. However the decomposition of diethylhydrazine was shown to be a radical chain, so that we may infer that even if propylamine follows a similar course, free propyl radicals will be formed at some step in the reaction and will decompose into methyl radicals and ethylene.

In our experiments, we used a commercial sample of propylamine which was carefully distilled, and the middle fraction, boiling over a range of 0.5°C was used. The *n*-propylamine was thermally decomposed to the extent of 2–3 percent at 650°C and 10 mm pressure and the results obtained are shown in Table IV. Since we were primarily interested in looking for the presence of lower amines, we did not make a complete over-all analysis of the products formed. There was no indication whatsoever in the distillation curve of the products of a methylamine plateau at −7°C, or of an ethylamine plateau at 17°C.

While our results indicate that reactions of the type

$$R + CH_3CH_2CH_2NH_2 \rightarrow RNH_2 + CH_3CH_2CH_2$$

either do not occur or are followed by redissociation into the original components, it should be pointed out that there is evidence for attack by methyl radicals on the nitrogen atoms in simple azocompounds[7] according to the equation

$$CH_3 + CH_3-N=N-CH_3 \rightarrow (CH_3)_2N=N-CH_3$$

followed by further reaction with radicals to give higher molecular weight compounds.

[5] Sickman and O. K. Rice, J. Am. Chem. Soc. **57**, 22 (1935).

[6] H. A. Taylor and Ditman, J. Chem. Phys. **4**, 212 (1936).

[7] See in this connection Davis, Jahn and Burton, J. Am. Chem. Soc. **60**, 10 (1938); Riblett and Rubin, *ibid.* **59**, 1537 (1937).

On the Predissociation of Several Diatomic Molecules

G. HERZBERG AND L. G. MUNDIE*
Department of Physics, University of Saskatchewan, Saskatoon, Saskatchewan, Canada
(Received November 13, 1939)

From the observed anomalous intensity distribution in the S_2 bands it is concluded that the dissociation limit for the first predissociation of S_2 lies appreciably below the predissociation limit (4.4 ev). It is found that the anomalous intensity as well as the diffuseness persists even at very low pressures (0.01 mm) and that therefore this is a case of genuine predissociation and not pressure broadening as assumed by Lochte-Holtgreven. The second predissociation of S_2 starting with the 18−0 band leads to an upper limit of 3.6 ev for the heat of dissociation of S_2. An anomalous intensity distribution similar to that of S_2 is found for NO assuming that the ϵ absorption bands are a continuation of the γ bands. This indicates a predissociation of NO in the upper $^2\Sigma$ state of the γ bands into normal atoms with a limit 1.3 ev above the dissociation limit. The remarkable intensity distribution found by Schüler and co-workers in the CuH emission band λ4280 at low pressure is explained as due to a predissociation into the $^3\Sigma^+$ state derived from normal $Cu(^2S)$ and normal $H(^2S)$. Such a state cannot cause the predissociation of the level $J'=0$ in agreement with observations. The heat of dissociation of CuH comes out to be $<23{,}325$ cm^{-1} (i.e., <2.892 ev). The method previously suggested by one of the authors for the detection of maxima of potential curves is applied to AlD (AlH) and BH. From the breaking off points observed in the visible bands of these molecules it is established that their $^1\Pi$ states have potential curves with maxima. Therefore the dissociation energies are appreciably lower than the energies of the observed breaking off points, i.e., $D_0(\text{AlH})<24{,}775$ cm^{-1}, $D_0(\text{AlD})<25{,}010$ cm^{-1}, $D_0(\text{BH})<28{,}350$ cm^{-1}.

A. Detection of Predissociation in S_2 and NO by Anomalous Intensity Distribution in Absorption

IT is well known that a diffuse absorption line (or band) under small dispersion appears with greater apparent intensity than a sharp line (or band) of the same true intensity. Therefore, if the true intensity is known in some way, a diffuseness may be detected indirectly by an anomalously large apparent intensity even if it is too slight for direct detection by the spectrograph used. This method has been applied, for example, in a number of cases to the detection of induced predissociation, where it is found that certain bands for the same number of absorbing molecules (that is, the same true intensity) appear more intense at higher pressure due to a predissociation (broadening) induced by collisions. In only one case, it seems, has this method of detection as yet been applied to ordinary predissociation, namely in the case of the D system of the H_2 molecule by Beutler, Deubner and Jünger.[1] This system exhibits in absorption only the bands with $v'\geq 3$ whereas those with $v'<3$ are so weak that they are not observed. Since the true intensity of the 2−0 and 3−0 bands must be of the same order of magnitude the sudden jump in apparent intensity can only be explained by the assumption that the bands with $v'\geq 3$ are broadened in consequence of predissociation even though no visible broadening is found. This conclusion is confirmed by the absence of emission bands with $v'\geq 3$.

Since, as in the above example, this method of detecting ordinary predissociation by anomalously large intensity in absorption is considerably more sensitive than the method employing an actual diffuseness of the bands it should prove useful also in other cases particularly when extremely large dispersion is not available.

In the following we shall describe two further cases in which the method has been applied, namely the absorption spectra of S_2 and NO.

(a) S_2

We have reinvestigated the absorption spectrum of diatomic sulphur vapor with a very long absorbing path (6 meters) hoping to find new weak systems of absorption bands (forbidden transitions) at longer wave-lengths than the well-known main system in the ultraviolet. Although we did find such absorption bands, extending as far as 8700A their analysis, due to small dispersion, has not yet been possible. However we

* Present address: Department of Physics, Purdue University, Lafayette, Indiana.
[1] H. Beutler, A. Deubner and H. O. Jünger, Zeits. f. Physik **98**, 181 (1935).

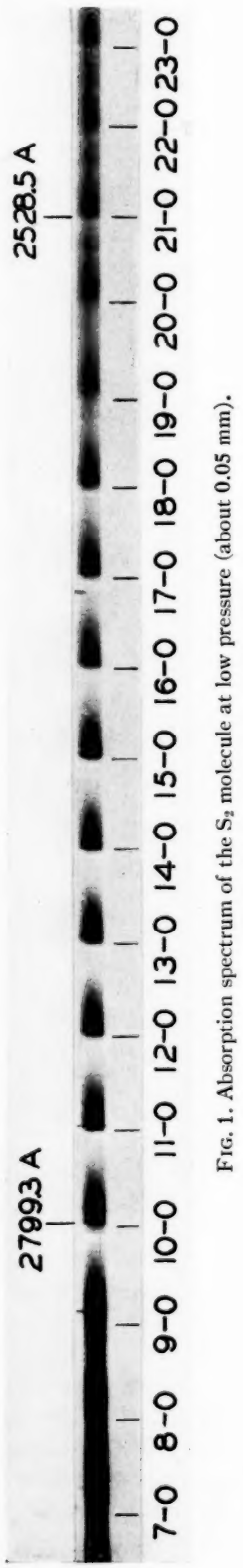

FIG. 1. Absorption spectrum of the S_2 molecule at low pressure (about 0.05 mm).

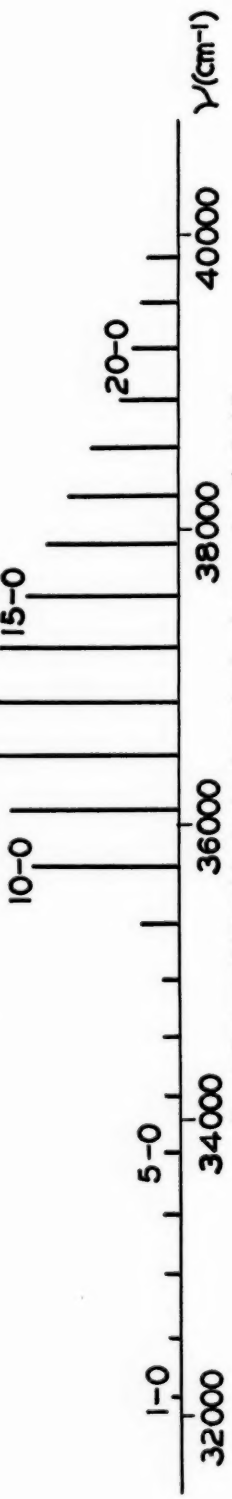

FIG. 2. Estimated intensities in the absorption band progression $v''=0$ of S_2.

also photographed the main absorption system with the long path at correspondingly low pressures and obtained some results that, we believe, are of interest particularly in view of recent controversies concerning the predissociation of the S_2 molecule.

As is well known, there are two points in the main absorption system of S_2 where the bands become diffuse: the first beginning with the $11-0$ band and the second with the $18-0$ band. This is shown by the spectrogram reproduced in Fig. 1. The fine structure lines of the $11-0$ band appear distinctly broadened compared to those of the $10-0$ band. Such a broadening is also present in the $12-0$, $13-0$, $\cdots$ $17-0$ bands although to a lesser and lesser extent. The $18-0$ band and the subsequent bands however are quite diffuse, no fine structure at all being noticeable.

While these facts concerning the predissociation of S_2 have been known for a long time, another point, which until now seems to have escaped consideration, is brought out by our spectrogram Fig. 1: The intensity distribution in the series of bands is quite different from what one would expect from the Franck-Condon principle. Since all the bands have $v''=0$ the intensity should first rise gradually and smoothly and then drop again in the same manner. Actually there is a *sudden jump in the intensity at the 10−0 band:* the bands from $10-0$ on are very strong whereas the preceding bands are quite weak. Within each group of bands, those with $v'<10$ and those with $v'\geq 10$, the intensity does not vary very greatly. Fig. 2 represents graphically the intensity distribution from estimated intensities.

It seems to us that the sudden intensity jump in the progression of S_2 absorption bands can be explained only by the assumption that this is a case, similar to the one observed for H_2 (see above), in which bands appear with an anomalously large intensity because of diffuseness of the fine structure lines. With the dispersion used the $10-0$ band appears to have a sharp fine structure whereas the following bands are visibly diffuse. However from the large intensity of the $10-0$ band we conclude that a diffuseness is present in this band as well, although to a lesser extent, and that therefore *predissociation sets in*

at the $v'=10$ level and not at $v'=11$. This conclusion is in agreement with results of Olsson[2] who investigated the spectrum with very large dispersion and found the 10−0 band to have slightly diffuse lines.

It is significant that as shown by the spectrogram Fig. 1 the fine structure lines of the 9−0 band appear much more intense at some distance from the head than at the head. This distribution is different from that in any other band and indicates that the higher rotational lines of this band are also broadened, i.e., that predissociation occurs for the higher rotational levels of the $v'=9$ state.

In this connection it should be mentioned that, in emission, only bands with $v'\leq 9$ occur (see Olsson[2]) and that the bands with $v'=9$ break off abruptly.[3] This confirms the conclusion that the limit for this particular predissociation lies between some high rotational level of the $v'=9$ state and the lowest rotational level of the $v'=10$ state.[4]

There are essentially two cases of predissociation that consist of radiationless electronic transitions from a discrete to a continuous state. In the first case (*Ib*[5]) the point of intersection of the potential curves of the two electronic states in question lies *below* the asymptote of the potential curve of the state causing the predissociation (see Fig. 3); in the second case (*Ic*) the point of intersection lies *above* the asymptote (see Fig. 4). In the first case predissociation sets in with maximum probability at a point corresponding to the asymptote (dissociation limit). In the second case the maximum probability of the radiationless transition corresponds to the point of intersection of the potential curves which is above the asymptote of one of them; but the predissociation will set in, though with smaller probability, somewhat below this point in consequence of the quantum-mechanical penetration of potential barriers. To be sure, this effect is very slight indeed for molecules as heavy as S_2, except when the potential hill formed by the two intersecting potential curves is very narrow.

In the first predissociation of S_2, however, as shown above, the level $v'=10$ is not predissociating as strongly as the level $v'=11$, and therefore this predissociation does represent an example of case *Ic* with a rather narrow potential hill. Thus we conclude that the *dissociation limit corresponding to this predissociation* (i.e., the asymptote of the potential curve of the state causing the predissociation) *lies appreciably below the predissociation limit.*

This conclusion is the opposite to the one obtained by Rosen, Désirant and Duchesne[4] who, from the observed breaking off in the emission bands with $v'=8$ and 9, according to a method of one of us,[6] concluded that this predissociation belongs to case *Ib*, i.e., that the predissociation limit coincides with the corresponding dissociation limit. However these authors have not analyzed in detail the fine structure of the bands in question. Also there are violent perturbations in the rotational levels of the states $v'=8$ and 9 (see Olsson[2]) so that the above-mentioned method cannot be applied safely, at least not without a detailed analysis of the rotational structure. We consider the arguments for case *Ic* given above as sufficiently strong to rule out definitely case *Ib*. Therefore the energy of the

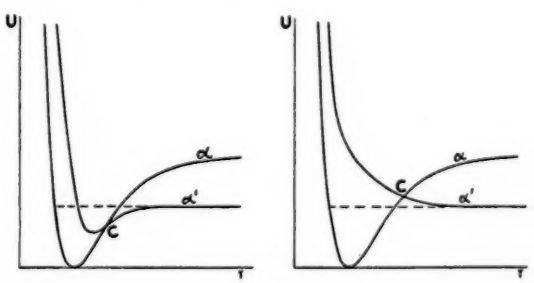

FIG. 3 (left). Potential curves for case *Ib* of predissociation (predissociation limit = dissociation limit).
FIG. 4 (right). Potential curves for case *Ic* of predissociation (predissociation limit > dissociation limit).

[2] E. Olsson, Zeits. f. Physik **108**, 40 (1937); also Thesis, Stockholm, 1938. We had reached the above conclusion before this paper appeared but unfortunately publication of our results was greatly delayed.
[3] G. Herzberg, Ann. d. Physik **15**, 701 (1932).
[4] Rosen, Désirant and Duchesne (Phys. Rev. **48**, 916 (1935)) and Rosen and Bouffieux (Bull. Acad. Belg. 1936, p. 885) have observed a termination of the fine structure of emission bands even with $v'=8$ at a higher value of the rotational quantum number (see however Olsson, reference 2, and further below).
[5] See G. Herzberg, Ergebn. exact. Naturwiss. **10**, 207 (1931); for a slight revision of the nomenclature concerning the subcases of case I of predissociation (radiationless electronic transition) see G. Herzberg, *Molecular Spectra and Molecular Structure I. Diatomic Molecules* (Prentice-Hall, New York, 1939). Case *Ia* is the limiting case between *b* and *c*.
[6] G. Herzberg, Ann. d. Physik **15**, 677 (1932); G. Büttenbender and G. Herzberg, Ann. d. Physik **21**, 577 (1935).

predissociation limit $E(v'=10)=4.4$ ev represents only an upper limiting value for the heat of dissociation of the S_2 molecule.

Lochte-Holtgreven[7] has obtained the absorption spectrum of S_2 in CS_2 vapor at a temperature sufficient to decompose the latter. He claims that in this way it is possible to obtain lower vapor pressures of S_2 with less admixture of polymers than by the usual method. From the spectra obtained he comes to the conclusion that at low vapor pressure the first point of diffuseness in the S_2 spectrum (starting with the $11-0$ band) disappears altogether, and therefore is not due to a genuine predissociation.[8] However, in our experiments even at the lowest pressures used the lines of the $11-0$ band were still broadened compared to those of the preceding and some of the following bands and the anomalous intensity distribution was still present. Since our absorbing layer was 600 cm compared to Lochte-Holtgreven's 65 cm his S_2 pressure was at least 9 times larger than that used by us for the same intensity of absorption. From the temperature of the side tube of our absorption tube (100–180°C) the vapor pressure is found to be between 0.01 and 1 mm. Most of this vapor at a temperature of 950°C of the main absorption tube is in the diatomic form. Furthermore we have carried out experiments also with a short tube (20 cm long) at a correspondingly higher pressure and have not found any noticeable difference in the broadening of the lines or, which is a more critical test, in the intensity distribution of the bands.

Therefore, on the basis of our experiments, covering a much wider range of pressures than Lochte-Holtgreven's, we conclude that *the first point of diffuseness in the S_2 absorption spectrum represents a genuine predissociation which supplies a definite upper limiting value for the dissociation energy of S_2, namely 4.4 ev.* Lochte-Holtgreven's value $D(S_2)=4.7$ volts therefore cannot be maintained.[8a]

The fact that Lochte-Holtgreven arrived at conclusions contrary to ours may be explained in the following way: Apparently he has not himself taken spectra at considerably higher pressures with correspondingly thinner layers and seems to have been under the impression that at high pressures the bands $11-0$ etc. are completely diffuse, which is not the case, the broadening of the fine structure lines even at high pressure being slight when observed with moderate dispersion. Therefore when he found only very slight or no broadening at the relatively low pressures used by him he considered the diffuseness found by others at higher pressures to be a case of pressure broadening. In support of our explanation of Lochte-Holtgreven's results is the fact that his published spectrogram looks exactly like many of those obtained by us under various conditions when the intensity of absorption was the same as his. Unfortunately he does not reproduce the $11-0$ and $12-0$ bands which show the maximum broadening whereas the bands $15-0$, $16-0$, $17-0$ which he does reproduce are rather sharp anyway.[8b] Also he uses a rather high intensity of absorption such that only a few lines of high rotational quantum number really come out on his spectrogram. The little that is left of the continuous background in such a spectrogram is more likely to appear sharp than when a moderate intensity of absorption is used.

In contrast to the first predissociation of S_2 the second one seems to set in with maximum probability, occurring at the $18-0$ band which is entirely diffuse. However on closer examination of the spectrogram it is seen that the lines of the $17-0$ band are not as sharp as those of the preceding bands.[9] This shows that the second predissociation, too, belongs to case *Ic*.[10] However, since for this second predissociation the maximum probability is at any rate not farther away from the limit than in the case of the first predissociation the two states causing the two predissociations cannot lead to the same combination of atoms, because, if they did, the potential hill for the second predissociation would be narrower than for the first and the second predissociation should set in more slowly. The simplest assumption then is that the first predissociation leads to normal atoms ($^3P+^3P$) whereas the second leads to one normal S atom (^3P) and one S atom in the first excited state (^1D, excitation energy $A=1.1$ ev). From the latter assumption it would follow (since, as shown, even the second

[7] W. Lochte-Holtgreven, Zeits. f. Physik **103**, 395 (1936).

[8] See also the controversy between Lochte-Holtgreven and Olsson in Zeits. f. Physik **109**, 147 (1938).

[8a] Compare also M. Burton and G. K. Rollefson [J. Chem. Phys. **6**, 416 (1938)] who accepted Lochte-Holtgreven's conclusion as correct in their discussion of photochemical primary processes.

[8b] It should be noted that Lochte-Holtgreven's numbering of the bands is not the same as the one adopted here and by most investigators of the S_2 spectrum.

[9] Cf. also the spectrogram reproduced by Lochte-Holtgreven, reference 7.

[10] The only alternative would be to assume that the broadening in the $17-0$ band is due to a predissociation other than that in the $18-0$ band and the subsequent bands.

predissociation limit is somewhat above the corresponding dissociation limit) that the *dissociation energy of* S_2 *into normal atoms is somewhat smaller than* $E(v'=17)-A(^1D)=3.6$ *ev.* In other words the potential hill for the first predissociation would be at least $4.4-3.6=0.8$ ev high. In view of this height, it is plausible that the hill is sufficiently narrow to allow a noticeable quantum-mechanical leaking through even for such a heavy molecule as S_2.

Since the upper limiting value 3.6 ev just derived for $D_0(S_2)$ is based on an assumption about the products of dissociation at the second predissociation of S_2 it is not quite as certain as the upper limiting value 4.4 ev derived from the first predissociation. However, we consider it very likely that the smaller upper limiting value, 3.6 ev, is also correct. Both upper limiting values are in agreement with the assumption that the pressure dependent broadening of the absorption bands 5−0 to 9−0 found by Kondratjew and Olsson[11] is a genuine induced predissociation and not just a pressure broadening since the energy of the $v'=5$ level is 4.2 ev above the ground state.

(b) NO

A case similar to that of S_2 seems to occur for NO. In recent compilations of band spectra four absorption systems of NO are given, the β, γ, δ and ϵ systems. An examination of the spectrograms published by Leifson[12] shows that the first four absorption bands of the γ system have roughly equal intensities. Hitherto the succeeding bands were thought to be hidden by the ϵ bands. These ϵ bands are very much stronger than the preceding γ bands but they lie exactly in the positions expected for the succeeding γ bands. This leads us to the conclusion, on the basis of the above discussion, that they simply are the 4−0, 5−0$\cdots\gamma$ bands which have anomalously large intensity in consequence of predissociation. Thus a *predissociation limit* is fixed *between 51,088 and 53,271* cm^{-1}.

TABLE I. *Wave numbers of the* γ *and* ϵ *absorption bands of* NO *according to Leifson.*[12]

	$v'-v''$	ν(cm^{-1})	$\Delta\nu=\Delta G'$
γ	0−0	44,156	2336
	1−0	46,492	2317
	2−0	48,809	2279
	3−0	51,088	2183
ϵ	4−0*	53,271	2297
	5−0*	55,568	2245
	6−0*	57,813	2187
	7−0*	60,000	

* This numbering is on the assumption that the ϵ bands belong to the γ system.

In Table I the wave numbers of the bands of the γ and ϵ systems in absorption are given according to the measurements of Leifson. It is seen that the differences between successive bands are quite compatible with the assumption that they form one system. A slight unevenness in the differences may either be due to a perturbation which is likely to occur near the point of intersection of two potential curves or to the fact that the two groups of bands have so widely different intensities and were measured on spectrograms of very small dispersion.

The dissociation energy of NO is known to be 5.29 volts. The next dissociation limit above this is 7.26 volts which is higher than the above determined predissociation limit 6.6 volts. Therefore we have a *predissociation into normal atoms* and the point of intersection of the potential curves of the $^2\Sigma$ upper state of the γ bands and the state causing the predissociation lies high above the asymptote of the latter, that is we have *case Ic of predissociation.* This is not surprising if we consider that the $^2\Sigma$ upper state of the γ bands has an r_e value appreciably smaller and an ω_e value appreciably larger than that of the ground state, so that the point of intersection of its potential curve with any repulsive curve is bound to be high above the asymptote. The state causing the predissociation is most probably the $^2\Sigma$ state arising from normal atoms $N(^4S)+O(^3P)$. Apart from this $^2\Sigma$ state and the $^2\Pi$ ground state only quartet states, which are not likely to cause such a strong predissociation, result from normal atoms. According to the noncrossing rule the potential curves of the $^2\Sigma$ state just mentioned and of the $^2\Sigma$ upper state of the γ bands must avoid each other. But the fact that only a predissociation of the stable $^2\Sigma$ state and no

[11] V. Kondratjew and E. Olsson, Zeits. f. Physik **99**, 671 (1936).

[12] S. W. Leifson, Astrophys. J. **63**, 73 (1926).

violent perturbations take place indicates that the interaction of the two states is slight and that the two potential curves *almost* cross.

Indications of other predissociations of the NO molecule have previously been found. Kaplan[13] attributed the absence in emission of β bands with $v'>4$ to a predissociation. Flory and Johnston[14] found a photochemical decomposition of NO by light of the wave-length of the $1-0$ and $2-0$ δ bands, whereas they noted that δ bands with $v'=0$ are the only ones observed in emission. This predissociation limit in the δ bands is at about the same height as that in the γ bands found above. It is quite likely that all three observed predissociations of NO are caused by the same repulsive $^2\Sigma$ state resulting from normal atoms. It should be pointed out that Flory and Johnston's experiments do not exclude the possibility of a photochemical decomposition by absorption of light of the $4-0$, $5-0$ γ bands which should occur according to the above interpretation of the anomalous intensity distribution. The observation of γ bands in emission with $v'>3$ (see Guillery[15]), which would contradict our explanation, does not appear to be definite.

B. Detection of Predissociation in CuH by Anomalous Intensity Distribution in Emission

Schüler, Gollnow and Haber[16] in a recent paper have found a remarkable intensity distribution in the CuH band at λ4280 when excited in a hollow cathode at low pressure (0.02 mm). Instead of the usual maximum of intensity in each of the branches they find that the first line of the P branch $P(1)$ is the most intense while all subsequent lines of the P branch and all lines of the R branch are much weaker and increasingly so with increasing J. The line $P(1)$ is the only line having $J'=0$ in the upper state. It is thus this *level $J'=0$* which under the conditions mentioned is *much more strongly populated than the others.* Schüler and his co-workers have suggested that this anomalous distribution is due to the process of formation of the CuH molecules. However it

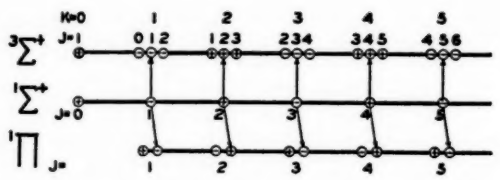

FIG. 5. Predissociation of a stable $^1\Sigma^+$ state into an unstable $^3\Sigma^+$ and an unstable $^1\Pi$ state. The level $J=0$ of the $^1\Sigma^+$ state cannot predissociate, according to Kronig's selection rules, even if such a predissociation were energetically possible.

seems impossible to picture a formation of CuH in a three-body collision at room temperature leading to CuH molecules practically only in the $J'=0$ level which would correspond to an extremely low temperature. Also the molecules would have to be formed directly in the upper state of the bands because, if first formed in the lower ground state, in a subsequent excitation about as many molecules with $J'=1$ should be formed as with $J'=0$.

We would like to propose an entirely different explanation for this phenomenon: Numerous cases are known of a breaking off of the fine structure of electronic bands at a certain J' value produced by predissociation. If above a certain energy (J' value) in the upper state of a band system predissociation is possible and if the radiationless transition probability is larger than the probability of transitions to the lower state with radiation a breaking off or at least a sudden decrease in intensity of the lines in a band will occur. But this is just the phenomenon occurring for CuH except that here the sudden decrease of intensity occurs for $J'\geq 1$ so that only one line in the band is strong. Therefore we propose to *explain the anomalous intensity* observed by Schüler and co-workers *as a predissociation.* This explanation would of course imply that the dissociation energy of CuH is smaller than the excitation energy of the $J'=1$ level of the upper electronic state, that is $<23{,}325$ cm^{-1} (or <2.892 ev). This is entirely possible since a linear extrapolation of the vibrational quanta of the ground state yields $D_0(\text{CuH})\approx 24{,}300$ cm^{-1} and since such linear extrapolations are known to give D_0 values which are usually somewhat too large.

It is however not necessary to make the assumption that the predissociation limit just

[13] J. Kaplan, Phys. Rev. **37**, 1406 (1931).
[14] P. J. Flory and H. L. Johnston, J. Am. Chem. Soc. **57**, 2641 (1935).
[15] M. Guillery, Zeits. f. Physik **42**, 121 (1927).
[16] H. Schüler, H. Gollnow and H. Haber, Zeits. f. Physik **111**, 484 (1939).

happens to fall between the levels $J'=0$ and $J'=1$ of the upper $^1\Sigma^+$ state of the CuH band as long as it is below 23,325 cm^{-1}, because *if the unstable state causing the predissociation is a* $^1\Pi$ *or* $^3\Sigma^+$ *state the* $J=0$ *level of the* $^1\Sigma^+$ *upper state of the CuH band cannot predissociate no matter where the predissociation limit lies.* This is illustrated by Fig. 5. According to Kronig's selection rules[17] only states with the same value of J and the same symmetry can predissociate into each other. But a $^1\Pi$ state has no level with $J=0$ and in a $^3\Sigma^+$ state the only level with $J=0$ has the opposite symmetry $(-)$ to that of the $J=0$ level $(+)$ of $^1\Sigma^+$ (see Fig. 5).

A Cu atom in the ^2S ground state and an H atom in the ^2S ground state give rise to two molecular states $^1\Sigma^+$ and $^3\Sigma^+$ of which the former is the ground state. Therefore if a predissociation into normal atoms is assumed the only state that can cause the predissociation is the $^3\Sigma^+$ state and such a state according to the above cannot cause a predissociation of the $J'=0$ level, in agreement with observation. Thus under this assumption the predissociation limit and, *a fortiori*, the corresponding dissociation limit may be appreciably below the energy of $J'=1$ (23,325 cm^{-1}).

It is not impossible although much less likely that the predissociation leads to a normal H atom and a Cu atom in the excited ^2D state. In that case six states arise from the separated atoms. For two of them, $^3\Sigma^+$ and $^1\Pi$ the same arguments as above would apply for the nonpredissociation of the $J'=0$ level (see Fig. 5). But the predissociation may also be caused by two of the other four states arising from $^2S+^2D$ (namely $^1\Sigma^+$ or $^3\Pi$) and then the nonpredissociation of the level $J'=0$ would not follow automatically. Moreover in this case the heat of dissociation of CuH into normal atoms would have to be $<12{,}125$ cm^{-1} (i.e., <1.503 ev) which appears to be too small although not impossible. Thus we consider it as most likely that the *predissociation is caused by the* $^3\Sigma^+$ *state resulting from normal atoms and that therefore* $D_0(CuH)<23{,}325$ *cm*$^{-1}$.

Our assumption that the upper $^1\Sigma^+$ state of the CuH band predissociates into $^3\Sigma^+$ contradicts Kronig's selection rule that the spin S should not change in a radiationless transition. But intercombinations between singlet and triplets have been found to occur for predissociations of the heavier molecules just as for transitions with radiation.[17]

In a predissociation $^1\Sigma^+\rightarrow{}^3\Sigma^+$ as well as in a predissociation $^1\Sigma^+\rightarrow{}^1\Pi$ the radiationless transition probability increases roughly proportionately to J. While for $^1\Sigma^+\rightarrow{}^1\Pi$ this has been known for a long time (Kronig) it follows for $^1\Sigma^+\rightarrow{}^3\Sigma^+$ from a recent paper of Budó and Kovács[18] who calculated the perturbations between a $^1\Sigma^+$ and a $^3\Sigma^+$ state. The observations of Schüler and co-workers are in qualitative agreement with this theoretical conclusion since they found that the intensity continues to drop even after the jump from $J'=0$ to $J'=1$ whereas if the radiationless transition probability were independent of J one would expect to find after the breaking off point an increase of intensity up to the usual thermal maximum which would occur at $P(5)$.

There remains to explain the fact that at higher pressures the complete CuH band appears with the usual intensity distribution, the line $P(1)$ having no longer any abnormally large intensity. It seems to us that this is the well-known *pressure effect of predissociation* also observed for AlH, CaH and SrH.[17, 19] At higher pressures in consequence of the collisions the molecules in the $J'=0$ state, whose natural life is longer than in the states with $J'\geq 1$, will go back to the ground state without radiation or will go over to the other rotational levels of the excited state, or will be dissociated by collisions (induced predissociation), and eventually a distribution corresponding to thermal equilibrium is set up. While this is the same explanation as for the other observed cases of pressure effect, the remarkable thing in the case of CuH is that such very low pressures are necessary in order to bring out the anomalous intensity distribution produced by predissociation. Even at a pressure as low as 2 mm the $P(1)$ line is not the most intense line of the band. This occurs only at a considerably lower pressure. However, this can easily be understood because here (unlike the

[17] See G. Herzberg, *Molecular Spectra and Molecular Structure I. Diatomic Molecules* (Prentice-Hall, New York 1939).

[18] A. Budó and I. Kovács, Zeits. f. Physik **111**, 633 (1939).

[19] See also Olsson, Dissertation, Stockholm, 1938.

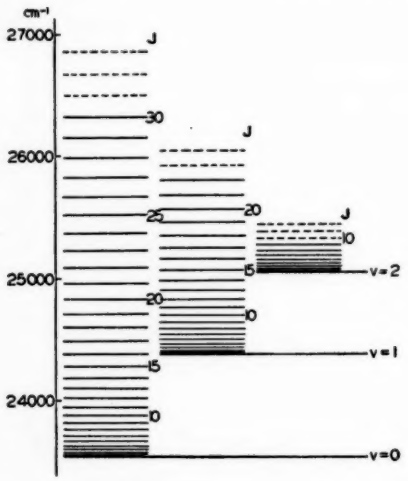

FIG. 6. Observed rotational levels in the $^1\Pi$ state of AlD according to Holst and Hulthén, reference 21. The broken lines refer to predissociating levels (see, however, reference 23).

other cases) we have an intercombination for which the radiationless transition probability is not very much larger than the probability for transitions with radiation, as is also evidenced by the fact that lines with $J'>0$ do appear at the lowest pressure used even though with much smaller intensity than the line with $J'=0[P(1)]$. Therefore it requires only comparatively few collisions to produce a nearly thermal distribution. To be sure the distribution is not yet entirely thermal at a pressure of 2 mm.

Very probably it will be possible to detect weak predissociations of other molecules by observing their band spectra in emission at such low pressures as were used by Schüler and co-workers for CuH.

It should be remarked that according to the above interpretation one would expect to find a similar intensity distribution in CuH bands of the same system with $v'>0$, but such bands have not been investigated by Schüler and his co-workers.

C. On Potential Hills in the Predissociation of AlH and BH

If one wants to determine the dissociation energy of a molecule from predissociation data it is necessary to know whether the predissociation occurs across a potential hill or not. The criterion used in Section A for deciding this question in the case of the predissociation of the S_2 molecule (noncoincidence of predissociation limit with maximum probability of radiationless transition) is in general not applicable to predissociations observed by a breaking off of emission bands. But as pointed out by one of us[20] a decision is possible *if a breaking off of the rotational fine structure can be observed in at least two but preferably three successive vibrational levels.*

In Fig. 6 the observed rotational energy levels in the $^1\Pi$ state of AlD are represented according to the data of Holst and Hulthén.[21] The predissociating levels are indicated by broken lines. The fact that predissociation starts at a higher energy for the lower vibrational levels is known to be due to the fact that the heights of the maxima of the effective potential curves increase with increasing rotational quantum number J.

The *effective potential energy* $U_J(r)$ for the rotating molecule (in cm^{-1} units) is given by

$$U_J(r)=U_0(r)+\frac{h}{8\pi^2 c\mu r^2}J(J+1), \qquad (1)$$

where $U_0(r)$ is the potential energy without rotation ($J=0$). If $U_0(r)$ has no maximum the maxima of $U_J(r)$ will shift to smaller r values with increasing rotation. If the *energies of the maxima* $U_{max}(J)$ are *plotted against* $J(J+1)$ a

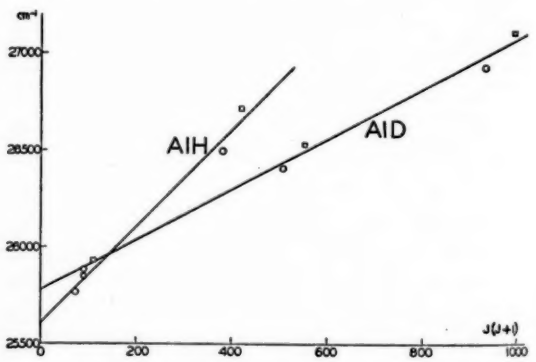

FIG. 7. Breaking off points of AlD and AlH for the various vibrational levels of the $^1\Pi$ state plotted as a function of $J(J+1)$. The circles represent the last nonpredissociating levels, the squares the first predissociating levels for the respective vibrational levels. The ordinate gives the energy above the minimum of the ground state $^1\Sigma$.

[20] G. Herzberg, Ann. d. Physik **15**, 677 (1932); J. Phys. Chem. **41**, 299 (1937); Astrophys. J. **89**, 290 (1939); see also reference 17.

[21] W. Holst and E. Hulthén, Zeits. f. Physik **90**, 712 (1934).

curve that is convex to the abscissa axis is obtained (limiting curve of dissociation). It intersects the ordinate axis with horizontal tangent at an energy value equal to $U_0(\infty)$, i.e., equal to the dissociation limit of the electronic state in question.[22] *If, however, $U_0(r)$ has a maximum* the maxima of the effective potential curves $U(r)$ will all be at approximately the same r value and therefore according to (1) *approximately a straight line will result for $U_{max}(J)$ if plotted as a function of $J(J+1)$*. This will intersect the ordinate axis at $U_0(r_{max})$, the potential energy at the point of the maximum (without rotation). This conclusion is independent of whether the potential maximum for zero rotation is due to an intersection of two potential curves or not.

From the experimental breaking off points a few points on the curve $U_{max}(J)$ as a function of $J(J+1)$ may be obtained since the breaking off will occur for those levels for which the sum of vibrational and rotational energy equals $U_{max}(J)$ for the particular J value. In Fig. 7 the breaking off points in the $^1\Pi$ *state of AlD*, represented in Fig. 6, are plotted as a function of $J(J+1)$ and thus the U_{max} curve is obtained. It is seen that the points lie very closely on a straight line which proves that the *potential energy without rotation has a maximum.*[23] Fig. 8 shows the corresponding plot for the $^1\Pi$ *state of BH* (calculated from the data of Almy and Horsfall[24]). Again a straight line is obtained proving that the potential curve without rotation has a maximum. This is not surprising since the two $^1\Pi$ states of AlD and BH are analogous also in other respects.

It is only in rare cases that a breaking off is observed (as for AlD and BH) in three successive vibrational levels of an electronic state of a diatomic molecule. If such a breaking off is only observed in two successive vibrational levels a decision as to whether the rotationless curve has a maximum or not may yet be obtained. The slope of the straight line through the two breaking off points in a diagram such as Figs. 7 and 8 according to (1) gives the mean r value of the two corresponding maxima of the effective potential curves. This r value is equal to the r value of the maximum of the rotationless curve if such is present. However, the maximum of a rotationless curve (or, in other words, the intersection of two potential curves) always lies at comparatively small r values, usually smaller than twice the equilibrium internuclear distance r_e of the state considered, whereas the maxima of the effective potential curves for an ordinary rotationless curve (without maximum) lie at appreciably larger r values, at least for not too large J values.

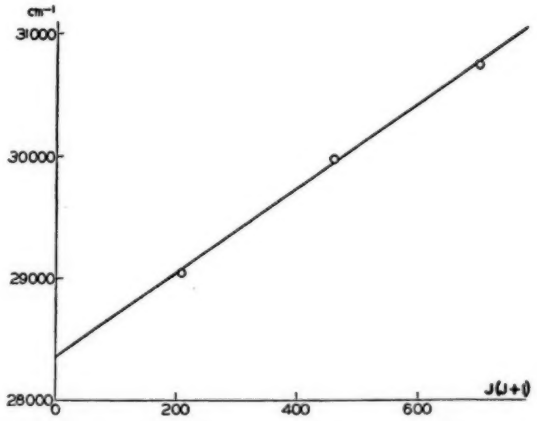

FIG. 8. Breaking off points of BH in the $^1\Pi$ state. Almy and Horsfall whose data have been used here give only the J value for the sudden decrease of intensity but do not state where the decrease starts. Therefore only one point is given for each vibrational level. The ordinate gives the energy above the level $v=0$, $J=0$ of the ground state.

Thus a *large slope* of the line connecting two breaking off points[25] in a diagram like Fig. 7 indicates a *maximum of the rotationless potential curve* or in case I of predissociation (radiationless electronic transition) it indicates the *subcase* (*c*) in which the point of intersection of the two potential curves lies above the asymptote of one of them (see Fig. 4). On the other hand, a *small slope* of the line in question indicates a *normal*

[22] See G. Büttenbender and G. Herzberg, Ann. d. Physik **21**, 577 (1935); G. Herzberg, J. Phys. Chem. **41**, 299 (1937); R. Schmid and L. Gerö, Zeits. f. Physik **104**, 724 (1937).

[23] Olsson, reference 19, gives slightly lower breaking off points obtained from unpublished observations at low pressure. If his data are plotted they do not fall as exactly on a straight line as the points in Fig. 7 (taken from Holst and Hulthén, reference 21). However, the curve obtained does not have a horizontal tangent for $J(J+1)=0$ and therefore the above conclusion as to the existence of a potential hill would not be changed by adopting his data. The curvature if real would be due to the fact that for large J values the position of $U_{max}(J)$ shifts slightly even when there is a potential hill in the rotationless curve.

[24] G. M. Almy and R. B. Horsfall, Phys. Rev. **51**, 491 (1937).

[25] Or a large initial slope of the curve obtained from more than two breaking off points (see reference 23).

potential curve or in case *I* the *subcase* (*b*) in which the point of intersection is below the asymptote (see Fig. 3).

As an example let us consider the $^1\Pi$ state of AlH which (unlike AlD) shows only two breaking off points. These also are indicated in Fig. 7. The slope of the line gives $r_{max}=2.643$ whereas $r_e=1.646$ thus indicating a maximum of the potential curve $U_0(r)$.[26] Of course this was to be expected since the maximum has already been proven for AlD. The r value for the maximum comes out to be the same for AlH and AlD within less than 0.01A.

As shown above, the intersection of the straight line in Fig. 7 or 8 with the ordinate axis gives the energy of the potential maximum of the rotationless curve (apart from the influence of the tunnel effect considered below). For AlD this energy comes out to be 25,173 cm^{-1} for BH 28,350 cm^{-1} above the $v=0$, $J=0$ level of the ground state. These values represent *upper bounds for the dissociation energies* of the respective molecules, but since there is a potential hill the actual values will be smaller by an appreciable amount.

If the energies are referred to the minimum of the potential curve of the ground state, as is done in Fig. 7, the points of intersection of the straight lines for AlH and AlD with the ordinate axis, that is the maxima of the rotationless potential curves of the two isotopic molecules, do not coincide exactly as one might perhaps expect. The values are 25,610 cm^{-1} and 25,775 cm^{-1}, respectively. The difference, as has previously been pointed out by Olsson,[27] is due to the quantum-mechanical penetration through potential barriers (*tunnel effect*) near the top of the hill. In consequence of this effect the breaking off points in Fig. 7 and 8 do not actually give the maxima of the effective potential curves but energies somewhat below. The difference will be larger for AlH than for AlD because H penetrates the potential hill more easily, that is, farther below the top, than D and this explains the small difference in the energies of the breaking off points for zero rotation of AlH compared to AlD. While of course the difference in energy between the top of the potential hill and the breaking off point for AlH is larger than the difference between the breaking off points for AlH and AlD it will certainly be of the same order of magnitude, that is the *influence of the tunnel effect is slight.* We are therefore justified in applying the above semi-classical method to the detection of the potential hills. The influence of the tunnel effect will be smaller yet for atoms heavier than H or D, and in general may be neglected for them except for very narrow potential hills, such as the one for S_2 discussed above where the influence is certainly present but yet slight.

The dissociation limit has of course the same energy above the minimum of the potential curve of the ground state in AlH and AlD and consequently the smaller of the two upper bounds (that for AlH) applies to both isotopic molecules. Subtracting the zero point energies we obtain for the *dissociation energies* referred to $v=0$, $J=0$ *of the ground state* $D_0(AlH)<24{,}775\ cm^{-1}$ $(=3.072\ ev)$ *and* $D_0(AlD)<25{,}010\ cm^{-1}$ $(=3.101\ ev)$.[28]

The above considerations concerning potential hills and the method of their detection, as has been mentioned before, are equally applicable for case *Ic* and *III* of predissociation[5] i.e., they are independent of whether the potential hill is formed by the intersection of two potential curves or whether it is present in a single zero rotation potential curve. According to von Neumann and Wigner if the potential curves of two electronic states of the same species cross in a zero approximation they will not do so in higher approximation. Thus, strictly speaking, case *Ic* is not possible for two states of the same species. But a maximum of a single potential curve may always be thought of as brought about by the intersection of two zero approximation curves of the same species (an attractive and a repulsive one), and it would depend on the

[26] As early as 1933 E. Hulthén and R. Rydberg [Nature **131**, 470 (1933)] suggested that there is a potential hill in the rotationless curve of the $^1\Pi$ state of AlH, but did not give a satisfactory proof for it. In a recent paper [Zeits. f. Physik **113**, 126 (1939)] Hulthén, in referring to this potential hill, says that it is so narrow and low that the breaking off at low pressure is not influenced by it and that therefore the breaking off point in the level $v'=2$ of AlD gives directly the dissociation limit of the $^1\Pi$ state. In our opinion this is by no means the case. Hulthén's discussion refers only to the very top of the potential hill that has been established here.

[27] E. Olsson, Zeits. f. Physik **108**, 322 (1938).

[28] If Olsson's data, reference 23, for the breaking off points were used very slightly smaller limits for D_0 would be obtained.

strength of the interaction of the two states whether one would consider the predissociation as case *Ic* or *III*.

In the cases of AlH (AlD) and BH we have apparently a case of two states of the same species interacting so strongly that these predissociations are most adequately described by case *III*. If the two states were not of the same species, or if for like species the interaction were small, and case *Ic* would apply one would expect to find, at least in absorption, transitions to higher vibrational levels beyond the predissociation limit, which at least for AlH is definitely not the case. The $^1\Pi$ state that predissociates may result from normal atoms Al (or B) (^2P)+H (^2S). But such a state also arises from the first excited ^2P state of Al (or B)+H (^2S). Apparently the former $^1\Pi$ state is "originally," that is in zero approximation, repulsive whereas the upper $^1\Pi$ state is attractive. The latter for smaller r presses the former downward giving rise to a minimum in its potential curve and a maximum at larger r values. Information about the height of the maximum can be obtained only after the heat of dissociation of these molecules has been obtained from other data.

MARCH, 1940 JOURNAL OF CHEMICAL PHYSICS VOLUME 8

The Partition Functions and Energy Levels of Molecules with Internal Torsional Motions

BRYCE L. CRAWFORD, JR.*
Mallinckrodt Chemistry Laboratory, Harvard University, Cambridge, Massachusetts
(Received December 11, 1939)

The complete energy matrix is set up for external and (hindered) internal rotations of "pseudo-rigid" molecules; i.e., molecules consisting of a rigid framework to which symmetric hindered rotators are attached. The reduced secular equation for the energy levels of such a molecule with one internal rotation is given explicitly. By using the perturbation method of Wilson, the partition function for this model is found, correct to the second order. Effects due to angular momentum couplings are included. A simple method for the calculation of thermodynamic contributions of hindered internal rotations is given. As an example, the application of the method to propylene is described; in this case, the coupling terms here included may amount to as much as 19 percent of the effect of the hindering potential on the thermodynamic contributions.

IT is now generally accepted that the internal rotations of methyl groups in organic compounds are restricted by potential barriers of appreciable magnitude. In order to determine these barrier heights from thermal, spectroscopic, and molecular structure data, it is necessary to study the dynamics of the molecules and to evaluate the partition functions for both the external and internal rotational degrees of freedom.

The quantum mechanics has been worked out by Nielsen[1] for the molecule consisting of two tops on a common axis. If these tops are identical, the wave-functions are periodic Mathieu functions; the thermodynamic contributions of such systems have been evaluated by Pitzer.[2] Ethane, C_2D_6,[3] and dimethyl acetylene[4] correspond to this model.

The quantum mechanics has not been worked out, however, for molecules in which the axis of the top does not pass through the center of gravity (e.g., methyl alcohol), or for molecules with several tops (e.g., propane). In this paper we present a study of the "pseudo-rigid" mole-

* Present address: Sterling Chemistry Laboratory, Yale University, New Haven, Connecticut. This research was carried out while the writer held a National Research Fellowship in Chemistry.

[1] H. H. Nielsen, Phys. Rev. **40**, 445 (1932). See also J. B. Howard, J. Chem. Phys. **5**, 451 (1937).

[2] K. S. Pitzer, J. Chem. Phys. **5**, 469 (1937).

[3] J. D. Kemp and K. S. Pitzer, J. Am. Chem. Soc. **59**, 276 (1937). G. B. Kistiakowsky, J. R. Lacher, and F. Stitt, J. Chem. Phys. **7** 289 (1939).

[4] B. L. Crawford, Jr., and W. W. Rice, J. Chem. Phys. **7**, 437 (1939).

cule, the over-all moments of inertia of which do not change with internal rotations. Such molecules consist of a rigid framework to which symmetric tops are attached. Examples of this class are propane, isobutene, acetone, and the methyl amines; simple molecules falling outside this class include ethyl alcohol and *n*-butane.

Thermodynamic Results

In this section we shall describe the nature of the partition function obtained, and shall give the final expressions for the thermodynamic contributions, postponing the rather involved derivation.

The partition function for the external and internal rotations may be written

$$Q=Q_R \prod_m Q_M(m), \tag{1}$$

where Q_R is the partition function for over-all rotation, and $Q_M(m)$ is the partition function for the internal hindered rotation of the mth top. The effects of angular momentum couplings, etc., are all included in the $Q_M(m)$. Hence the thermodynamic contributions of the over-all rotations are the usual ones for a rigid molecule; the moments of inertia, I_1, I_2, I_3, are to be evaluated for the molecule as a whole. The symmetry number for these contributions is obtained by considering the internal rotations to be frozen; e.g., $\sigma=6$ for ethane, $\sigma=1$ for propylene and for methyl alcohol.

The contributions of the internal hindered rotations being additive, we may describe $Q_M(m)$ for a single such motion. Let the mth top have a moment of inertia A_m about its axis, and let λ_{m1}, λ_{m2}, λ_{m3} be the direction cosines of the top axis with respect to the principal axes of the molecule as a whole. For the hindering potential, we use $(V_m/2)(1-\cos \nu_m\alpha_m)$, where α_m is the angle of rotation of the top about its axis, ν_m is the number of minima encountered in one complete rotation, and V_m is the height of the maxima.

The energy levels for the internal motion depend on the eigenvalues a_{mr} of the Mathieu equation

$$(d^2\psi/dx^2)+(a_{mr}+2\theta_m \cos 2x)\psi=0.$$

These a_{mr} depend upon the quantum number r ($r=0, \pm1, \pm2$, etc.), and upon the quantity θ_m, which is essentially the hindering potential:

$$\theta_m=V_m(8\pi^2A_m\Omega_m/h^2\nu_m^2). \tag{2}$$

Here h is Planck's constant and Ω_m is an important geometrical parameter:

$$\Omega_m=1-\sum_{i=1}^{3}(A_m/I_i)\lambda_{mi}^2. \tag{3}$$

The nature of Ω_m is best understood from the fact that $(A_m\Omega_m)$ may be regarded as a "reduced moment" for the top. Tables of the necessary a_{mr} exist.

The internal energy levels are vibrational in character for low values of the quantum number r, and rotational for high r; the angular momentum interactions for these two types of level are different. The partition function $Q_M(m)$ is found by summing over the energy levels in the usual way; it turns out that the interactions can be included if we break the sum into two parts, one for the "vibrational" and one for the "rotational" levels, and use appropriate factors for the two. The point of separation, $r=r_0$, is easily found on inspection of the a_{mr} for the particular case.

Writing

$$Y_{mr}=(h^2\nu_m^2/32\pi^2A_m\Omega_mRT)a_{mr}, \tag{4}$$

where R is the gas constant, we find

$$Q_M(m)=\exp(-q_m)\,[\Omega_m^{\frac{1}{2}}G_R+G_V], \tag{5}$$

$$G_R=\sum_R \exp(-\Omega_m Y_{mr}),$$
$$G_V=\sum_V \exp(-Y_{mr}). \tag{6}$$

The index R indicates that the sum is over all $r\geqslant r_0$, and the index V indicates summation over all $r<r_0$. The factor $\exp(-q_m)$ merely adjusts the zero of energy:

$$q_m=V_m/2RT. \tag{7}$$

The thermodynamic contributions due to the mth top may be written:

$$(E/T)_M=R[q+(H/G)],$$
$$(F/T)_M=R[q-\ln G],$$
$$S_M=R[\ln G+(H/G)],$$
$$C_M=R[(J/G)-(H/G)^2], \tag{8}$$

where

$$G=(\Omega_m{}^{\frac{1}{2}}G_R+G_V);\quad H=(\Omega_m{}^{\frac{1}{2}}H_R+H_V);$$
$$J=(\Omega_m{}^{\frac{1}{2}}J_R+J_V),$$
$$H_R=\sum_R \Omega_m Y_{mr}\exp(-\Omega_m Y_{mr}),$$
$$H_V=\sum_V Y_{mr}\exp(-Y_{mr}),\qquad (9)$$
$$J_R=\sum_R \Omega_m{}^2 Y_{mr}{}^2\exp(-\Omega_m Y_{mr}),$$
$$J_V=\sum_V Y_{mr}{}^2\exp(-Y_{mr}).$$

It will be seen that for cases in which Ω_m may be taken as unity, the distinction between G_R and G_V vanishes, and the partition function (5) reduces to the simple sum over states for a Mathieu system. The corresponding thermodynamic contributions have been given by Pitzer[2] in his Eqs. (2) and (3) and tables, so that no direct calculation is necessary in such cases. The "reduced moment," $A_m\Omega_m$, becomes simply the moment of the top.

The "quantum effects," which require the introduction of the symmetry number in Q_R, are particularly easy to take into account in $Q_M(m)$. It turns out that the result obtained by using only levels of a certain symmetry, say of class A, in our sums G_R, G_V, etc., gives a very good approximation, except at very low temperatures. The error may be estimated by evaluating $G_V(A)$, using A levels only, and $G_V(B)$, using B levels only, and noting the difference, r_0 being taken so that $G_V(A)$ and $G_V(B)$ have the same number of levels. No symmetry number factor is used.

These A and B eigenvalues are those which are given in the ordinary tables such as those of Ince;[5] with his notation, the eigenvalues a_n and b_n belong to the A class if n is even, and to the B class if n is odd. In evaluating G_R, H_R, J_R, the following approximate expression is useful for finding higher values of a_{mr}; in Ince's notation,

$$a_n=b_n=n^2+[\theta^2/2(n^2-1)].$$

This formula is valid for small θ and large n; for $n=6$, $\theta=16$, the error in a_n is less than 1 percent. A convenient method of finding the eigenvalues accurately is given in reference 11.

For very small values of Ω_m, it may be necessary to use the exact expressions for G_R and G_V given in Eq. (42); the error due to use of the above expressions (6) may be estimated by noting the effect of changing the position of r_0 to include one more or less level in G_V.

The application of this method to the case of propylene is discussed in the last section. We now proceed to the derivation of the energy matrix and the partition function described above.

Kinetic Energy

Let there be N symmetric tops in the molecule, attached to a rigid framework. Let I_1, I_2, I_3 be the moments of inertia of the molecule as a whole (framework and tops) about the principal axes. These axes and moments are independent of the rotations of the tops. We retain the notations described in the previous section. Then it is not hard to show[6] that the classical kinetic energy is given by the expression

$$2T=\sum_{m=1}^{N} A_m\dot{\alpha}_m{}^2+\sum_{i=1}^{3} I_i\omega_i{}^2+2\sum_{i=1}^{3}\sum_{m=1}^{N} A_m\lambda_{mi}\omega_i\dot{\alpha}_m, \qquad (10)$$

where ω_i is the instantaneous angular velocity of the molecule about the principal axis i.

This expresses the kinetic energy as a quadratic form in the $(N+3)$ velocities, ω_i and $\dot{\alpha}_m$. The Hamiltonian form of the kinetic energy is a quadratic form in the conjugate momenta

$$P_i=(\partial T/\partial\omega_i),\quad P_m=(\partial T/\partial\dot{\alpha}_m).$$

The matrix of the Hamiltonian quadratic form is the inverse of the matrix of (10); carrying out this inversion (see below) yields the expression

$$2T=\sum_m \frac{1}{F_m}P_m{}^2+\sum_i\sum_j \beta_{ij}P_iP_j+\sum_m\sum_{n\neq m}{}' \Delta_{mn}P_mP_n$$
$$+2\sum_m\sum_i \gamma_{mi}P_mP_i, \qquad (11)$$

where the terms have the following meanings. The first term gives the energy of over-all rotation of the molecule; the β_{ij} are analogous to

[5] E. L. Ince, Proc. Roy. Soc. Edinburgh **52**, 355 (1931), especially p. 363. Ince's θ corresponds to our θ_m; his a_n, b_n correspond to our a_{mr}, for positive and negative r, respectively, if n is even, and vice versa if n is odd.

[6] L. S. Kassel, J. Chem. Phys. **4**, 276 (1936); or one may use the method of E. B. Wilson, Jr., and J. B. Howard, J. Chem. Phys. **4**, 260 (1936).

reciprocal moments of inertia, and are best defined through the matrix

$$(g_{ij})=(\delta_{ij}-\tau_{ij}), \tag{12}$$

where

$$\tau_{ij}=(I_iI_j)^{-\frac{1}{2}}\sum_m A_m\lambda_{mi}\lambda_{mj} \tag{13}$$

and δ_{ij} is the Kronecker symbol. Then

$$\beta_{ij}=(I_iI_j)^{-\frac{1}{2}}g^{ij}, \tag{14}$$

where (g^{ij}) is the matrix inverse to (g_{ij}). If g is the determinant of (g_{ij}), then the determinant of β is

$$|\beta|=(I_1I_2I_3g)^{-1}. \tag{15}$$

The second term in (11) gives the energy of the internal motions; the F_m are corrected moments of inertia:

$$(1/F_m)=(1/A_m)+\Delta_{mm}, \tag{16}$$

where

$$\Delta_{mn}=\sum_i\sum_j\lambda_{mi}\beta_{ij}\lambda_{nj}. \tag{17}$$

The third term expresses the coupling between different tops (note that only terms between *different* tops are included in the summation), while the last term gives the angular momentum coupling between the top motions and the overall rotations; here

$$\gamma_{mi}=-\sum_j\lambda_{mj}\beta_{ji}. \tag{18}$$

Since the coefficients in (12) are constants, this equation gives the quantum-mechanical kinetic energy operator, if for P_i we write $\mathbf{P}_i$, and for P_m, $\mathbf{P}_m$.[7] Here the $\mathbf{P}_i$ are the angular momentum operators studied by Klein,[8] and $\mathbf{P}_m=(h/2\pi i)(\partial/\partial\alpha_m)$. The wave functions must be periodic in α_m with period 2π.

The inversion of (10) is conveniently carried out by matrix technique.[9] Denoting the matrix of the quadratic form (10) by (T), we may break it up into four sub-matrices:

$$(T)=\begin{pmatrix}T_1 & T_3\\ \tilde{T}_3 & T_2\end{pmatrix}.$$

Here

$$(T_1)_{mn}=A_m\delta_{mn},\quad (T_2)_{ij}=I_i\delta_{ij},\quad (T_3)_{mi}=A_m\lambda_{mi},$$

and $\tilde{T}_3$ is the transpose of T_3, these two being rectangular matrices. If we break up (T^{-1}) in the same way, writing

$$(T^{-1})=\begin{pmatrix}\zeta & \gamma\\ \tilde{\gamma} & \beta\end{pmatrix},$$

and use the fact that $(T)(T^{-1})=(T^{-1})(T)=E$, where E is the identity matrix, we can find relationships between the sub-matrices. We obtain

$$\beta^{-1}=T_2-\tilde{T}_3T_1^{-1}T_3,$$
$$\gamma=-T_1^{-1}T_3\beta,$$
$$\zeta=T_1^{-1}+\Delta=T_1^{-1}+T_1^{-1}T_3\beta\tilde{T}_3T_1^{-1},$$

and the problem is reduced to the inversion of the 3-by-3 matrix (β^{-1}), since T_1^{-1} and T_2^{-1} can be written down at once.

Case in which $N=1$

For a molecule with a single top, (11) reduces to

$$2T=\sum_i\sum_j\beta_{ij}P_iP_j+\frac{1}{F_m}P_m^2+2\sum_i\gamma_{mi}P_mP_i. \tag{19}$$

The elimination of the sum over m results in simple expressions for the parameters:

$$g=\Omega_m=1-\sum_i\tau_{ii}=1-\rho_m,$$
$$F_m=A_m\Omega_m=\rho_m/\Delta_{mm}, \tag{20}$$
$$\gamma_{mi}=-\lambda_{mi}/I_i\Omega_m.$$

For the molecule composed of two tops on a common axis, (19) can be transformed into Nielsen's equation,[1] which involves no interaction terms. Unless the tops are identical, however, the new boundary conditions demand nonperiodic solutions, as Nielsen points out. It is more convenient to work with periodic solutions, retaining the interaction, therefore, except in the case of ethane-like molecules.

[7] B. Podolsky, Phys. Rev. **32**, 812 (1928). This procedure has been justified for $\mathbf{P}_x$, $\mathbf{P}_y$, $\mathbf{P}_z$ by Wilson and Howard, reference 6.

[8] O. Klein, Zeits. f. Physik **58**, 730 (1929).

[9] See, for example, R. A. Frazer, W. J. Duncan, and A. R. Collar, *Elementary Matrices* (Cambridge University Press, 1938).

Case in which $N>1$

For a molecule containing several tops, it proves convenient to regard the τ_{ij} as small, and neglect terms of second order in τ_{ij}. In most applications of interest, methyl groups will be involved; if there are two or more methyl groups attached to a framework, the ratio A_m/I_i will indeed be small, and it will be reasonable to neglect τ_{ij}^2. On this basis we find

$$\begin{aligned} \Omega_m &= (1-\rho_m), \\ g &= \prod_m \Omega_m, \\ F_m &= A_m \Omega_m, \\ \gamma_{mi} &= -\lambda_{mi}/I_i, \\ \Delta_{mn} &= \sum_i (\lambda_{mi}\lambda_{ni}/I_i), \end{aligned} \tag{21}$$

where

$$\rho_m = \sum_{i=1}^{3} (A_m/I_i)\lambda_{mi}^2.$$

Energy Matrix

Potential energy

The energy operator consists of the kinetic energy (11) plus the potential energy, which we write

$$2V = \sum_m V_m(1-\cos \nu_m \alpha_m), \tag{22}$$

neglecting possible interaction terms of the type $V_{mn}(\alpha_m,\alpha_n)$. The use of the cosine form is desirable for mathematical simplicity, and is supported (though not conclusively) by the heat capacity data on ethane.[3] The parameters defining the potential barrier, are ν_m, the number of minima encountered in one complete rotation, and V_m, the height of the maxima, as described in the first section.

The complete Hamiltonian may be written:

$$\mathbf{H} = \mathbf{H}_0 + \mathbf{H}_1, \tag{23}$$

where

$$\begin{aligned} \mathbf{H}_0 &= \mathbf{P}^2 + \sum_m \mathbf{H}_m, \\ \mathbf{H}_1 &= \sum_m \mathbf{P}_m \mathbf{p}_m + (1/2) \sum_m \sum_{n\neq m}{}' \Delta_{mn}\mathbf{P}_m\mathbf{P}_n, \\ 2\mathbf{H}_m &= (1/F_m)(\mathbf{P}_m)^2 + V_m(1-\cos \nu_m\alpha_m), \\ \mathbf{P}^2 &= (1/2) \sum_i \sum_j \beta_{ij}\mathbf{P}_i\mathbf{P}_j, \\ \mathbf{p}_m &= \sum_i \gamma_{mi}\mathbf{P}_i. \end{aligned} \tag{24}$$

Zeroth-order energy

The term $\mathbf{P}^2$ gives the rotational energy of a top which has the moment of inertia tensor (β^{-1}). The rotational energy matrix may be written down in terms of the usual quantum numbers J, K, M.[8]

The term $\mathbf{H}_m$ gives the energy of internal rotation for the mth top. The wave-equation obtained from the operator $\mathbf{H}_m$ may be written in the form

$$\partial^2\psi_{mr}/\partial x^2 + (a_{mr} + 2\theta_m \cos 2x)\psi_{mr} = 0, \tag{25}$$

which is one form of Mathieu's equation,[10] with $2x = \nu_m\alpha_m$. For the quantum number, r, we use that of the limiting free rotator derived by setting $\theta_m = 0$; hence $r = 0, \pm 1, \pm 2, \cdots$. The degeneracy of the "positive" and "negative" levels is lifted for $\theta_m \neq 0$, if r is a multiple of $(\nu_m/2)$; the "negative" level has the lower energy. In general, the energy will be

$$w_{mr} = (a_{mr} + 2\theta_m)(h^2\nu_m^2/32\pi^2 F_m). \tag{26}$$

The parameter θ_m is given by Eq. (2). Unfortunately, a_{mr} is not a simple function of r and θ_m.

As was mentioned above, the lower levels of this Mathieu system closely approximate those of a harmonic oscillator, while as r increases, the levels change and become like those of a free rotator. This transition takes place quite abruptly, so that we may speak of "vibrational" and "rotational" levels in this connection.

Energy matrix

It will be convenient to write the energy matrix $\mathbf{H}$ in terms of sub-matrices, each sub-matrix corresponding to certain sets of Mathieu quantum numbers, r, and being itself a function of J, K, and M. (Throughout we shall use r and s as Mathieu quantum numbers for the mth and nth tops, respectively.) If we write

$$v_{mrr'} = \int \psi_{mr}^* \mathbf{P}_m \psi_{mr'} d\tau, \tag{27}$$

[10] This form is chosen to conform to Ince, reference 5, as his tables of the eigenvalues a_{mr} are the most extensive we have found. The discrepancy in the sign of the term in $\cos 2x$ arises because we choose to regard V_m and θ_m as positive; this difference does not affect our results.

then the sub-matrices of $\mathbf{H}$ are

$$\mathbf{H}^{rs,\,rs}=\mathbf{P}^2+\sum_m v_{mrr}\mathbf{p}_m + \{\sum_m w_{mr}+\tfrac{1}{2}\sum_m\sum_n{}'\Delta_{mn}v_{mrr}v_{nss}\}\mathbf{E},$$
$$\mathbf{H}^{rs,\,r's'}=\sum_m v_{mrr'}\mathbf{p}_m+\{\tfrac{1}{2}\sum_m\sum_n{}'\Delta_{mn}v_{mrr'}v_{nss'}\}\mathbf{E}, \quad r\neq r' \tag{28}$$

where $\mathbf{E}$ is the identity matrix. This expression is valid for any form of potential energy which does not include interactions $V_{mn}(\alpha_m,\alpha_n)$.

The large $\mathbf{H}$ matrix can be factored by using the symmetry properties of the Mathieu functions. The levels can be classified into the symmetry classes of the group $\mathbf{D}_{\nu_m}$[11] (e.g., $\mathbf{D}_3$ for the methyl group in C_2H_6). Using the fact that $\mathbf{P}_m$ has symmetry A_2, we can show that $v_{mrr'}$ must vanish unless the r and r' levels belong to one of the pairs (A_1,A_2), (B_1,B_2), (E_k,E_k). By expanding the E_k functions in exponentials instead of sine and cosine terms, we may eliminate interactions between E_k^+ and E_k^-. Thus we have $\mathbf{H}$ factored in $\Pi_m\nu_m$ factors, of symmetries (A_1+A_2), (B_1+B_2), E_k^+, E_k^- for each top.

Limiting values

For the "rotational" levels in each factor, the limiting value of a_{mr} is $4r^2/\nu_m^2$. If we use exponential expansions for the "rotational" wave functions of the (A_1+A_2) factor, as we may without difficulty, the limiting value of $v_{mrr'}$ is the same for all factors; *viz.*,

$$v_{mrr'}=(h/2\pi)r\delta_{rr'}. \tag{29}$$

For the "vibrational" levels, there will be ν_m levels, one of each symmetry factor, with the same energy. Writing t for the "vibrational" quantum number which we may use in place of r,[12] we find

$$a_{mt}=2(2t+1)(\theta_m)^{\frac{1}{2}}-2\theta_m \tag{30}$$

and the nonvanishing elements $v_{mtt'}$ are

$$v_{m,\,t,\,t+1}=-v_{m,\,t+1,\,t}=(h/4\pi i)\nu_m(t+1)^{\frac{1}{2}}\theta_m^{\frac{1}{4}}. \tag{31}$$

Energy levels

To find the separate energy levels from the energy matrix, we must write out $\mathbf{P}^2$ and $\mathbf{p}_m$ in terms of J, K, M. First, however, we shall find it convenient to rotate axes so that the matrix β becomes diagonal. This rotation also affects the $\mathbf{p}_m$. If C is the orthogonal transformation (rotation of axes) which diagonalizes β, so that

$$\sum_k\sum_l \tilde{C}_{ik}\beta_{kl}C_{lj}=(1/I_i')\delta_{ij},$$

then we can easily show that we must take

$$\mathbf{p}_m=\sum_i \mu_{mi}\mathbf{P}_i',$$
$$\mu_{mi}=\sum_j \gamma_{mj}C_{ji},$$
$$\mathbf{P}_i'=\sum_j C_{ij}^{-1}\mathbf{P}_j.$$

The insertion of Klein's matrices[8] for the $\mathbf{P}_i'$ yields the energy sub-matrices $\mathbf{H}^{r,\,r}$ and $\mathbf{H}^{r,\,r'}$ as explicit functions of J, K, and M. The complete energy matrix $\mathbf{H}$ is diagonal in J and M. By regarding the matrices $\mathbf{H}^{r,\,r'}$ as perturbations, and applying perturbation methods,[13] the energy matrix may be rendered diagonal in r, correct to the third order in the elements of $\mathbf{H}^{r,\,r}$. The expression for the energy of a molecule with a single top, for example, may be written (the subscript m has been dropped)

$$W_{J,\,K,\,M,\,r}=(h^2/8\pi^2)\times\{\tfrac{1}{2}(B_1+B_2)J(J+1)+B_0\eta\}+w_r, \tag{32}$$

where η is the root of the secular equation whose

---

[11] E. B. Wilson, Jr., J. Chem. Phys. **6**, 740 (1938), gives the symmetries for $\nu_m=6$, corresponding to C_2H_6 in his coordinates. The general case is in exact analogy. It may be pointed out that these symmetry properties do not depend on our use of the cosine-form potential energy; they demand only that V_m be an even function of α_m with period $(2\pi/\nu_m)$.

[12] As $\theta_m\to\infty$, or $r\to 0$, a group of ν_m levels will coalesce to give the ν_m-fold degenerate vibrational level designated by the vibrational quantum number t. ($t=0, 1, 2, \cdots$.) In this group there will be one level belonging to each of the symmetry factors mentioned above. The relation between r and t may be written

$$\nu_m t=|2r|-k$$

with $0\leqq k<\nu_m$ for r positive, and $0<k\leqq\nu_m$ for r negative. The plot of w_{mr} against θ_m (reference 1) makes this clear.

[13] J. H. Van Vleck, Phys. Rev. **33**, 484 (1929); O. M. Jordahl, Phys. Rev. **45**, 87 (1934); Wilson and Howard, reference 6. In applying this method, we have regarded the spacing between interacting Mathieu levels r, r' as large compared to the over-all rotational spacing; i.e. $w_{r'}-w_r>B^0(2K+1)$. This will be true for the "vibrational" levels; for the "rotational" levels, the value of $v_{mrr'}$ decreases to zero and the interaction becomes negligible as $(w_{r'}-w_r)$ becomes small.

nonvanishing elements are

$$(K,K)=-\eta+K^2+(4\pi\mu_3 v_{rr}/hB_0)K,$$

$$(K,K+1)=(\mu_1-i\mu_2)[(J-K)(J+K+1)]^{\frac{1}{2}}\times[(2\pi/h)v_{rr}-d\mu_3(2K+1)]/B_0, \quad (33)$$

$$(K,K+2)=\frac{1}{2C_0}\left(\frac{1}{I_1'}-\frac{1}{I_2'}\right)f(J,K+1).$$

The matrix is of course Hermitian; the symbols have the following meanings:

$$f(J,K)=-\tfrac{1}{2}[(J-K)(J-K+1)\times(J+K)(J+K+1)]^{\frac{1}{2}},$$

$$d=\sum_{r'\neq r}{}' v_{rr'}{}^2/(w_{r'}-w_r),$$

$$B_i=(1/I_i)-2d\mu_i{}^2, \quad i=1,2,3,$$

$$B_0=B_3-(B_1+B_2)/2.$$

The secular equation for the molecule with several tops may be found by the same technique.

Partition Function: Single Top

We shall use the method given by Wilson[14] to find the partition function from the energy matrix (28). It is not necessary to diagonalize β. We shall first develop the case $N=1$, and then extend our results to the general case.

Zeroth-order expression

If we include only the terms of $\mathbf{H}_0$, as given in (24), we see at once that the partition function, Q, for internal and external rotational motion, is given by

$$Q=Q_R(I_1I_2I_3g)\ Q_M{}^{(0)}(q_m,\theta_m), \quad (34)$$

where Q_R is the usual rotational partition function for an asymmetric top of moment of inertia product $|\beta^{-1}|=I_1I_2I_3g$ (Eq. (15)).

$$Q_R=(8\pi^2/h^3)(2\pi kT)^{\frac{3}{2}}(I_1I_2I_3g)^{\frac{1}{2}} \quad (35)$$

$Q_M{}^{(0)}$ is the sum-of-states for a Mathieu system, as evaluated by Pitzer.[2]

$$Q_M{}^{(0)}=\sum_{r=0}^{\infty}\exp(-w_{mr}/RT)=\exp(-q_m)\sum_{r=0}^{\infty}\exp(-a_{mr}q_m/2\theta_m), \quad (36)$$

$$q_m=V_m/2RT.$$

First-order correction

The interaction term in $\mathbf{H}^{r,r}$, the term $(v_{mrr}\mathbf{p}_m)$, is linear in the $\mathbf{P}_i$. We may take account of this term by a change of variable which eliminates linear terms; the transformation

$$\mathbf{P}_i=\mathcal{P}_i-\sum_j(\beta^{-1})_{ij}\gamma_{mj}v_{mrr} \quad (37)$$

reduces $\mathbf{H}^{r,r}$, after simplification, to

$$\mathbf{H}^{r,r}=\mathcal{P}^2+\mathbf{E}(w_r-\tfrac{1}{2}\Delta_{mm}v_{rr}{}^2). \quad (38)$$

Here

$$\mathcal{P}^2=\tfrac{1}{2}\sum_i\sum_j\beta_{ij}\mathcal{P}_i\mathcal{P}_j.$$

Since Q_R is classical, and since the transformation (37) has a Jacobian equal to unity and leaves the matrix of $\mathbf{P}^2$ unaltered, we may leave Q_R unchanged and write

$$Q=Q_R(I_1I_2I_3g)\ Q_M{}^{(1)}(q_m,\Omega_m,\theta_m). \quad (39)$$

The evaluation of $Q_M{}^{(1)}$ is more complex. If we define two parameters κ_{mr} and ϵ_{mr}, such that

$$\kappa_{mr}=1-\epsilon_{mr}=(16\pi^2/h^2\nu_m{}^2)(v_{mrr}{}^2/a_{mr}),$$

then we may write, after algebraic manipulation,

$$Q_M{}^{(1)}=\sum_{r=0}^{\infty}\exp-(w_r-\tfrac{1}{2}\Delta_{mm}v_{mrr}{}^2)/RT$$

$$=\exp(-q_m)\sum_{r=0}^{\infty}\exp\left[-\frac{a_{mr}q_m}{2\theta_m}(1-\rho_m\kappa_{mr})\right]$$

$$=\exp(-q_m)\sum_{r=0}^{\infty}\exp\left[-\frac{a_{mr}q_m\Omega_m}{2\theta_m}\times\left(1+\frac{\rho_m}{\Omega_m}\epsilon_{mr}\right)\right], \quad (40)$$

the two forms being equivalent. Now for "rotational" Mathieu levels, $\epsilon_{mr}\leqq 0$; for "vibrational" levels, $\kappa_{mr}\leqq 0$. We may fix a transition point

[14] E. B. Wilson, Jr., J. Chem. Phys. 7, 948 (1939). This method is based on the perturbation technique of reference 13.

$r=r_0$, and write

$$Q_M^{(1)}=\exp(-q_m)[G_R(\theta_m, q_m\Omega_m) + G_V(\theta_m, q_m)], \quad (41)$$

where

$$G_R=\sum_{r\geq r_0}\exp\left[-\frac{q_m\Omega_m}{2\theta_m}a_{mr}\right]\exp\left[-\frac{q_m\rho_m}{2\theta_m}a_{mr}\epsilon_{mr}\right],$$
$$G_V=\sum_{r<r_0}\exp\left[-\frac{q_m}{2\theta_m}a_{mr}\right]\exp\left[+\frac{q_m\rho_m}{2\theta_m}a_{mr}\kappa_{mr}\right]. \quad (42)$$

This expression is exact; the sharpness of transition between the two types of Mathieu level is such that we may neglect the second exponentials and write, as in Eq. (6),

$$G_R=\sum_{r\geq r_0}\exp[-(q_m\Omega_m/2\theta_m)a_{mr}],$$
$$G_V=\sum_{r<r_0}\exp[-(q_m/2\theta_m)a_{mr}]. \quad (43)$$

Second-order correction

In taking account of the $\mathbf{H}^{r,r'}$ matrices, we assume at once that the levels with $r<r_0$ are strictly vibrational, and those with $r>r_0$ strictly rotational. Using the limiting values (29) to (31), we find the second-order correction $(\mathbf{H}_2)^{r,r}$ vanishes for $r>r_0$ (rotational); and for $r<r_0$, we may write, using the quantum-number t,[12]

$$(\mathbf{H}_2)^{t,t}=\mathbf{p}_m^2\{[|v_{mt,t+1}|^2/(w_{mt}-w_{m,t+1})] + [|v_{mt,t-1}|^2/(w_{mt}-w_{m,t-1})]\}$$
$$=-F_m\mathbf{p}_m^2/2,$$

where

$$\mathbf{p}_m^2=\sum_i\sum_j\gamma_{mi}\gamma_{mj}\mathbf{P}_i\mathbf{P}_j.$$

The transformed diagonal sub-matrix, $\mathfrak{IC}^{r,r}$, correct to the third order, is now given by

$$\mathfrak{IC}^{r,r}=\mathbf{H}^{r,r}+(\mathbf{H}_2)^{r,r}$$
$$=\mathcal{P}^2-F_m\mathbf{p}_m^2/2+\mathbf{E}(w_{mr}-\tfrac{1}{2}\Delta_{mm}v_{mrr}^2) \quad (44)$$

for "vibrational" levels, and by (38) for "rotational" levels. Since the transformation (37), involving v_{mrr}, justifies us in taking $\mathcal{P}^2=\mathbf{P}^2$ for vibrational levels, we may combine the matrices of the first two terms of (44), writing

$$\mathbf{H}_R{}^r=\mathbf{P}^2-F_m\mathbf{p}_m{}^2/2$$
$$=\sum_i(1/2I_i)\mathbf{P}_i^2.$$

Hence for the vibrational levels we must use $Q_R(I_1I_2I_3)$ for the over-all rotational partition function, and not $Q_R(I_1I_2I_3g)$. Thus we have, recalling (41) and (35)

$$Q=\exp(-q_m)[Q_R(I_1I_2I_3)\ G_V+Q_R(I_1I_2I_3g)\ G_R]$$
$$=Q_R(I_1I_2I_3)\ Q_M,$$

where

$$Q_M=\exp(-q_m)\ [\Omega_m{}^{\frac{1}{2}}G_R+G_V]. \quad (45)$$

PARTITION FUNCTION: GENERAL CASE

In extending the treatment to the case in which $N>1$, we assume that terms in τ_{ij}^2 are negligible. The neglected terms encountered in the algebra do in fact tend to cancel, reducing the error.

One of the most unfavorable cases is dimethyl ether, for which $\tau_{11}=0.23$, $\tau_{22}=0.089$, other $\tau_{ij}=0$. Here, fortunately, the error is reduced to a negligible amount by cancellation due to symmetry; such beneficial effects are found for any molecule in which the tops are symmetrically placed (symmetry C_{2v} or higher). In cases of such large τ_{ij}, however, it is better to calculate the needed parameters from Eq. (12) to (18) and the definition $\Omega_m=F_m/A_m$, rather than from (21).

The zeroth-order approximation is quickly written down:

$$Q=Q_R(I_1I_2I_3g)\prod_{m=1}^{N}Q_M{}^{(0)}(q_m, \theta_m).$$

The first-order correction is found as it was for the single-top case; here the transformation (37) becomes

$$\mathbf{P}_i=\mathcal{P}_i-\sum_j\sum_m(\beta^{-1})_{ij}\gamma_{mj}v_{mrr}.$$

The transformation results in the cancellation of terms in Δ_{mn}, giving

$$\mathbf{H}^{r,r}=\mathcal{P}^2+\mathbf{E}\left\{\sum_m\left(w_{mr}-\frac{\Delta_{mm}}{2}v_{mrr}{}^2\right)\right\}.$$

This is exactly similar to (38); proceeding as

TABLE I.

T, °K	(C_M-C_f), Eq. (45)	$(C_M^{(0)}-C_f)$, Eq. (36)	Percent Deviation
148.1	0.85	0.69	−19
225.35	1.16	1.04	−10
333.9	0.99	1.02	+ 3
367.1	0.90	0.97	+ 7

before, we find

$$Q=Q_R(I_1I_2I_3g)\prod_m Q_M^{(1)}(q_m,\theta_m,\Omega_m)$$

with $Q_M^{(1)}$ given by (41).

In finding the second-order correction, we neglect terms in Δ_{mn} (the corrections from these terms would be of order τ_{ij}^2); proceeding as for the former case, we get one term for each "vibrating" top:

$$\mathbf{H}_2^{r,r}=-\sum_n(F_n/2)\mathbf{p}_n^2,$$

the sum being over all tops with $r<r_0$. We neglect the error caused by adding this matrix to that of $\mathcal{P}^2$, and write

$$\mathcal{H}^{r,r}=\mathbf{H}_R{}^r+\mathbf{E}\left\{\sum_m\left(w_{mr}-\frac{\Delta_{mm}}{2}v_{mrr}{}^2\right)\right\}.$$

Evaluating the moment of inertia product corresponding to $\mathbf{H}_R{}^r$, we find the corresponding over-all rotational partition function to be

$$Q_R(I_1I_2I_3g/\prod_n\Omega_n),$$

the product being over all "vibrating" tops. It follows that the complete partition function is

$$Q=Q_R(I_1I_2I_3)\prod_{m=1}^{N}Q_M(q_m,\Omega_m,\theta_m), \qquad (46)$$

Q_M being given by (45).

Symmetry Effects

The "quantum effects" due to symmetry have not yet been mentioned. Except at very low temperatures (below 50°K for ordinary methyl group rotations), these may be included just as in the case of over-all rotation, by summing over levels of *all* symmetries in (42) or (43) and then dividing the partition function by the symmetry number ν_m. However, if we take $\Omega_m=1$, and write $G(A)$ for the sums taken over levels of symmetry A_1 and A_2 only, etc., then except at very low temperatures we find that $G(A)=G(B)=G(E_k{}^+)$, etc. While it does not follow that $G_R(A)=G_R(B)$, etc., it turns out that this is a good approximation. Therefore we may adopt the procedure discussed in the first section, using only the A levels, and omitting the symmetry number factor.

An Example: Propylene

The results of the application of this method to the internal hindered rotation in propylene have been published;[15] a few details of the calculation will be given here by way of illustration. The interatomic distances were taken to be: C−H, 1.09; C−C, 1.54; C=C, 1.33A; the angles of the CH_3 group were assumed to be tetrahedral, and all other angles were taken to be 120°. The value of Ω_m was found to be 0.7622, appreciably different from unity; the "corrected moment" of the methyl groups was thus $F_m=4.014(10^{-40}$ g cm$^2)$. The value $\theta_m=12$ ($V_m=2119$ cal./mole) gave the best agreement with thermal data. Two levels each were taken for $G_V(A)$ and $G_V(B)$, values of a_{mr} being taken from Ince;[5] these sums were found to be 7.0918 and 7.0923, respectively, at the boiling point, 225.35°K. It is apparent that we may take $G_V(A)=G_V(B)$ without appreciable error. When three levels were included in $G_V(A)$, the value of S_M increased by 0.01 e.u.

A comparison of the results obtained from the zeroth-order expression (36) with those obtained from the more complete form (45) is of interest. At 225.35°K, the entropy difference due to the barrier, (S_f-S_M), where S_f is the entropy contribution for free rotation, was found to be 1.08 e.u., from (45); the zeroth-order approximation gave $(S_f-S_M{}^{(0)})=1.21$ e.u., the difference amounting to 12 percent. A similar comparison of the calculated heat capacity contributions is given in Table I.

In concluding, I wish to express my thanks to Professor E. B. Wilson, Jr., for many helpful suggestions during the course of this study, and for permission to quote the calculations on propylene, carried out in his laboratory.

[15] B. L. Crawford, Jr., G. B. Kistiakowsky, W. W. Rice, A. J. Wells, and E. B. Wilson, Jr., J. Am. Chem. Soc. **61**, 2980 (1939).

An Experimental Determination of the Electron Affinity of Chlorine

J. J. MITCHELL* AND JOSEPH E. MAYER**
Chemical Laboratory of The Johns Hopkins University, Baltimore, Maryland

(Received December 8, 1939)

The electron affinity of chlorine has been determined to be about 92.7 kcal. by measuring the ratio of ions to electrons and atoms leaving a hot tungsten surface. Owing to the reactivity of the chlorine a certain erratic behavior leads to some possible scepticism as to the accuracy of the result.

INTRODUCTION

BY using a hot (~2000°K) tungsten filament exposed to an atmosphere of dilute ($P \sim 10^{-2}$ mm Hg) chlorine gas in the center of a magnetron tube the ratio of negative ions to electrons leaving the filament can be determined, whereas the number of neutral atoms may be calculated from the pressure of surrounding chlorine gas. These data permit the calculation[1,2] of the equilibrium constant for the reaction

$$Cl_g + e_g^- \rightarrow Cl_g^- \qquad (1)$$

as

$$K = \frac{P_{Cl^-}}{P_{Cl} P_{e^-}} = \frac{I_i}{I_{e^-}} \left(\frac{M_{Cl} T_R}{2 m_e T_f P_{Cl_2}} \right)^{\frac{1}{2}}, \qquad (2)$$

in which: I_i and I_{e^-} are the negative ion and electron currents, M_{Cl} and m_e the masses of chlorine atoms and electrons, P_{Cl_2} the pressure of Cl_2 gas in the apparatus measured at the temperature T_R, and T_f is the temperature of the filament.

Since, for the reaction (1)

$$RT \ln K = -\Delta F^0 = E_0 + F_{e^-}{}^0 + F_{Cl}{}^0 - F_{Cl^-}{}^0, \qquad (3)$$

in which the free energies F^0 are at unit pressure measured from free energy zero at absolute zero, the electron affinity E_0 may be calculated from the data used in (2).

The free energy of the chlorine monatomic gas is

$$F_{Cl}{}^0 = RT \left[\ln \left(\frac{h^2}{2\pi m_{Cl} kT} \right)^{\frac{3}{2}} \frac{1}{kT} \frac{1}{Q_{iCl}} \right]. \qquad (4)$$

The internal partition function,

$$Q_{iCl} = \sum_i e^{-\epsilon_i / kT} = 4 + 2e^{-881 \times 1.4316/T}, \qquad (5)$$

depends on the temperature. Call

$$x = 1 + \tfrac{1}{2} e^{-881 \times 1.4316/T}, \qquad (6)$$

and then

$$\ln Q_{iCl} = \ln 4 + \ln x. \qquad (7)$$

Now if $\ln x$ is expanded in a McLaurin's series around 2140°K, one finds that the second-order terms are negligible.

Finally one obtains

$$\log_{10} x = T(2.5964 \times 10^{-5}) + 0.04077. \qquad (8)$$

The resulting complete equation from (4), (3) and (2) for E_0 is

$$E_0 = \frac{T_f}{1000} 4.5738 \left[\log_{10} \frac{I_i}{I_{e^-}} - \log_{10} P_{Cl} + 2 \log_{10} \frac{T_f}{1000} + T_f(2.5964 \times 10^{-5}) + 9.832 \right]. \qquad (9)$$

Here E_0 is the electron affinity in kcal. and P_{Cl_2} is the pressure of chlorine in mm of Hg times a thousand.

EXPERIMENTAL

The chlorine was fractionally distilled eight times in a baked out all glass vacuum system. It was stored in 5-liter bulbs which were connected to the apparatus as shown in Fig. 1. The chlorine was released by breaking the glass tip with a magnetic hammer after the pressure had been reduced to the order of a millimeter or less by cooling the lower bulb in a slush of dry ice and petroleum ether which was under reduced pressure.

* This author wishes to acknowledge a grant-in-aid received from The Hynson, Westcott and Dunning Research Fund.

** Now located at Columbia University.

[1] P. P. Sutton and J. E. Mayer, J. Chem. Phys. **3**, 20 (1935).

[2] H. B. Weisblatt, Johns Hopkins, Dissertation (1938).

The pressure of the chlorine in the reaction chamber was controlled by obtaining a steady-state flow through the reaction tube between the reservoir and a liquid-air-cooled trap. The flow was regulated by means of a capillary device shown in Fig. 2 which was between the chlorine reservoir and the reaction vessel. When the rod was inserted all of the way into the capillary, the pressure in the reaction tube was reduced to 1/10 of the value obtained when the rod was free.

The chlorine pressure was measured with a quartz fiber manometer designed and built by H. B. Weisblatt.[2]

The magnetron tube in which the measurements were made is shown in Fig. 3.

The tube and the solenoid were packed in dry ice in order to freeze out any reaction products formed by the Cl_2 and the metal parts. Before use these metal parts were baked out with an induction furnace. The plate, 4.7 cm diameter and 3.0 cm long, the guard plates, 4.7 cm diameter and 4.0 cm long, and the grid, 2.5 cm diameter and 7.5 cm long, were made of tantalum. The leads were made of tungsten and nickel.

The first filament used had been previously operated in an atmosphere of bromine gas in measuring the electron affinity of bromine. After several days of operation the filament was removed and it was found that it had grown to about twice its original diameter, presumably due to the decomposition of some volatile metallic chloride on its surface. During these experiments the reaction tube had *not* been packed in dry ice.

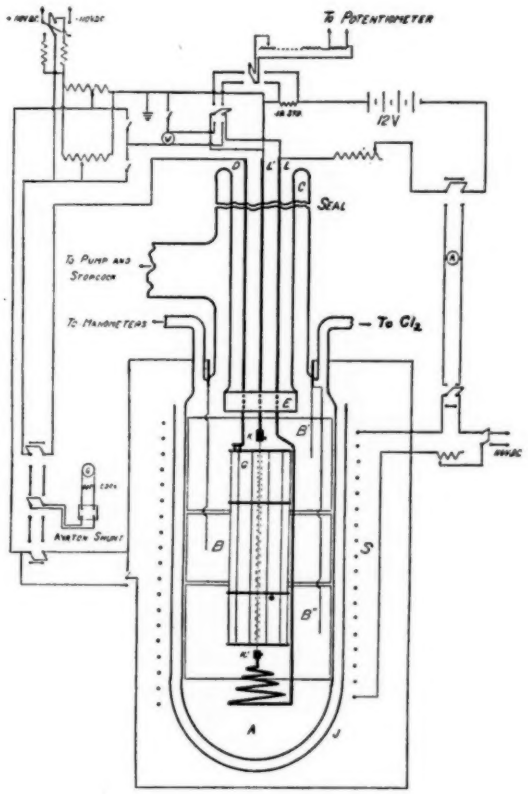

FIG. 3.

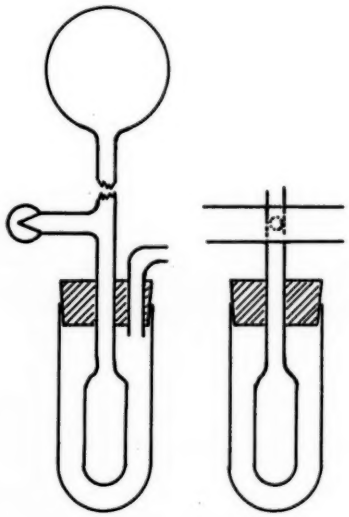

FIG. 1.

FIG. 2.

Since the temperatures are determined from the current voltage characteristics of the filament one may legitimately feel considerable scepticism concerning the value of these results.

Joseph Hickman, of this laboratory, kindly made an x-ray powder photograph of the filament. The resulting interplanar distances are given in Table I. They corresponded to none of the expected materials.[3] Before the apparatus was opened a yellow powder was noticed inside; on exposure to air it turned white. This is characteristic of tantalum pentachloride which hydrolyzes in moist air.[4]

A second filament led to erratic results, the

[3] Hanawalt, Rinn and Frevel, Ind. Eng. Chem. Analyt. Ed. **10**, 457 (1938).
[4] H. Rose, Pogg. Ann. **99**, 65 (1856).

calculated electron affinity being much lower than any probable value.

Through the kindness of Dr. Irving Langmuir a pure tungsten filament of diameter 0.0199 cm was obtained, filament III.

The first 31 measurements on this filament were taken in the course of 7.5 hours, and led to reasonable results, which are arranged in chronological order in Table II. A slight tendency for the calculated E_0 values to decrease with time is observable.

Some 50 measurements taken later gave erratic results with calculated E_0 values as low as 70 kcal., and few results as high as 85 kcal.

Errors

This method of determination of electron affinity is based on only one assumption other than the obvious ones of accuracy in the measurements themselves: namely, that the reflection coefficients of ions, atoms, and electrons on the filament surface are unity. This means that the probability of a chlorine nucleus leaving the surface as a negative ion, or as a neutral atom, is independent of its past history, that is whether it struck the filament as molecule, ion or atom. The correctness of this assumption can only be tested by the independence of the resulting E_0 on the temperature and Cl_2 pressure, which determine the nature of the filament surface.

Since the results were apparently independent of temperature and pressure, but strongly dependent on the time for which the filament had been exposed to chlorine these authors believe that the error is to be ascribed to some difficulties in the data themselves, rather than on the reflection coefficients.

Of the data, only the filament temperature, T_f, appears to be in reasonable doubt. These temperatures were calculated by the method suggested by Langmuir and Jones,[5] in which the voltage

Table I. $d=0.7093/2 \sin \theta$.

3.20	1.61	0.876
2.40	1.47	0.774
2.12	1.28	0.732
1.83	1.04	0.644
		0.600

[5] Langmuir and Jones, Gen. Elec. Rev. **419**, 310 (1927).

Table II.

R_f	I_i/I_e	$P_{Cl_2}\times10^3$	T_f	E_{0f}
		Filament III		
1.39	5.1	0.85	1845	94.5*
1.39	3.4	0.44	1845	95.4*
1.57	1.5	5.41	2034	92.5*
1.57	129.	7.19	2033	109.3*
1.56	9.2×10^{-2}	0.43	2032	91.4
1.58	1.3×10^{-1}	0.71	2034	90.8
1.63	9.6×10^{-2}	0.86	2094	91.7
1.62	1.6×10^{-1}	1.47	2092	91.5
1.69	2.9×10^{-1}	2.49	2141	94.2
1.66	2.2×10^{-1}	2.46	2126	94.0
1.68	4.5×10^{-1}	2.69	2132	95.3
1.69	4.5×10^{-1}	2.69	2134	95.3
1.74	2.3×10^{-1}	2.84	2180	94.5
1.74	1.8×10^{-1}	3.20	2179	92.8
1.81	3.4×10^{-1}	4.22	2186	94.7
1.76	3.8×10^{-1}	4.17	2187	95.3
1.84	1.1×10^{-1}	3.58	2258	93.8
1.85	1.2×10^{-1}	3.73	2263	94.3
1.95	3.0×10^{-2}	3.92	2320	90.3
1.94	2.8×10^{-2}	4.72	2315	88.9
1.96	3.1×10^{-2}	1.69	2325	94.5
1.93	2.9×10^{-2}	1.73	2299	93.0
1.86	4.8×10^{-2}	2.46	2231	90.6
1.85	5.9×10^{-2}	2.72	2229	91.0
1.78	8.9×10^{-2}	3.48	2164	88.7
1.79	1.0×10^{-1}	3.48	2167	89.4
1.79	1.5×10^{-1}	3.68	2166	90.9
1.65	3.5×10^{-1}	4.03	2054	88.8
1.63	3.5×10^{-1}	4.17	2049	88.4
1.51	1.0	5.90	1987	88.2*
1.49	1.1	4.62	1980	89.2*

* I_i/I_e is uncertain when its value exceeds unity. Average $E_0=92.7$ kcal.

Table III.

Filament I
35 observations covering the range

I_i/I_e	P_{Cl_2}	T	E_0
1.1×10^{-2} to 5.3	0.5 $\times10^{-3}$ mm to 22. $\times10^{-3}$ mm	1972°K to 2203°K	79.9 to 99.1 kcal. 85% within 90.1 to 95.1

Filament observed to be coated thickly with foreign metallic coating after observations.

Filament II
74 observations covering the range

I_i/I_e	P_{Cl_2}	T_f	E_0
6×10^{-4} to 10.4	0.24×10^{-3} to 14. $\times10^{-3}$	1717°K to 2309°K	75 to 106 kcal.

Calculated E_0 values decreased uniformly with time at first, then rose abruptly at end of experiments.

Filament III
first 31 observations in Table II
next 49 observations covering the range

I_i/I_e	P_{Cl_2}	T_f	E_0
9×10^{-5} to 3 $\times10^{-1}$	0.34×10^{-3} mm to 11.11×10^{-3} mm	1869°K to 2249°K	66 to 87.5 kcal.

Calculated E_0 values decreased uniformly with time at first, then rose at end of the experiments.

times cube root of current over the length of filament is used. This function gives the temperature provided the surface is that of clean tungsten. The cooling due to the chlorine gas itself at the pressures used can be calculated to be negligible. It was assumed that a monomolecular Cl layer on the surface would not affect its optical properties.

Presumably this is true, and only after considerable exposure when the filament surface has become covered, as noted particularly with filament I, does the temperature calculated differ appreciably from the true filament temperature.

The average of the first 31 measurements, on filament III, recorded in Table II are taken as giving a probable value for E_0.

In Table III a brief summary of the other results are indicated for completeness.

The authors wish to acknowledge the help of Dr. Harold B. Weisblatt in much of the experimental work.

MARCH, 1940 JOURNAL OF CHEMICAL PHYSICS VOLUME 8

The Structure of Phosphine and Related Hydrides

D. P. STEVENSON*
California Institute of Technology, Pasadena, California
(Received November 20, 1939)

It is shown that Badger's rule when applied to the frequencies of some hydrides gives values for the interatomic distances which are in agreement with values deduced from the moments of inertia of the hydrides and with values predicted from the covalent radius suggested for hydrogen, 0.315A. Using the value 1.415A. for the phosphorus-hydrogen distance in phosphine and a reliable spectroscopic value for one of the moments of inertia of the molecule one finds the bond angle to be 93°. Values are suggested for the bond angles and bond distances in a number of hydrides whose structures have not been experimentally determined.

IN the course of calculating the thermodynamic functions of some compounds from spectroscopic data it became apparent that the structure of phosphine as well as the structures of the hydrides of the heavier elements of the fourth, fifth, and sixth groups of the periodic system are either unknown or only partially known. Due to the complicated nature of the vibration-rotation interactions it is very difficult if not impossible to determine the structure of these hydrides from the fine structure of the rotation-vibration absorption bands in the infra-red. Although it has been proved possible to determine the interatomic distances in methane[1a] and ammonia[1b] by the electron diffraction method, it is, at present, not feasible to use this method for the heavier hydrides because of the excessive atomic scattering of the heavy atom and the very severe temperature factors that arise when the vibrational frequencies become relatively small.

Inasmuch as the structures of the hydrides are of interest from several points of view it seems worth while to report the results of an indirect determination of the structure of phosphine and of some of the heavy hydrides.

Wright and Randall[2] have found 6.22×10^{-40} g cm^2 for the perpendicular moments of inertia of phosphine. These moments of inertia are related to the structural parameters of the molecule by the equation

$$I_2=I_3$$
$$=mr_0^2\left[2\sin^2\frac{\alpha}{2}+\frac{3M}{M+3m}\left(1-\frac{4}{3}\sin^2\frac{\alpha}{2}\right)\right], \quad (1)$$

where m is the mass of the hydrogen atom, M is the mass of the phosphorus atom, r_0 is the phosphorus-hydrogen distance, and α is the bond angle. In Table I are given the values of r_0 and α which are compatible with the value $I_2=6.22\times10^{-40}$ g cm^2, as well as the corresponding values of I_1, the moment of inertia about the

* Contribution from the Gates and Crellin Laboratories of Chemistry, California Institute of Technology, No. 749.

[1a] V. Schomaker and D. P. Stevenson, J. Am. Chem. Soc. **62** (1940).

[1b] P. P. Debye, Physik. Zeits. **40**, 404 (1939).

[2] Wright and Randall, Phys. Rev. **44**, 391 (1933).

symmetry axis.

$$I_1 = 4mr_0^2 \sin^2 \frac{\alpha}{2}. \qquad (2)$$

The angle α is plotted against r_0 in Fig. 1.

The interatomic distances found in methane,[3] ammonia,[2] water,[4] and hydrogen sulfide[5] taken with the covalent radii of carbon, nitrogen, oxygen, and sulfur as given by Pauling[6] give 0.315±0.005A for the covalent radius of hydrogen. The covalent radius of phosphorus is 1.100±0.010A, hence $r_0 = 1.415 \pm 0.015$A. Interpolating by means of the graph of r_0 *vs.* α (Fig. 1), one obtains $\alpha = 93 \pm 2°$.

One may obtain a check on the reliability of r_0 as estimated by the use of the covalent radius table by the application of Badger's rule[7] to the known frequencies of phosphine.[8] Furthermore a measure of the accuracy of Badger's rule may be obtained by comparing the interatomic distances given by the frequencies of methane, ammonia, water, and hydrogen sulfide with those found from the moments of inertia. In Fig. 2 a plot of r_0 *vs.* $(1/k_e)^{\frac{1}{3}}$ is given for a number of diatomic molecules of the type 1-*H*, 2-*H*, and 3-*H*, the Arabic numerals indicating rows of the periodic system. The values of k_e were calculated from the formula

$$k_e = 0.0586 M' \nu^2, \text{ dynes per cm,}$$

where ν is the observed frequency in wave numbers and M' is the reduced mass in atomic weight units. The values of r_0 and ν were taken from Sponer.[9] It was assumed that for the

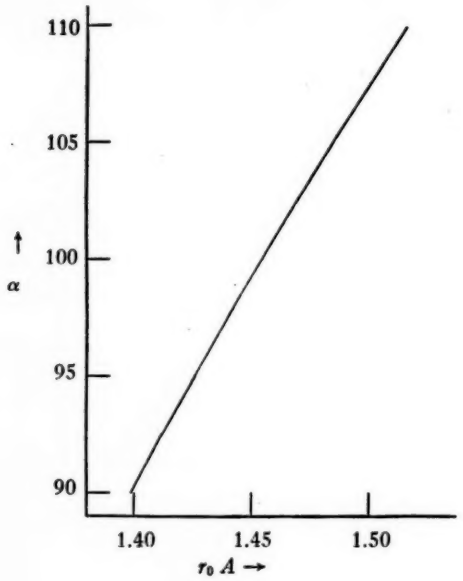

FIG. 1.

polyatomic hydrides k_e has a form similar to that for the diatomic hydrides,

$$k_e = 0.0586 M' \left(\frac{\nu_{\|} + \rho_\perp \nu_\perp}{1 + \rho_\perp} \right)^2$$

$$= 0.0586 M' \bar{\nu}^2 \text{ dynes per cm,}$$

where $M' = Mm/(M+m)$, M is the mass of the central atom, m is the mass of the hydrogen atom, and $\rho_\perp$ is the degeneracy of the perpendicular vibration. This assumption is reasonable for the hydrides since the interaction between the various modes of vibration is quite small. There is practically no difference between the force constants calculated according to Eq. (4) and those calculated for more complicated potential functions in which allowance is made for interaction. The values of r_0 obtained for the hydrides whose vibrational frequencies are known are given in column 4 of Table II with the values from the moments of inertia in column 5 and those predicted from the covalent radius table in column 6.

The quality of the agreement indicates that in general the interatomic distances predicted for hydrides by the covalent radius table or by Badger's rule are accurate to within 0.02A.

The values obtained for the Si-H distance in silane are considerably higher than the value

TABLE I.

α	r_0 IN A	$I_1 \times 10^{40}$ G CM²
90°	1.399	6.51
95°	1.426	7.35
100	1.455	8.26
105	1.484	9.22
110	1.515	10.24

[3] N. Ginsburg and E. F. Barker, J. Chem. Phys. **3**, 668 (1935).
[4] Freudenberg and R. Mecke, Zeits. f. Physik. **81**, 465 (1933).
[5] P. C. Cross, Phys. Rev. **46**, 536 (1934); **47**, 7 (1935).
[6] L. Pauling, *The Nature of the Chemical Bond* (Cornell University Press, 1939), p. 154.
[7] R. M. Badger, J. Chem. Phys. **2**, 128 (1934).
[8] Hibben, *The Raman Effect* (Rheinhold Press, 1939).
[9] H. Sponer, *Molekülspektren* (Springer, 1935).

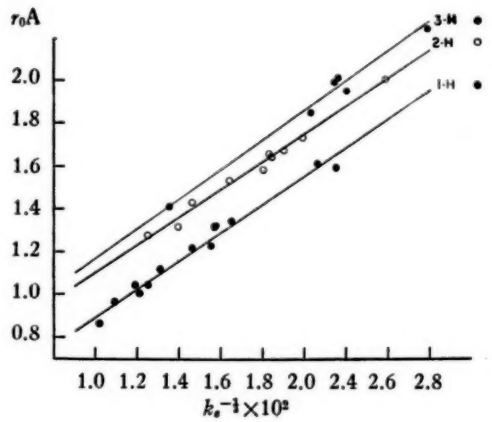

FIG. 2.

TABLE II.

MOLECULE	$\bar{\nu}$ cm^{-1}	$k_e^{-1}\times10^2$	r_0 A (CALC.)	r_0 A (OBS.)	r_0 A (COVALENT)	REFERENCE
CH_4	2990	1.27	1.07	1.09	1.085	9
NH_3	3257	1.20	1.02	1.01	1.015	9
H_2O	3675	1.10	0.96	0.97	0.975	9
SiH_4	2185	1.54	1.46	1.42*	1.485	8
PH_3	2390	1.46	1.40		1.415	8
H_2S	2625	1.37	1.34	1.35	1.355	9
AsH_3	2155	1.55	1.54		1.525	8
H_2Se	2305	1.48	1.50		1.485	12

* See reference 10.

1.42A calculated from the moment of inertia found by Steward and Nielsen.[10] Their value is probably less reliable than that given by the covalent radius table, inasmuch as an inspection of their data reveals that the fine structures of the bands in question are less accurately known than those of the corresponding bands of methane.

It has been suggested by Pauling[6] that the elements of the fifth and sixth groups should tend to form p bonds rather than hybrid $s-p$ bonds because of the much greater stability of the s electrons in the atoms. The fact that the bond angles in ammonia and water are so much greater than the 90° predicted for pure p bonds was explained on the basis of partial ionic character due to the large electro-negativities of nitrogen and oxygen. If this is so one would expect the bond angles to decrease when the nitrogen or oxygen atom is replaced by heavier atoms. The value 93° obtained for phosphine adds to the confirmation of this hypothesis already provided by Cross's[4] value for the bond angle in hydrogen sulfide, 92°. One would thus expect that the bond angles in arsine, stibine, hydrogen selenide, and hydrogen telluride to be within 1° of 90°.

On the basis of the conclusion reached in the preceding paragraphs we may predict the interatomic distances and bond angles for the hydrides shown in Table III.

Cameron, Sears and Nielsen[11] have recently obtained approximate values for the moments of inertia of hydrogen selenide by assuming the molecule to be almost a symmetrical top, $I_2 \cong I_3 = I/2$. From the spacing of lines of the 4.3μ band of H_2Se they find $I_2 = 3.6\times10^{-40}$ g cm^2. The structure suggested in Table III leads to 3.69×10^{-40} g cm^2 for this moment of inertia.

TABLE III.

MOLECULE	M-H A	H-M-H°
SiH_4	1.49	109.5°
PH_3	1.42	93°
GeH_4	1.54	109.5°
AsH_3	1.53	90°
SeH_2	1.49	90°
SnH_4	1.72	109.5°
SbH_3	1.73	90°
TeH_2	1.69	90°

In conclusion, the author expresses his thanks to Professor L. Pauling for his interest and helpful suggestions.

[10] W. B. Steward and H. H. Nielsen, Phys. Rev. **47**, 828 (1935).

[11] D. M. Cameron, W. C. Sears and H. H. Nielsen, J. Chem. Phys. **7**, 994 (1939).

The Relation Between the Energy of a Hydrogen Bond and the Frequencies of the O—H Bands*

RICHARD M. BADGER
Gates and Crellin Laboratories of Chemistry, California Institute of Technology, Pasadena, California
(Received November 6, 1939)

IT has previously been pointed out[1] that there appears to be a relation between the energy of a hydrogen bond and the shift in frequency of the O—H bands which accompanies the formation of the bond. Recently additional data have been obtained in this laboratory[2,3] which confirm the existence of this useful relation and it seems worth while to discuss them in this connection.

The data here presented all relate to linkages in which a hydroxyl hydrogen is concerned, though the atom to which it is weakly bound may be oxygen, chlorine, or carbon in an aromatic ring. It is surprising that the same connection between energy and frequency shift should be found in these various cases but such appears to be the fact. For other types of bond, for example those involving the hydrogen of an amino group, a slightly different relation may well be expected.

The data plotted in Fig. 1, with one exception, relate to cases in which a hydroxyl group which is initially in a relatively ideal, unperturbed condition enters into a hydrogen bond. The observed shift in frequency of the third harmonic O—H band which accompanies this change is plotted against the energy of the bond.[4] There is a fairly strong indication that the relation between frequency and energy is not linear, though the curve drawn is indeed somewhat arbitrary. The inaccuracy in the energy values may be at least as great as 500 cal. and the precision of the frequency measurements is uncertain. The frequencies employed are those of the band maxima. This is satisfactory in the case of narrow bands but the association bands are broad and unsymmetrical and it is not certain to what point one should measure. It seems quite certain that resolvable features which these bands have sometimes been supposed to possess are merely superposed C—H bands or other harmonic or combination bands. At present the maximum seems to be the least arbitrary point of reference for measurement.

The abscissae of the points for *o*-chloro phenol and ethylene chlorohydrin are differences in energy of two molecular configurations in one of which an intramolecular hydrogen bond is present. The energy difference of the two states may be partly due to other factors beside the hydrogen bond, but at present it is not possible to make allowance for them. Similar difficulties, however, are encountered in the estimation of the energy of any hydrogen bond. For example, in obtaining the energy of the two bonds in the dimer organic acids from the dissociation energy one should probably make some allowance for van der Waals interactions.

It is not certain that it is permissible to include the point for phenol in benzol solution in the diagram. The spectroscopic data[5] indicate a very low O—H frequency for the phenol monomer in

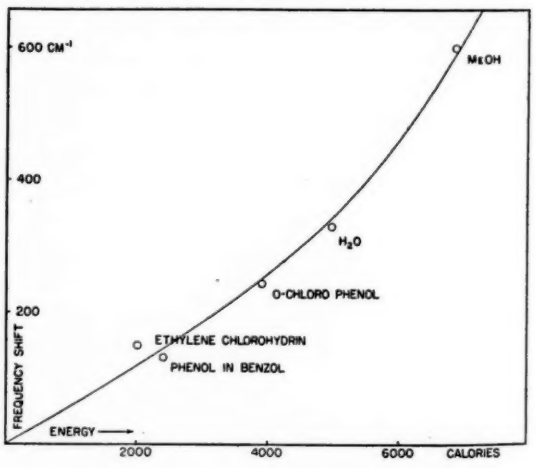

FIG. 1. A plot of the frequency shift in the third harmonic O—H bands against energy of the hydrogen bond.

* Contribution No. 744 from the Gates and Crellin Laboratories of Chemistry.

[1] Badger and Bauer, J. Chem. Phys. **5**, 839 (1937).

[2] Lassettre and Dickinson, J. Am. Chem. Soc. **61**, 54 (1939).

[3] Zumwalt and Badger, J. Am. Chem. Soc. (in press).

[4] The data for water and methyl alcohol are those of reference 1.

[5] A. Naherniac, Ann. de physique **7**, 528 (1937).

benzol solution, which may be taken as evidence for solvation through the agency of a hydrogen bond. The energy quantity evaluated by Lassettre and Dickinson[2] may thus be regarded as the difference in energy of two hydrogen bonds. If the energy frequency relation is nonlinear one should expect the point for phenol to lie somewhat above the curve fitting the other points. A similar situation may be expected for the carboxylic acids. The low O−H frequency and the rather rigid planar COOH group of the acid monomers[6] suggest some tendency for the formation of a weak hydrogen bond in a four-membered ring.

The frequency shifts plotted in the figure are all for the third harmonic O−H bands in the region λ9500–11,000. The photograph region, beside being convenient for investigation, has the advantage that shifted and unshifted bands are better separated and more accurately measured than in the fundamental region. It would no doubt be preferable to deal with frequencies extrapolated to zero amplitude but the data are at present too incomplete to permit this. In any case the frequency shifts in the third harmonic bands will usually be nearly proportional to those in the ω_e's, since the convergence of most O−H band progressions is about the same.

A very important exception to this is the case of the carboxylic acids. By a somewhat unjustifiable method of plotting Badger and Bauer brought a point for acetic acid in line with other data, but actually the bands of the associated organic acids are quite anomalous. Badger and Bauer have discussed the character of the O−H vibrations in these substances and the nature of the potential function. As they pointed out, an unsymmetrical O−H vibration is responsible for the infra-red association bands. Owing to the somewhat special character of the potential function the succession of energy levels corresponding to this vibration must diverge rather than converge, as is customary. One is consequently not surprised to find that the progression of O−H bands for the double molecules diverges at about the same rate as other O−H progressions converge. Such anomalous cases are probably rare.

Many applications of the relations here discussed must be obvious and need not be discussed. Recently spectroscopic data relating to hydrogen bonds have been accumulating rapidly and in many cases they may greatly assist in interpreting observations of other kinds.

[6] Bauer and Badger, J. Chem. Phys. **5**, 852 (1937).

LETTERS TO THE EDITOR

This section will accept reports of new work, provided these are terse and contain few figures, and especially few halftone cuts. The Editorial Board will not hold itself responsible for opinions expressed by the correspondents. Contributions to this section should not exceed 600 words in length and must reach the office of the Managing Editor not later that the 15th of the month preceding that of the issue in which the letter is to appear. No proof will be sent to the authors. The usual publication charge ($3.00 per page) will not be made and no reprints will be furnished free.

The Second Virial Coefficient of Ethane

This is to make known an error in the value of a constant in the second virial temperature coefficient equation for ethane of Eucken and Parts.[1] The equation is given by these workers as

$$B=+59.0-\frac{3.9\times10^{6}}{T^{1.7}}-\frac{9.5\times10^{12}}{T^{5.4}}, \qquad (1)$$

and tabulated data appended for B observed and B calculated, over the temperature range investigated. However, comparing values of B calculated from Eq. (1) it will be found that they do not agree with those given in the table of Eucken and Parts. Upon inspection of the situation, it becomes apparent that the equation should have been given as

$$B=+59.0-\frac{3.9\times10^{6}}{T^{1.7}}-\frac{9.5\times10^{13}}{T^{5.4}}, \qquad (2)$$

that is, the exponent for the constant of the last term should be 13 instead of 12. The values in Table I, calculated for three of the temperatures of Eucken and Parts demonstrate the situation. This comparison can leave but little doubt that Eq. (2) above was the one employed by Eucken and Parts for calculating the values given in the third column of the above table. The use of the incorrect equation will lead to an error of *ca.* 8 percent at the lowest temperature and of 2.6 percent at the highest, in B.

TABLE I.

	Values of $-B$ in cc per mole			
	From E. & P. Table		Calc. from above equations	
T, °K	Obs.	Calc.	(1)	(2)
191.86	498	499	458.4	498.5
224.50	354	353	335.5	352.7
273.20	227.5	228	222.9	228.8

TABLE II.

	dB/dT, cc/mole/deg.		d^2B/dT^2, cc/mole/deg.^{2}	
T, °K	Eq. (1)	(2)	(1)	(2)
191.86	4.67	5.80	−0.0681	−0.1058
272.07	1.783	1.90	−0.0179	−0.0207
364.78	0.804	0.822	−0.00597	−0.00629

It is of importance to ascertain the resulting errors in dB/dT and in d^2B/dT^2 that will occur from employing the incorrect equation. The results of some calculations are given in Table II. It will be observed that appreciable error will be made in the derivatives, especially at the lower temperatures.

Mr. W. W. Rice of these laboratories has kindly checked the calculations in the above two tables.

A search of volumes of *Zeitschrift für physikalische Chemie* later than **B19** failed to reveal any recorded correction of this error.

EDWIN E. ROPER

Mallinckrodt Chemical Laboratories,
Harvard University,
Cambridge, Massachusetts,
February 6, 1940.

[1] Eucken and Parts, Zeits. f. physik. Chemie **B20**, 184 (1933).

The Crystal Structure of Sodium Sulfate III

Of the five modifications of anhydrous sodium sulfate,[1,2] thenardite is the only form that has been examined structurally. To help understand the nature of the temperature transition from thenardite to Na_2SO_4 III, the structure of the latter modification has been determined. Na_2SO_4 III belongs to the orthorhombic space group Pb nn. The unit cell contains $4Na_2SO_4$ and has the following dimensions at room temperature:

$$a=5.59\pm0.02\text{A}, \quad b=8.93\pm0.02\text{A}, \quad c=6.98\pm0.02\text{A}.$$

The tetrahedral $SO_4^{=}$ groups are located at $\pm(\frac{1}{4}, v, \frac{1}{4})$ and $\pm(\frac{1}{4}, \frac{1}{2}-v, \frac{3}{4})$ with $v=0.097\pm0.001$. The two sets of sodium ions have the following parameters: $\pm(\frac{1}{4}, v_1, \frac{1}{4})$, $\pm(\frac{1}{4}, \frac{1}{2}-v_1, \frac{3}{4})$ with $v_1=0.435\pm0.010$; and $\pm(u, \frac{1}{4}, o)$, $\pm(\frac{1}{2}-u, \frac{1}{4}, \frac{1}{2})$ with $u=-\frac{1}{4}$. The sixteen oxygens occupy two sets of general positions $\pm(x, y, z)$, $\pm(x, \frac{1}{2}-y, -z)$, $\pm(\frac{1}{2}-x, y, \frac{1}{2}-z)$, $\pm(\frac{1}{2}-x, \frac{1}{2}-y, z+\frac{1}{2})$ with x_1, y_1, z_1 $=0.030\pm0.002$, 0.197 ± 0.003, $\frac{1}{4}$ and x_2, y_2, $z_2=\frac{1}{4}$, 0, 0.072 ± 0.002.

LUDO K. FREVEL

The Dow Chemical Company,
Midland, Michigan,
January 23, 1940.

[1] F. C. Kracek and R. E. Gibson, J. Phys. Chem. **33**, 1304 (1929).
[2] F. C. Kracek and C. J. Ksanda, J. Phys. Chem. **34**, 1741 (1930).

Zeeman Effect From Liquids, Solutions of Salts of Europium

Among liquids, the solutions of the salts of europium appear to be unique in the sharpness of their absorption spectra. The absorption lines cluster in groups which owe their origin to the splitting of the energy levels of the europium ions by the electric fields of their environment. Should the symmetry of the fields about the ions be reduced, as by superimposing an external field, a further splitting is to be expected in general and also an increase in the number of lines within the groups. It is in the study of the structures of the groups that we have turned to the effect of a magnetic field on the spectra.

Zeeman effects from crystals at low temperatures have indicated that the lines must be very sharp before the effect of the magnetic field can be resolved. It has actually been found, notably from aqueous solutions of europium nitrate, that some of the Zeeman components at the fields available could be separated with an instrument of rather modest resolving power and dispersion, a three-prism Steinheil spectrograph having a dispersion of about 13A per mm at 4650A.

The group of absorption lines at 4650A which, in the absence of the field, had consisted of three lines at 4645.$_0$A, 4649.$_8$A, 4654.$_5$A increased to five, when the radiation passed through the solution transverse to the field. However, the existence of one of these lines was somewhat uncertain. As the magnetic field was increased, a component was observed to split off the line at 4649.$_8$ toward long wave-lengths until at 33,000 gauss, the separation from the undisplaced component amounted to 7 cm^{-1} ± 1.5 cm^{-1} or about six to eight times the normal Larmor precession. Another component also appeared to separate off from the same line toward shorter wave-lengths, but it was much less sensitive to the magnetic field and indeed the displacement was very small relative to the dispersion of the spectrograph. However, its presence seemed to be confirmed on examining the polarization of the spectra. The sensitive component represented absorption of radiation having its electric vector at right angles to the magnetic field; the insensitive component was polarized in the same sense. However, the undisplaced component remained unpolarized. The line at 4645.$_0$A displaced by the field to 4644.$_8$A also remained unpolarized.

The effect of a magnetic field on the spectrum from a solution of europium chloride was altogether different from what occurred with the nitrate.

At some later occasion, a more detailed description of the spectra arising in the magnetic field will be given.

We gratefully acknowledge the support of the Penrose Fund of the American Philosophical Society.

G. H. Jones Laboratory,
University of Chicago,
Chicago, Illinois,
January 27, 1940.

SIMON FREED
S. I. WEISSMAN
G. J. ROTARIU

Raman Effect of Symmetric Difluorotetrachloroethane

We have observed twenty-two Raman shifts in symmetric difluorotetrachloroethane. The results are shown in Table I. Three exposures were made on Eastman Spectroscopic Plates Type 1-J using our usual set-up of a three-prism Steinheil spectroscope and eight concentric mercury discharge tubes as a source of radiation. Exposure times employed were 22 and 42 hours with a slit width of 0.05 mm, and 46 hours with a slit at 0.1 mm. The spectroscope was thermostated at 33.4±2°C. The average temperature of the sample was about 40°C.

A separate exposure was necessary in order to obtain the line at 81.4 cm^{-1} since the region of the plate close to 4358 and 4046 is blocked off by dihedral light stops to prevent overexposure and consequent halation of the strong lines.

TABLE I. *Raman lines of symmetric tetrachlorodifluoroethane.*

$\Delta\nu$ cm^{-1}	Estimated Relative Intensity	% Mean Deviation	Exciting Lines		No. of Readings
81.4	5	0.25		*c*	2
165.5	3	.36		*c*	4
181.2	5	.38		*c*	6
231.0	7	.30	*a*	*c*	12
264.3	7	.45	*a*	*c*	12
297.2	5	.47	*a*	*c*	12
329.1	7	.21	*a*	*c*	12
402.1	3	.32	*a*	*c*	5
421.2	10	.26	*a*	*c*	12
444.7	8	.22	*a*	*c*	10
455.5	2	.50	*a*	*c*	7
523.8	8	.34	*a*	*c*	12
578.2	6	.27	*a*	*c*	10
625.9	8	.23	*a*	*c*	12
778.9	0	.25		*c*	2
854.8	4	.19	*a*	*c*	8
906.8	2	.40	*a*	*c*	6
1027.2	4	.20	*a*	*c*	8
1046.0	0	.26	*a*	*c*	7
1086.0	0	.23		*c*	2
1143.0	2	.17		*c*	3
1167.5	3	.08		*c*	3

a = 4046, *c* = 4358A.

An exposure of 13.5 hours with a slit width of 0.1 mm was made with the stops out. The line was found between the halated excitation line and the circular halo which is formed about 100 cm^{-1} from it.

The material used was furnished by the E. I. duPont de Nemours & Company and was specified as "carefully fractionated a number of times, practically 100 percent pure." We wish to thank Dr. A. F. Benning of the Jackson Laboratory for the loan of this substance. Further considerations of these results will be published later.

GEO. GLOCKLER
C. G. SAGE

University of Minnesota,
Minneapolis, Minnesota,
February 1, 1940.